AN ASSESSMENT OF THE SPATIO-TEMPORAL URBAN DYNAMICS IN THE CITY OF TSHWANE, SOUTH AFRICA

BY

JAMES TAKAWIRA MAGIDI (1254935)

A thesis submitted to the School of Geography, Archaeology and Environmental Studies, Faculty of Science in fulfilment of the requirements for the degree of Doctor of Philosophy in Geography.

Supervisor: Professor Fethi Ahmed

May 2018

Declaration

I, James Takawira Magidi, declare that this thesis is my own unaided work except as stated in the acknowledgements. No other person's work has been used without due acknowledgment in the main text of the report. It is submitted in fulfilment of the requirements for the degree of Doctor of Philosophy in Geography at the University of the Witwatersrand, Johannesburg. It has not been submitted before for any degree or examination at any other universities.

Signature: _____

ABSTRACT

Urbanisation, urban sprawl and loss of biodiversity in urban environments are major phenomena of the 21st Century cities and towns in both developing and developed countries. A study of the City of Tshwane (CoT), South Africa has shown that the city had been affected by unprecedented urbanisation, which led to encroachment of urban areas into non-urban environments. There is a need to monitor, quantify and predict urban dynamics for the sustainable management of urban environments. The advent of remote sensing and Geographical Information Systems (GIS) techniques have enabled researchers and decision-makers to have a historical perspective of the earth and detect change in urban areas. Remote sensing and GIS are powerful, cost-effective and efficient tools that are used in quantifying, monitoring and predicting land cover change using multi-temporal and multi-spectral spatial datasets. This helps decision-makers in designing decision support systems that are useful in evaluating alternative management scenarios and in the formulation of land use policies that are effective in the sustainable management of urban areas. Landsat TM (Thematic Mapper), ETM+ (Enhanced Thematic Mapper Plus) and OLI (Operational Land Imager) satellite imagery from 1984 to 2015 were used for the long-term change detection. These remotely sensed data were classified into two classes, which are built-up (urban) and non-built-up (non-urban) areas using the supervised maximum likelihood classifier (MLC) Post-classification change detection methods and landscape metrics were used to assess change and quantify the degree of urban sprawl. Short-term change detection was performed in the low, medium and high-density areas using classified SPOT (Satellite Pour l'Observation de la Terre) satellite imagery of 2008, 2012 and 2015. To predict future scenarios in urban dynamics the study made use of the classified land cover maps of 1986, 2005, 2009 and 2009 (Landsat TM and Landsat OLI) coupled with transitional areas, transitional probabilities and the Cell Automaton-Markov (CA-Markov) model. The prediction model was validated using the predicted maps and classified maps of 2009 and 2013. Change in vegetation was assessed using time series analysis, which was run on MODIS (MODerate-resolution Imaging Spectroradiometer) NDVI (Normalized Difference Vegetation Index) datasets with a 250m spatial resolution and a 16-day temporal

resolution. Temporal (NDVI) profiles generated in different land cover classes coupled with the Mann-Kendall Statistic and Sen's Estimator were used to assess the seasonal trends in vegetation from 2000 to 2016. Retrieval of change in land surface temperature (LST) was done using winter (August) and summer (December) Landsat imagery of 1997 and 2015. NDVI, emissivity and satellite temperature of the two different years and seasons were inputs in the retrieval of LST. There was a comparison of LST between the two years (1997 and 2015) and between seasons (winter and summer). Cross-sectional transects were run across different land cover types to show variations in LST. Results revealed an increase in urban areas in the CoT between 1984 and 2015. Urban predictions revealed an anticipated future increases in urban sprawl. Short-term land cover changes using SPOT imagery revealed an increase in urban areas in the high-density as compared to the low-density and the medium-density areas. Human settlements in the high-density areas especially the informal ones are also encroaching into areas earmarked for conservation. There were also remarkable seasonal variations in vegetation cover based on the MODIS NDVI temporal profiles. Mann Kendall trend analysis revealed a decreasing trend in vegetation cover in different land cover types. Temperature change in the CoT is evident as there was an increase in LST between 1997 and 2015 with high LST in summer and low in winter. The main aim of this study was to use remote sensing and GIS techniques to quantify, monitor and predict urban dynamics in the CoT. The objectives were to assess long-term and short-term land cover changes, to predict urban dynamics and to use available proxies such as vegetation cover, land surface temperature to assess urban growth.

Keywords: Urban Sprawl, Urban growth, Predictive Modelling, GIS, Remote Sensing, Sustainable Development, Landscape Metrics, Land Surface Temperature, Time Series Analysis

ABBREVIATIONS

ASTER	Advanced Spaceborne Thermal Emission and Reflection Radiometer
AVHRR	Advanced Very High Resolution Radiometer
AWMPFD	Area Weighted Mean Patch Fractal Dimension
AWMSI	Area Weighted Mean Shape Index
CA	Class Area
CA-Markov	Cell Automaton Markov
CBAs	Critical Biodiversity Areas
CBD	Central Business District
CoT	City of Tshwane
DN	Digital Number
ED	Edge Distance
EOS	Earth Observation System
ESAs	Ecological Support Areas
ETM+	Enhanced Thematic Mapper Plus
EVI	Enhanced Vegetation Index
FCC	False Colour Composite
GCRO	Gauteng City Region Observatory
GIS	Geographical Information Systems

KIA	Kappa Index of Agreement
LIDAR	Light Detection and Ranging
LST	Land Surface Temperature
LULC	Land Use Land Cover
MCE	Multi-Criteria Evaluation
SDG	Sustainable Development Goals
MLC	Maximum Likelihood Classification
MODIS	MODerate-resolution Imaging Spectroradiometer
MPAR	Mean Perimeter - Area Ratio
MPE	Mean Patch Edge
MPI	Mean Proximity Index
MPS	Mean Patch Size
MRT	MODIS Projection Tool
MSI	Mean Shape Index
MVC	Maximum Value Composite
NDVI	Normalized Difference Vegetation Index
NGI	National Geo-Spatial Information
NIMP	Number of Patches
NOAA	National Oceanic and Atmospheric Administration

OLI	Operational Land Imager
PRD	Patch Richness Density
PSCOV	Patch Size Coefficient of Variation
PSSD	Patch Size Standard Deviation
RDP	Reconstruction and Development Programme
SANSA	South Africa Space Agency
SHEI	Shannon’s Diversity Index
SPOT	Satellite Pour l'Observation de la Terre
SVM	Support Vector Machine
TE	Total Edge
TM	Thematic Mapper
TOR	Top of Atmosphere Reflectance
UHI	Urban Heat Islands
UN	United Nations
USGS	United State Geological Survey
UTM	Universal Transverse Mercator

ACKNOWLEDGEMENTS

Firstly, I would like to acknowledge Professor Fethi Ahmed for the tremendous work in supervising and guiding me in this study. I would also like to acknowledge the Tshwane University of Technology and National Research Foundation (NRF) for financing this study. I also would like to express my gratitude to the anonymous reviewers of the research papers for the contributions they have made.

I also would like to acknowledge Mr Mufaro Magidi, Mr John Mambambo, James Madzimure, Ms Cynthia Maringo, Mr Edward Kurwakumire and Mr Kerrison Munyorwi for the assistance rendered in editing and proofreading this report.

To my wife Talent and my daughter Jewel Ngaakudzweishe, I appreciate your patience during the years of this study.

DEDICATION

To the King of kings for his tender mercy which endures forever and ever.

I dedicate this to my wife Talent and daughter Jewel Ngaakudzweishe for the support and love. Also to my mother Mrs T. Magidi and late father Mr J.C. Magidi who sacrificed a lot for my education.

TABLE OF CONTENTS

LIST OF FIGURES

LIST OF TABLES

CHAPTER ONE

1 Quantifying, Monitoring and Modelling of urban spatial patterns in the CoT: towards a sustainable management of an urban environment.

1.1 Background

Urbanisation, urban sprawl and loss of biodiversity (decrease of natural habitats) in urban environments are the major phenomena of the 21st Century urban areas (Kamusoko and Aniya, 2007, Kamusoko and Aniya, 2009, Liu *et al.*, 2011, Shafizadeh Moghadam and Helbich, 2013). Urbanisation, is defined as the increase in urban population as a result of natural increase and migration (UNHABITAT, 2016). Urbanisation is one of the most powerful and recognisable anthropogenic and transformative force that has and is still leading to land cover changes in both developing and developed countries (UNHABITAT, 2016).

Currently, more than half of the world's population dwells in urban areas (United Nations, 2014). Urban growth in developing countries is due to the high natural population increase and migration whereas in developed countries it is mainly due to migration (UNHABITAT, 2016). Developed countries are more urbanised than the developing world (United Nations, 2014). North America, Latin America (including the Caribbean) and Europe's current urban population is sitting at 82%, 80% and 73% respectively (United Nations, 2014). Africa and Asia which constitute most of the developing countries have 40% and 48% respectively, of their respective population in urban areas (United Nations, 2014). The developing countries urbanise faster than the developed world and it is projected that by 2050 about 56% and 64% of the population will be urban dwellers in Africa and Asia respectively (United Nations, 2014).

Africa is projected that more than 1.3 billion people who will be living in urban areas in 2050 as compared to the current 0.35 billion urban dwellers (United Nations, 2014). Sub-Saharan Africa had about 27% of its population living in urban areas in 1990, 37% in 2014 and this is projected to increase to 56% in 2050 (United Nations, 2014). The average rate of increase per annum between 2010 and 2015 was 1.4% for Sub-

Saharan Africa, 0.3% for developed countries, 1.7% for the developing countries and 0.8% in South Africa (United Nations, 2014). In South Africa, 19 million (52%) people were living in urban areas by 1990, 34 million (64%) in 2014 and it was anticipated to increase to 49 million (77%) in 2050 (United Nations, 2014). Decentralisation policies have been taking centre stage in most of the developing cities (UNHABITAT, 2016). With an increase in urbanisation, one of the challenges that is affecting urban areas is the development of informal settlements (UNHABITAT, 2016). Development of informal settlements is continuing and there is need for policy formulation that can helps the sustainable growth of formal and informal settlements. This forms part of the Sustainable Development Goals (SDG) to ensure environmental sustainability (Griggs *et al.*, 2013, United Nations, 2015, Statistics South Africa, 2015, UNHABITAT, 2016). In Sub-Saharan Africa, more than 90% of urbanisation takes place in informal settlements and is mostly characterised by poverty, unemployment, environmental degradation and uncontrolled growth of informal settlements (Pieter and Mark, 2006, United Nations, 2015, UNHABITAT, 2016). Another challenge is the failure by the authorities to provide adequate infrastructure and basic services such as water and sanitation (UNHABITAT, 2016). An increase in the number of urban dwellers brings in a change in consumption and production patterns of urban dwellers which leads to an increase in carbon emissions thereby accelerating climate change (UNHABITAT, 2016).

1.2 Urban Growth in the Developing World (Problem Statement)

The biggest obstacle to development in developing countries is the rapid and the uncontrolled population growth (Pauchard *et al.*, 2006). This comes with its own socio-economic challenges such as poverty, power struggles and lack of basic needs such as food, clean water, shelter and basic health care which culminate in a negative impact on sustainable development (United Nations, 2015). Rapid and uncontrolled population growth has led to an accelerated increase in the formal and informal settlements (Pauchard *et al.*, 2006, Pieter and Mark, 2006). Most of the urban growth that will take place in the world in the next 15 years will be as a result of population growth (United Nations, 2014).

Transitions of governments in Africa, modernisation of agriculture, urbanisation and industrialisation are among the main drivers of land cover dynamics (Liu *et al.*, 2011). Urbanisation and urban growth lead to horizontal and vertical infrastructure developments thereby affecting land cover change (Misago *et al.*, 2010, Landau *et al.*, 2011). Third World cities are also vulnerable to the urbanisation, intensive urban growth, inner city decay, escalating pollution (water, land and air) and increase in environmental degradation (McGranahan *et al.*, 2009, Mubea *et al.*, 2011).

City of Tshwane in South Africa is not exempt from these challenges as it was affected by rapid population growth and economic developments (Pieter and Mark, 2006, Wang *et al.*, 2010, Ogra and Onatu, 2013, Chikowore and Willemse, 2017). In the CoT the population 1.770 330 in 1996, 2,142,322 in 2001 and 2,921,488 in 2011 (STATSSA, 2012) and is expected to increase by 1.7% in 2030 (United Nations, 2016). Urbanisation and uncontrolled urban growth are the main effects of urban-urban, rural-urban and international migration and natural population growth (Pieter and Mark, 2006, Wray, 2010, Chikowore and Willemse, 2017). People migrate to urban areas usually in search of economic prospects, escaping socio-political problems, better living conditions and employment opportunities (Wray, 2010, Ogra and Onatu, 2013).

Due to the apartheid laws (pass laws), mobility of none-white races into white communities was restricted however, the year 1994 saw the formulation of de-racialization policies which allowed everyone to move freely without a pass thereby encouraging rural-urban and urban-urban migration (Seekings, 2000, Pieter and Mark, 2006, McLennan *et al.*, 2016). On the other hand, socio-political and economic problems in neighbouring countries in the Southern African region and beyond for example Zimbabwe, Mozambique and Somalia also led to legal and illegal immigrants streaming into the South African cities (Misago *et al.*, 2010, Landau *et al.*, 2011).

The CoT as the political capital of South Africa is facing these migration challenges of resulting aggravated increases in the population of urban dwellers (Misago *et al.*, 2010, Landau *et al.*, 2011, Mubiwa and Annegarn, 2015). Consequently, there is a congestion of the city centre with businesses and residents relocating to the urban periphery (malls, residential areas, new business parks and informal settlements)

thereby putting more pressure on the available resources (McGranahan *et al.*, 2009, Misago *et al.*, 2010, Landau *et al.*, 2011).

The focus of sustainable development and issues relating to South Africa should be directed towards the urban environments and challenges caused by unprecedented urban growth (Grizans, 2009). With the challenges in urban areas raised above, there is an urgent need for fast decision-making and planning by the decision-makers to control the growth of urban areas and there is a need for up-to-date spatial and temporal information on various aspects such as cadastre, socio-economic and remotely sensed data (Mundia and Aniya, 2005). An analysis of these spatio-temporal change in urban dynamics will provide a better understanding of the spatio-temporal urban dynamics (Sudhira and Ramachandra, 2007).

1.3 Roles of GIS and Remote Sensing

Quantifying, monitoring and modelling spatial patterns, trends and characteristics of urban dynamics are necessary for the sustainable management of urban environments (Sudhira *et al.*, 2003a, Sudhira *et al.*, 2003b, Sudhira *et al.*, 2003c, Sudhira and Ramachandra, 2007, Araya and Cabral, 2010). These patterns and trends can be mapped, quantified and analysed using remote sensing, GIS techniques and spatial statistics (landscape metrics) (Sudhira *et al.*, 2003a, Sudhira *et al.*, 2003b, Sudhira *et al.*, 2003c, Sudhira and Ramachandra, 2007, Araya and Cabral, 2010). GIS and remote sensing have been proved to be powerful, cost-effective and efficient tools that are used in quantifying, monitoring and predicting land cover change using multi-temporal and multi-spectral spatial datasets (Sudhira *et al.*, 2003a, Sudhira *et al.*, 2003b, Sudhira *et al.*, 2003c, Sudhira and Ramachandra, 2007, Araya and Cabral, 2010). Remote sensing technology with its multi-temporal and multi-spectral observations allows for both short-term and long-term monitoring to assess, quantify and predict spatial growth (Taubenböck and Esch, 2011). GIS and remote sensing are the best tools that can be used to assess the spatio-temporal dynamics compared to the socio-economic indicators such as population growth (Maktav *et al.*, 2005). Advances in GIS, remote sensing and landscape ecology have made it easier for researchers and planners to map, quantify, monitor and predict urban growth (Araya

and Cabral, 2010, Subedi *et al.*, 2013, Deep and Saklani, 2014). This has contributed to the creation of detailed urban land cover maps that are aiding planners, researchers and ecologists to have a well-informed understanding of urban dynamics (Subedi *et al.*, 2013). There are numerous techniques and algorithms applied to quantify, assess, predict and characterise the urban processes, patterns and trends (Weng, 2007, Taubenböck and Esch, 2011, Abebe, 2013).

1.4 Rationale and Research Questions

Negative impacts of unprecedented urbanisation in the developing countries includes rapid urban growth (horizontal and vertical), traffic congestion, environmental degradation, pollution (air, water and land), the establishment of formal and informal settlements and other socio-economic problems (Dodman *et al.*, 2017). There are a number of legislations in the form of policies and strategies that have been developed by the international bodies and government that are aimed at improving lives of urban dwellers especially those in informal settlements (National Planning Commission, 2012). The South African government legislated a number of these policies that are aimed at improving the livelihoods in both formal and informal urban settlements (National Planning Commission, 2012). One of the policies and strategies is the National Development Plan (NDP), 2030 which is aimed at breaking apartheid spatial patterns in South Africa so that all races have equal access to affordable housing in a better and sustainable environment (National Planning Commission, 2012). The projects that are currently being implemented include the provision of government subsidised houses (Reconstruction and Development Programme (RDP)) and provision of basic services or amenities (Cameron, 1996). Both these interventions require access to reliable, up-to-date spatial information on location, quantity and growth of both formal and informal settlements. To contribute to the Sustainable Development Goals (SDGs), there is need for accurate spatial information on informal settlements to report on progress towards improvement of slum dwellers (Griggs *et al.*, 2013, United Nations, 2014, Statistics South Africa, 2015).

This purpose of this study was to address the problem of urban growth and its implications for the planning and sustainable management of urban areas. The

research provided necessary information for informed decision-making towards the sustainable management of the CoT. The techniques of quantifying, monitoring and predicting land cover changes were used in this study. This study used GIS and remote sensing techniques to measure, assess and predict urban land cover change in the CoT. It focused on characterising land cover types in the CoT using remotely sensed data to quantify, assess and predict land cover change between the years using both high and low-resolution satellite imagery. This study integrated the following: GIS, remote sensing, urban growth modelling techniques, landscape metrics, retrieve LST and vegetation phenology in monitoring urban dynamics. This will enable planners and ecologists to deal with undesired effects of urban land cover change and encourage sound urban planning and sustainable management of resources. It will help them to set management guidelines, which are important in conserving and managing the available resources.

Relevant research questions discussed in this study were:

1. How do spatial patterns evolve with time in the CoT?
2. Can the connectivity relationship of the new spatial patterns be studied using satellite imagery/landscape metrics?
3. Can spatial patterns (extent) in CoT be detected / mapped using information from medium and/high-resolution imagery?
4. What are the future scenarios of urban growth?
5. Is there any difference in the pattern of land cover change between the townships and newly developed suburbs?
6. What is the impact of urban sprawl in CBAs?
7. What would be the impact of urban growth on the environment for example vegetation, temperature?

1.5 Aims of the Study

The aim of this study was to assess the spatio-temporal urban patterns and trends in the CoT, South Africa using GIS and remote sensing techniques.

The objectives of the study were to:

1. Characterise land cover for the CoT using remote sensing between 1984 and 2015
2. Analyse land cover changes between two or more dates (Assessing changes [gains/losses] in each land cover class between two years (1984 and 2005) for example residential, informal settlements among others) at a short-term and long-term scale between 1984 and 2015.
3. Assess the degree and direction of urban dynamics in the CoT using remotely sensed data and landscape metrics between 1984 and 2015.
4. Use transitional probabilities to simulate future trends in land cover types and validate the methodology between 2013 and 2030.
5. Analyse the change in vegetation in the CoT.
6. Compare spatio-temporal variations of vegetation between different areas in the CoT from 2000 to 2015.
7. Assess the change in LST between 1984 and 2016.

1.6 Study Area

The study area is the CoT (Figure 1) popularly known as the City of Pretoria located in the North of the Gauteng Province which was founded in 1855 by Marthinus Pretorius as Pretoria and changed to Tshwane in 2000 (Raper, 2008, Van der Vyver, 2015). It merged with Metsweding District following the Gauteng Global City Region Strategy (Matlala, 2015). The city is the single-largest metropolitan municipality in the country with 7 regions, 105 wards and 210 councillors. CoT lies between latitudes 25^{o}6’34.60” S to 26^{o}4’41.12” S and longitudes 27^{o}53’24.26E to 29^{o}5’54.31” E. It has a landmass of 629 618 ha, 2 921 490 people and 911 536 households based on the 2011 Census (STATSSA, 2012). The population of the CoT was, 1770330 in 1996, 2142,322 in 2001 and 2,921,488 2011 (STATSSA, 2012).

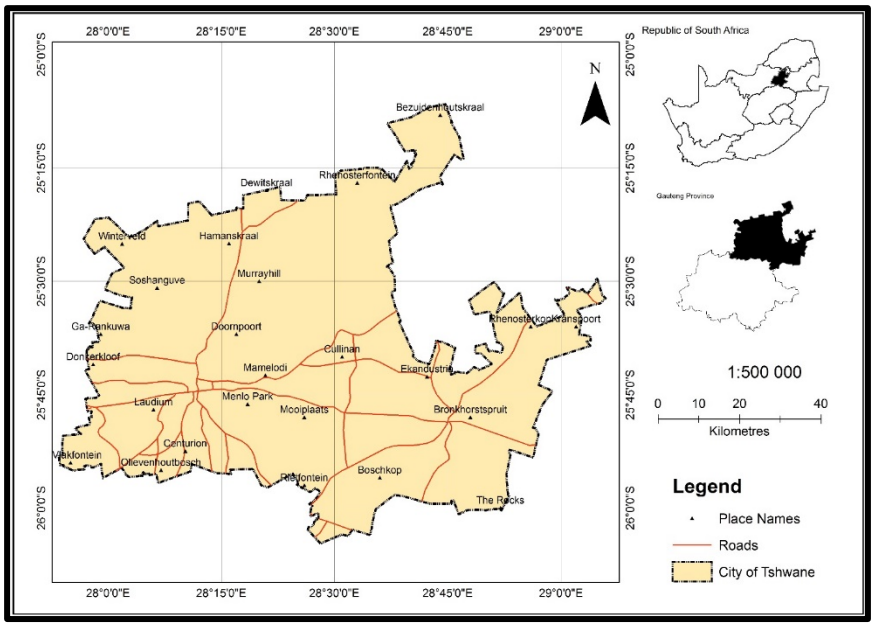

Figure 1: The location of the study area (Municipality of the CoT) which is situated in Gauteng Province, South Africa.

1.7 Conceptual Framework

To assess the spatio-temporal urban dynamics the conceptual framework in Figure 2 was followed. Land cover change analysis was done using both medium and high-resolution satellite imagery. Medium resolution imagery used were Landsat TM, ETM+ and OLI to assess long-term change in the CoT. Landsat imagery were used to predict future land cover scenario. High-resolution SPOT 5, 6 and 7 imagery was used for short-term change and to have a closer look at the changes (at a large scale) in urban areas and this focused on high, medium and low-density areas. This short-term assessment evaluated the impact of urban growth on CBAs. Thereafter, low-resolution satellite data (MODIS) was used to assess the temporal changes in vegetation in different parts of the study area. Lastly, the medium resolution satellite (Landsat TM and OLI) was used to retrieve LST and map urban heat islands. Changes in vegetation and LST were used as proxies for potential impacts of urbanisation.

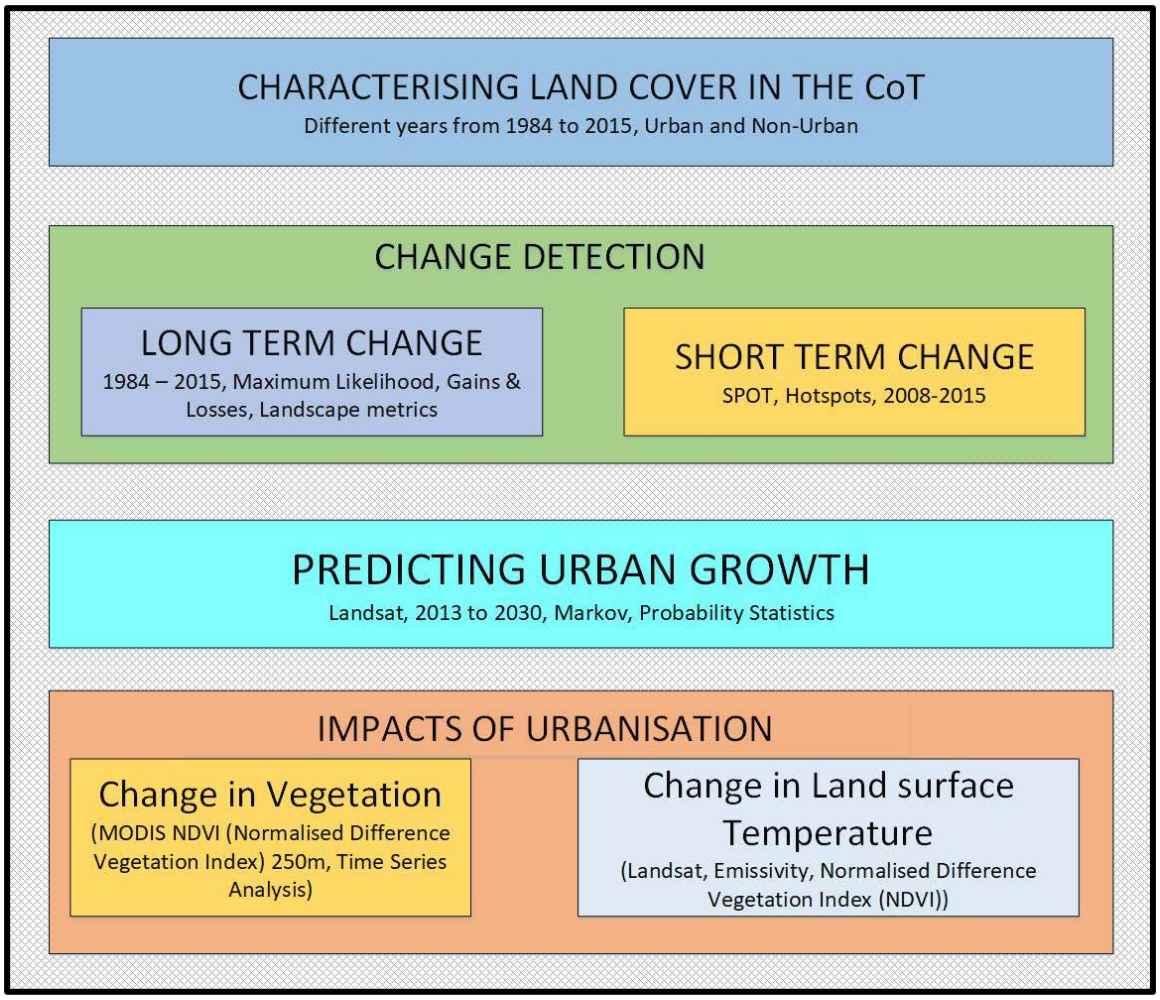

Figure 2: Conceptual Framework showing the approach in accomplishing the objectives of the study.

1.8 Structure of the Thesis

This thesis was written in paper format.

Chapter 1 provided an overview of spatial and temporal land cover changes because of rapid population growth. The chapter explored the population differences in the developed and developing countries. The problem statement, research rational and questions were articulated in this chapter. Aims and objectives of this study were also outlined in this chapter. Application of GIS and remote sensing techniques in assessing, quantifying and modelling urban land cover changes were also highlighted.

Chapter 2 reviewed literature on the application of GIS and remote sensing in urban dynamics. The chapter examined the different methods and datasets (remotely sensed data) used to quantify, monitor and model urban land cover changes.

Chapter 3 focused on assessing and quantifying land cover changes between 1984 and 2005 using Landsat TM, ETM+ and OLI satellite imagery. This chapter explained the methods used to classify the available satellite imagery of different dates. It also explored how urban sprawl was quantified using landscape metrics between the years. The spatial extent of urban areas, gains in urban growth were calculated in this chapter.

Chapter 4 explained how the CA-Markov algorithm, transitional probabilities and transitional areas were used to predict future urban changes. The chapter also included how the CA-Markov models were validated. It showed the capability of CA-Markov Model to predict land cover change in urban areas.

In Chapter 5, high-resolution imagery (SPOT 5 and SPOT 6) was used to quantify urban sprawl and a comparison between low-density, medium-density and high-density was performed. The chapter outlines the methods used to classify, quantify and assess changes in urban sprawl. In this chapter, areas that experienced a high degree of change in the low, medium and high-density were revealed. The impact of urban growth on the sensitive areas (CBAs) was examined in this chapter.

Chapter 6 dealt with the time series analysis of vegetation cover using MODIS NDVI of 250m spatial resolution and a 16-day temporal resolution. Time series analysis was run on different land cover types and the results of the time series analysis were explained in this chapter. The chapter showed the results of spatio-temporal analysis of vegetation cover in different land cover types.

Chapter 7 dealt with LST, which is an indicator of urban dynamics (growth). Landsat TM and Landsat OLI imagery of different years and seasons (winter and summer) were used in this chapter to retrieve LST and the normalised LST. In this chapter, urban heat islands and spatial variations in LST were mapped and results were outlined.

Chapter 8 gave a synthesis of the different methods and datasets that were used to assess, quantify and predict urban dynamics. It showed the results and the conclusions drawn in respect to the objectives used in this study. The effectiveness of the methods used in this study was explained in detail. The relevance and importance of the research in aiding decision-makers and researchers to make well-informed decisions in urban environments was also explained in detail.

CHAPTER TWO

2 THE QUANTIFICATION, ASSESSMENT AND MODELLING OF URBAN SPRAWL: A REVIEW *

2.1 Abstract

Urbanisation is an issue of major concern for decision-makers and resource managers as it is growing at an alarming rate due to migration and natural population increase. Urbanisation, which can be defined as the increase in the number of urban dwellers, has led to both controlled and uncontrolled urban growth. This has a negative impact on the surrounding environment. With the dynamism of urban environments, there is a need for continuous spatio-temporal monitoring, quantification and prediction of urban land cover change to aid decision-makers in the sustainable management of urban ecosystems. The introduction of GIS and remote sensing techniques has enabled researchers and planners to make informed decisions. The purpose of this paper is to review how GIS and remote sensing techniques are used to assess, quantify and predict change in urban land cover. Different techniques, algorithms and remotely sensed datasets were used in different studies to assess, monitor and predict urban dynamics. Other proxies such as LST and vegetation are also used to assess the impact of urban growth. There was a positive correlation between urban growth and LST but the extent of green spaces in urban areas reduces LST. There was an increase in urban areas, which in turn reduces the size of vegetation and agricultural areas. Urban modelling/prediction also revealed that there is an anticipated increase in urban areas. The result showed that for sustainable management of urban environment remote sensing and GIS techniques are the best tools in informing researchers and decision-makers.

---

* In preparation for submission in the South African Journal of Geomatics

Keywords: Urban Sprawl, Urban growth, Predictive Modelling, GIS, Remote Sensing, Sustainable Development, Landscape Metrics, Land Surface Temperature

2.2 Introduction

Urbanisation is a phenomenon of the 21st Century urban areas. Urbanisation in both developing and developed countries has led to unprecedented land cover change (Kong *et al.*, 2012, Shafizadeh Moghadam and Helbich, 2013). Cities in the developing countries are vulnerable to unprecedented urbanisation, intensive urban growth (formal and informal), inner city decay, increase in pollution and biodiversity loss (Shafizadeh Moghadam and Helbich, 2013). Urban growth also leads to traffic congestion, loss of agricultural areas, increase in LST, lack of parking space, pollution (water, air and land), informal settlements and other socio-economic problems.

One of the critical causes of urban dynamics is the change in political leadership especially in Africa where most of the countries were under the colonial leadership (Cohen, 2006). In South Africa, with the dawn of democracy in 1994 de-racialisation laws were enacted which allowed non-white races to move freely without any pass (Saff, 1994). In some African countries such as Zimbabwe (Mutambirwa and Potts, 1990), Zambia (Potts, 2005), Mozambique (Garenne, 2003) independence brought about change in urban management and it also encouraged urbanisation. This accelerated urban-urban, rural-urban and international migration as people are looking for economic prospects, (Chikowore and Willemse, 2017) and escaping socio-political problems (Weber and Puissant, 2003, Pieter and Mark, 2006). These factors triggered urban growth and depletion of non-urban areas such as natural vegetation, agricultural areas and many others.

The extent of urban expansion can be quantified using different indicators. One of the indicators is the size of impervious surfaces, which can be derived using remote sensing techniques (Sudhira *et al.*, 2003a). Quantifying, monitoring and predicting spatial patterns, trends and characteristics of urban dynamics are necessary for the sustainable management of urban environments (Kong *et al.*, 2012). Assessing change in urban environments implies the need to consider these two points into account: the extent and location of current and future changes (Herold *et al.*, 2003,

Kong *et al.*, 2012). GIS and remote sensing are powerful, cost-effective and efficient tools used to quantify, monitor and predict urban land cover change (Herold *et al.*, 2003, Deka *et al.*, 2011, Kong *et al.*, 2012, Noor and Rosni, 2013). GIS and Remote Sensing techniques are widely applied in assessing natural resources and monitoring spatio-temporal changes, thereby contributing to the creation of detailed urban land cover maps that are aiding planners, researchers and ecologists to have a better and well-informed understanding of urban dynamics (Herold *et al.*, 2003, Weber and Puissant, 2003, Kong *et al.*, 2012, Noor and Rosni, 2013). This paper intends to review prior literature in the application of GIS and remote sensing on assessing, quantifying and predicting urban growth.

2.3 Urban Sprawl

Urban sprawl can be referred to as a process of land development, a cause of land use behaviour, a result of land use behaviour or patterns of land use (Bhatta *et al.*, 2010). There are varying and debatable definitions of urban sprawl (Sudhira *et al.*, 2003b, Bhatta *et al.*, 2010, Taubenböck *et al.*, 2012). Urban sprawl can be defined as the unplanned, uncontrolled, uncoordinated and poorly planned encroachment of urban-like environments (housing, shopping centres, industry) into non-urban areas (open spaces watershed land, green spaces, agricultural land or rural areas) (Sudhira *et al.*, 2003b, Bhatta *et al.*, 2010, Noor and Rosni, 2013). Some scholars define urban sprawl as one of the dimensions of land use patterns where some urban characteristics (administration, business, settlements, industry) are decentralised from the urban core to the outskirts (Sudhira *et al.*, 2004). This outward expansion of urban areas has negative impacts on infrastructure and the sustainability of urban areas (UN-HABITAT, 2010). Spatial development of urban areas can be divided into three forms which are: low-density sprawl, ribbon sprawl, nucleated and leapfrog sprawl (Farooq and Ahmad, 2008). Low-density sprawl: is caused by outward spreading of low-density suburban land use and it leads to the high consumptive use of land for urban purposes (Torrens and Alberti, 2000). Ribbon Sprawl is when development follows major transport routes outward from the urban core and land that is close to these linear features become developed but a distance from the transport route is not developed (Torrens and Alberti, 2000, Farooq and Ahmad, 2008). Leapfrog sprawl is when the developments

are sporadic and they grow in an irregular pattern (Torrens and Alberti, 2000). It is a scattered form of urban growth which leads to disjointed urban land uses and interspersed undeveloped areas (Torrens and Alberti, 2000).

Urban sprawl is a major contributor to land cover change as it induces the increase in built-up (impervious surfaces) (Sudhira *et al.*, 2004, Araya and Cabral, 2010, Deep and Saklani, 2014). Urban land cover change has led to the loss of agricultural land and natural vegetation in both developing and developed countries including in South Africa (Araya and Cabral, 2010, Deep and Saklani, 2014). There are severe and unsustainable consequences due to uncoordinated urban development, which are lack of infrastructure (sewer, accommodation, roads and transport networks), increase in congestion, environmental pollution, loss of natural resources and sanitation challenges (Shafizadeh Moghadam and Helbich, 2013, Noor and Rosni, 2013). In addition, this has promoted increases in crime and some socio-economic problems (Shafizadeh Moghadam and Helbich, 2013, Noor and Rosni, 2013). Impervious surfaces which refer to the built-up areas (residential, commercial, industrial areas, pavements, tarred roads) is the main parameter that is used to quantify urban sprawl and can only be measured from physical surveys or remotely sensed data (Jat *et al.*, 2008).

2.3.1 Quantifying Urban Sprawl

There is a need to assess and quantify urban sprawl for sound land use management policies and strategies (Sudhira *et al.*, 2003a, Sudhira *et al.*, 2003b, Sudhira *et al.*, 2003c, Ji *et al.*, 2006). Quantifying urban land cover change and urban sprawl requires land cover change analysis and identification of proper change detection algorithms. The advent of GIS and remote sensing techniques has enabled researchers and resource managers to detect urban land cover change (Sudhira *et al.*, 2003a, Sudhira *et al.*, 2003b, Sudhira *et al.*, 2003c, Sudhira *et al.*, 2005, Sudhira and Ramachandra, 2007, Araya and Cabral, 2010).

Remote sensing imagery (ground-based, aerial and satellite-based) are mainly used to derive land cover classification maps, which are used in analysing land cover change (Jensen and Lulla, 1987, Sudhira *et al.*, 2003a, Sudhira *et al.*, 2003b, Sudhira *et al.*,

2003c, Sudhira *et al.*, 2005, Sudhira and Ramachandra, 2007, Araya and Cabral, 2010). Many satellite sensors were used to map land cover changes in urban areas, these include Landsat TM, ETM+ and OLI (Deka *et al.*, 2011, Vermeiren *et al.*, 2012, Ahmed and Ahmed, 2012, Abutaleb *et al.*, 2013, Aduah and Baffoe, 2013), Indian Remote Sensing (IRS) LISS-III (Jat *et al.*, 2008) SPOT 5 (Weber and Puissant, 2003, Kong *et al.*, 2012, Noor and Rosni, 2013), IKONOS (Herold *et al.*, 2003, Taubenböck *et al.*, 2006, Noor and Rosni, 2013). There are many pre-processing and processing techniques, used to extract useful information on remotely sensed data which will be used to analyse change (Jensen and Lulla, 1987). Multi-temporal (repetitive) observations of the earth surface allow for both short-term and long-term monitoring (Jensen and Lulla, 1987, Taubenböck and Esch, 2011). These techniques include: support vector machine (SVM) classifier, object-oriented classification (Taubenböck *et al.*, 2006, Araya and Cabral, 2010, Tewolde and Cabral, 2011, Noor and Rosni, 2013), unsupervised and supervised classification (maximum likelihood) (Weber and Puissant, 2003, Jat *et al.*, 2008, Deka *et al.*, 2011, Vermeiren *et al.*, 2012, Aduah and Baffoe, 2013), fuzzy method (Reveshty, 2011), fisher classifier (Ahmed and Ahmed, 2012) principal component and discriminant analyses (Jensen and Lulla, 1987).

There are numerous change detection techniques such as principal component analysis, image-rationing, image differencing, cross-tabulation, time series analysis, landscape metrics (Jensen and Lulla, 1987, Kong *et al.*, 2012), change vector analysis and post-classification (delta) comparison that have been applied in urban dynamics (Jensen and Lulla, 1987, Singh, 1989, Weber and Puissant, 2003, Taubenböck and Esch, 2011, Aduah and Baffoe, 2013, Abebe, 2013). These techniques are used to quantify and assess change between images of two or more dates and will be used to inform decisions (Abebe, 2013). Among these change detection techniques the most commonly used are the post-classification (delta) change detection methods, which includes cross-tabulation techniques and are the most intuitive and can analyse the amount, location and nature of change (Jensen and Lulla, 1987, Abebe, 2013).

2.3.2 Quantifying Urban Sprawl Landscape Metrics

Remote sensing lacks the capability to fully describe the underlying urban processes and patterns hence the need to augment the techniques with landscape metrics (Mcgarigal *et al.*, 2002, Abebe, 2013). Landscape metrics are algorithms used to quantitatively determine and fully describe the underlying spatio-temporal structures and patterns in any landscape and are important in informing decision-makers (Herold *et al.*, 2005, Aguilera *et al.*, 2011, Abebe, 2013). Determination of landscape dynamics using landscape metrics was mainly conducted in developed countries and little has been done for the developing urban environments in Africa (Abebe, 2013).

There are two types of landscape metrics: composition and configuration metrics (Gustafson, 1998). Composition metrics are indices that are related to the presence, proportion, variety, the richness of patch type without considering the spatial character of patches (Gustafson, 1998). The commonly used composition metrics are Shannon's Diversity Index (SHEI) (Aithal and Ramachandra, 2013) and patch richness density (PRD) (Gustafson, 1998). Shannon's entropy reflects the degree of spatial concentration and dispersion of spatial variable and can be used to quantify and differentiate types of sprawl (Araya and Cabral, 2010). Entropy value varies from 0 to 1 and if the distribution is maximally concentrated in one region, the lowest entropy value (0) is obtained, while an evenly dispersed distribution across space gives a value of 1 which is the maximum (Deka *et al.*, 2011, Aduah and Baffoe, 2013). The Shannon's entropy and landscape metrics (patchiness and map density) have been computed in terms of the spatial phenomenon, in order to quantify the urban form (impervious area) (Jat *et al.*, 2008).

Configuration metrics refer to the spatial arrangement, character, orientation and position of patches in the landscape (McGarigal and Marks, 1995, Mcgarigal *et al.*, 2002). Class Area (CA) index measures in acres/hectare/m^2/km^2, the total area of built-up areas and non-built-up areas in the landscape (Araya and Cabral, 2010). Area Weighted Mean Patch Fractal Dimension (AWMPFD) of a patch equals two times the logarithm of patch area (m^2), while the perimeter is adjusted to correct for its raster bias. Number of Patches (NUMP) quantifies the number of built-up and non-built-up patches (Jat *et al.*, 2008, Araya and Cabral, 2010, Ahmed and Ahmed, 2012). There are many indices such as Edge Distance (ED), Mean Patch Size (MPS), Mean

Proximity Index (MPI), Mean Shape Index (MSI), Patch Size Coefficient of Variation (PSCOV), Patch Size Standard Deviation (PSSD), that are used to monitor change in urban sprawl (Sudhira *et al.*, 2004, Abebe, 2013).

2.3.3 Urban Prediction (Modelling)

Urban Prediction (Modelling) is a way of evaluating future urban land cover transitions and establishing relationships with driving forces of urban change (Herold *et al.*, 2001, Sudhira *et al.*, 2003a). This can help urban planners in designing spatial decision support systems that can be used to evaluate alternative management scenarios and to formulate land use policies that are effective in the sustainable management of urban areas (Sudhira *et al.*, 2003a, Wray and Cheruiyot, 2015). There are a number of modelling algorithms which are developed for different applications and they differ in their levels of complexity (Subedi *et al.*, 2013, Wray and Cheruiyot, 2015). Three main types of prediction models are logistic regression, cell automaton and multi-agents (Sudhira *et al.*, 2003b, Shoko and Smit, 2013, Abebe, 2013). These models can either be stochastic or process-based (Abebe, 2013). Stochastic based models include the Markov, logistic regression and Cell Automaton while the process-based model is the dynamic ecosystem model (Fu *et al.*, 2010, Rossetti *et al.*, 2013, Abebe, 2013).

There are many predictive models used to map future urban scenarios, which are applied in different fields. There are agent-based models, multi-agent simulation, expert models, cell automata (CA) and logical regression (Vermeiren *et al.*, 2012, Abebe, 2013, Shoko and Smit, 2013, Shoko and Smit, 2014, Wray and Cheruiyot, 2015). The mainly used predictive models are the CA, Markov and the combination of the CA and Markov Chain (CA-Markov) (Reveshty, 2011, Ahmed and Ahmed, 2012). The integration of Markov, logistic regression and cellular automaton algorithms gives CA-Markov a competitive and phenomenal modelling advantage over other prediction models (Kamusoko *et al.*, 2009). Hence the CA-Markov is rated the most powerful model in simulating future land cover scenarios (Kamusoko *et al.*, 2009) and it is widely utilised to predict future land cover changes (Subedi *et al.*, 2013). The model is an improvement to the performance of standard logistic regression model in predicting

urban areas (Araya and Cabral, 2010, Vermeiren *et al.*, 2012, Deep and Saklani, 2014). CA models do not interact with main elements that drive the infringement of urban-like environment into none urban environments such as population, city centre and transport networks (Araya and Cabral, 2010, Vermeiren *et al.*, 2012, Deep and Saklani, 2014). These models can as well represent complex systems with spatio-temporal characteristics and they enable understanding of urbanisation phenomenon and explore the 'if' scenarios (Araya and Cabral, 2010, Vermeiren *et al.*, 2012, Deep and Saklani, 2014).

Another modified CA model which is used to simulate urban sprawl is the SLUETH (Herold *et al.*, 2003, Jantz *et al.*, 2004, Xian and Crane, 2005, Oguz *et al.*, 2007). The model was used to predict urban growth using historical data to calibrate the model. It incorporates slope, land cover, exclusion layer (where growth cannot occur), urban, transportation and relief layers in the simulation (Herold *et al.*, 2003, Jantz *et al.*, 2004, Xian and Crane, 2005, Oguz *et al.*, 2007).

Agent-based modelling (ABM) is another prediction model that is made up of several interaction agents within a simulated environment (Sudhira *et al.*, 2005, Rui and Ban, 2010, Shoko and Smit, 2013, Shoko and Smit, 2014). These agents might represent entities in the real world for example buildings, people, land parcels (Rui and Ban, 2010). These agents are active in land cover simulations and rules derived from observation, knowledge-based approaches and data analysis are set for these agents which affect the behaviour and relationships of these agents (Rui and Ban, 2010). ABM has developed into multi-agent simulation where there are complex interactions between agents and the environment which are simulated (Rui and Ban, 2010).

After prediction, there is a need to validate the prediction model using an algorithm(s) that compare the predicted map with a reference map (usually classified images) (Araya and Cabral, 2010, Tewolde and Cabral, 2011). Validation algorithms evaluate the predictive power of the model (Araya and Cabral, 2010, Tewolde and Cabral, 2011). It measures how well the model represents the characteristics of the real world and is expressed in terms of quantity of cell in each class ($K_{quantity}$) and location of cells of each category ($K_{location}$), (Deepa and Ramachandra, 1999, Araya and Cabral, 2010,

Tewolde and Cabral, 2011, Eastman, 2015). Validation gives the traditional Kappa Index of Agreement (KIA) ($K_{standard}$) and some Kappa variations such as K_{no}, $K_{location}$ and $K_{quantity}$ and they are an indication of how well the simulated map agrees with the reference (Deepa and Ramachandra, 1999, Tewolde and Cabral, 2011, Eastman, 2015). K_{no} shows the proportion classified correctly relative to the expected proportion classified correctly by a simulation (Deepa and Ramachandra, 1999, Araya and Cabral, 2010, Eastman, 2015). $K_{location}$ is the success due to a simulation's ability to indicate location divided by the maximum possible success due to a simulation's ability to specify location perfectly (Deepa and Ramachandra, 1999, Araya and Cabral, 2010, Eastman, 2015). $K_{quantity}$ is a measure of validation of the simulations to predict quantity accurately (Deepa and Ramachandra, 1999, Araya and Cabral, 2010, Tewolde and Cabral, 2011, Eastman, 2015).

In Pudong, Shanghai City land cover change analysis and predictions were done using the CA-Markov models (Xie *et al.*, 2007). Land cover change predictions were run using the remotely sensed data for 2012 and 2018 and it proved that CA-Markov Model is useful in predicting future land cover change scenarios in both quantity and space (Xie *et al.*, 2007). The same model was also run in Tripoli, Libya and land cover maps of 2020 and 2015 were predicted and mapped and the accuracy of the projected images was 85% (Al-sharif and Pradhan, 2014). There was a predicted increase in urban areas due to a decrease in agricultural land (Al-sharif and Pradhan, 2014). In Setubal and Sesimbra, Portugal urban land cover change was modelled and examined using CA-Markov and landscape metrics and the kappa index was 87% and 83%, for location and quantity respectively (Araya and Cabral, 2010). CA-Markov coupled with multi-criteria evaluation (MCE) was used to map future land cover scenarios in Mashdad City (Tajbakhsh *et al.*, 2016). There was a predicted increase in urban areas and the Kappa index was 91.89% and 95.29% for quantity and location respectively (Tajbakhsh *et al.*, 2016). CA-Markov used to predict land cover change in many urban areas including Arak in Iran (Nadoushan *et al.*, 2015), Isfahan in Iran, Butwa in Nepal (Mandal, 2014) and many other urban environments.

2.4 Change in Urban Vegetation

Urban vegetation is important in the sustainable management of urban ecosystems. There are changes in vegetation cover in urban environments due to the effects of urbanisation (Jin *et al.*, 2018). Establishment of residential, industrial and commercial areas has negatively affected the environments as natural vegetation is cleared (Grobler *et al.*, 2006). Vegetation cover has been exposed to urban transformation and has negatively affected the sustainability of urban ecosystems (Jin *et al.*, 2018). In urban areas the local authorities, land developers and residents plant their own trees and grass (lawn, stadiums), thereby establishing their own urban ecosystems (Walters, 2013, Wood, 2014). There are well-managed and well-maintained open areas like nature reserves, stadiums and some riparian areas. As urban areas develops its leads to habitat fragmentation (Grobler *et al.*, 2006). Nature reserves, riparian areas and parks in the CoT are among the places with high-density of natural vegetation; some of the areas and the un-conserved areas suffered from massive deforestation for firewood and for clearing housing space (Chishaleshale *et al.*, 2015). Some of the natural areas still maintain thick bushes as compared to the natural areas in close proximity of residential areas especially the informal ones where the source of energy is firewood (Grobler *et al.*, 2006, NPC, 2011).

To measure vegetation cover there are transformational indices that can be used, the most popular being Normalised Difference Vegetation Index (NDVI). NDVI is a slope-based vegetation index, derived from the reflectance values of near-infrared and red portions of the electromagnetic spectrum (Tucker, 1979, Eckert *et al.*, 2015). NDVI is used to quantify photosynthetic capacity, moisture stress and vegetation productivity (Tucker, 1979, Eckert *et al.*, 2015). Chlorophyll, which is the primary photosynthetic pigment in the plant absorbs visible light (0.4-0.7µm) bands but reflects infrared light (0.7-1.1 µm) wavelengths (Tucker, 1979). Vegetated areas reflect more infrared and absorb more red but poor vegetation in arid areas and the dry season does not absorb more red as compared to green vegetation and there is a low reflection of infrared energy (Eckert *et al.*, 2015). NDVI values range from -1 to +1 with 0 standing for no vegetation, less than 0 is non-vegetated surfaces for example. water glaciers and above zero (0) represents vegetated areas (Eckert *et al.*, 2015).

Vegetation change in urban areas can be used as a proxy for urban growth. So this study assessed the spatio-temporal variation in urban vegetation using NDVI derived from satellite imagery.

2.5 Critical Biodiversity Areas (CBAs)

One of the important concepts is that of sensitive areas, known as Critical Biodiversity Areas (CBAs) and Ecological Support Areas (ESAs) (Pence, 2008, Pence, 2014, GRARD, 2014). These are terrestrial and aquatic areas that need protection from transformation by human beings because of their landscape, fauna, flora or historical significance (Carroll, 1992). These areas must be protected in order to meet the biodiversity targets as determined by the systematic conservation planning (Maree and Vromans, 2010, Pence, 2014, GRARD, 2014). Systematic conservation planning is critical in identifying areas where unique biodiversity needs to be conserved in order to reduce the global loss of biodiversity (Ralston *et al.*, 2009). There are ESAs, which are also earmarked to safeguard the CBAs for example. if a river is classified as a CBA, there is a need to set a buffer surrounding it to prohibit any form of activity close to it to avoid siltation, pollution among other effects. (Ralston *et al.*, 2009, Maree and Vromans, 2010, Pence, 2014, GRARD, 2014). Areas classified as CBAs and ESAs are regarded as highly sensitive areas, which are *"no-go"* areas for any development. They are used as biodiversity informants that are used to support land use planning and decision-making areas (Ralston *et al.*, 2009, Maree and Vromans, 2010, Pence, 2014, GRARD, 2014).

2.6 Urban Thermal Features

Transformation of landscapes into urban environments has led to replacement of natural vegetation and agricultural areas by impervious surfaces (roads, pavements and buildings) and has also led to high concentration of pollutants in the urban areas as a result of release of gases from industries and cars (Abutaleb *et al.*, 2014, Peres *et al.*, 2018). Urban growths have negative impacts on the quality of the environments, which include air quality and temperature (Abutaleb *et al.*, 2014). There will be an increase in temperature in urban areas as a result of impervious surface and high concentration of pollutants leading to the establishment of urban heat islands (UHI)

(Yang *et al.*, 2016). UHI can be defined as a microclimate where the temperature of the urban area is higher than that of the surrounding areas (Ngie *et al.*, 2014, Abutaleb *et al.*, 2014, Yang *et al.*, 2016). It is a result of anthropogenic activities such as construction of impervious surfaces which influence the increase in temperature in the areas and these cause an increase in precipitation, increase in energy (Huang *et al.*, 2008), affect the quality of air and rise in global warming (Ngie *et al.*, 2014, Peres *et al.*, 2018). These effects can be detrimental to the human health which will in turn increase mortality (Ngie *et al.*, 2014). UHI thermal profiles are used to graphically illustrate spatial variations of temperature in the urban environment and its surroundings (Peres *et al.*, 2018). Typical thermal curves of UHI variations will show cliffs, peaks, depression and plateau will reveal the thermal variations (Huang *et al.*, 2008, Abebe, 2013, Abutaleb *et al.*, 2014). Anthropogenic activities cause changes in the surface (from natural to impervious) which affect the albedo, thermal capacity, heat conductivity (Ngie *et al.*, 2014, Abutaleb *et al.*, 2014, Peres *et al.*, 2018). An urban area with green vegetation suffers less from UHI than a non-vegetated urban area (Tomlinson *et al.*, 2012) hence the use of vegetation indices such as Normalised Difference Vegetation Indices in retrieving LST in satellite imagery (Qin *et al.*, 2001, Peres *et al.*, 2018).

Many methods were employed to measure, quantify and assess UHI. These include ground-based measurements using thermometers (Ngie *et al.*, 2014, Abutaleb *et al.*, 2014). For proper spatial mapping, GIS and remote sensing technology have provided a new avenue of studying and retrieving LST (Rhinane *et al.*, 2012). Thermal remote sensing coupled with micrometeorology has helped scientists in studying UHI (Rhinane *et al.*, 2012, Abutaleb *et al.*, 2014). Measuring of surface or air temperatures can be used in mapping UHI, (Rhinane *et al.*, 2012). Usually, the nature of surface affects the surrounding air, with vegetated environments having lower temperature as compared impervious surfaces (urban built-up areas) which contribute to higher air temperatures (Peres *et al.*, 2018). Satellite remote sensing is used in measuring UHI to overcome the limitations of manual recording of (Yue *et al.*, 2007) meteorological information (Yue et al., 2007, Rhinane et al., 2012). Remote sensing have proved to be the most powerful tool in assessing the spatio-temporal variation in UHI in relation to the change in land cover using surface radiance and emissivity (Sobrino *et al.*, 2004). There are

many methods that can be used to retrieve LST and these are the radiative transfer methods, split-window (Kerr *et al.*, 1992), mono-window (Qin *et al.*, 2001) and the algorithm by Jimenez-Munoz and Sobrino (Sobrino *et al.*, 2004). The mono-window and the algorithm by Jimenez-Munoz and Sobrino are put to use when there is no need for ground verification whereas the radiative methods need an in situ atmospheric profile that operates at the same time with satellite pass (Qin *et al.*, 2001). The temperature at the sensor is slightly lower than the temperature measured at meteorological stations (ground level). There is a need to use ground emissivity and atmospheric corrections to accurately quantify LST (Qin *et al.*, 2001, Sobrino *et al.*, 2004). Vegetation cover and soil background influence the emissivity and the vegetation vigour can be estimated NDVI hence the use of NDVI in calculating emissivity (Qin *et al.*, 2001, Sobrino *et al.*, 2004). Many studies have used the thermal band in the Landsat TM and Landsat OLI as well as ASTER Images to calculate LST. Different sensors have been used to assess and quantify UHI and these are NOAA, MODIS, AVHRR, Landsat TM (MA *et al.*, 2008, Kumar and Shekhar, 2015, Sheng *et al.*, 2017), Landsat ETM+ (Yue *et al.*, 2007, Mallick *et al.*, 2008), Landsat OLI, ASTER, SPOT, IKONOS and other sensors with thermal band/s on board (Abutaleb *et al.*, 2014). In Africa UHI studies using remote sensing were done in Cairo in Egypt (Abutaleb *et al.*, 2014), Durban in South Africa (Ngie *et al.*, 2016). and Johannesburg in South Africa (Hardy and Nel, 2015).

2.7 Urban Dynamics in South Africa

Object-oriented and pixel-based image classification were used to classify some land cover in some urban environments of South Africa (Kleyn *et al.*, Schoeman *et al.*, 2014, Otunga *et al.*, 2014). In Port Elizabeth (now Nelson Mandela Bay Metropolitan) remote sensing was used to monitor major land cover changes using delta change detection techniques between 1990 and 2009 (Odindi and Mhangara, 2011, Odindi *et al.*, 2012). Urban growth was attributed to pre-1994 legislations and other post-democracy policies on the provision of infrastructure (Odindi *et al.*, 2012). In Gauteng Province, Landsat images were used to quantify urban sprawl between 1991 and 2009 using post-classification change detection (Mubiwa and Annegarn, 2015). Object-oriented images classification was performed on SPOT 5 imagery in the City of Rustenburg and

change detection techniques were used to monitor urban growth between 2007 and 2012 (Mudau *et al.*, 2014). In Stellenbosch, South Africa, the global and local Moran Index was used to identify urban sprawl hot and cold spots (Musakwa and Van Niekerk, 2014).

Using urban prediction models to predict future scenarios in urban growth is now key in monitoring and managing urban areas (Wray and Cheruiyot, 2015). The multi-criteria analysis was used in the City of Potchefstroom to predict urban growth for the year 2030 (Cilliers, 2010). Agent-Based Models were used to predict the growth of slum communities in the City of Cape Town (Shoko and Smit, 2014, Wray and Cheruiyot, 2015). Another variation of the CA model called the Dyna-Clue cellular automata was used to predict change in the City of Johannesburg using two different scenarios (Le Roux, 2012). CA was applied in predicting land cover change in the city of Johannesburg by Abutaleb *et al.* (2013). In eThekwini Municipality the Land Change modeller and Markov chain analysis was used to predict land cover change (Otunga *et al.*, 2014).

CoT Municipality like any other African city has been affected by urban growth and reduction in the non-urban environment due to migration and natural population increase (Wray, 2010). Some urban areas that were transformed in South Africa include Port Elizabeth (Odindi and Mhangara, 2011, Odindi *et al.*, 2012, Odindi and Mhangara, 2012), Rustenburg (Mudau *et al.*, 2014) Gauteng Province (Mubiwa and Annegarn, 2015), EThekwini (Otunga *et al.*, 2014). In Africa Nairobi, Kenya (Mubea *et al.*, 2011), Cape Town (Shoko and Smit, 2013), Tripoli, Libya (Alsharif and Pradhan, 2014, Al-sharif and Pradhan, 2014) and Kampala Uganda (Abebe, 2013) were also transformed. The CoT as the provincial capital there is need to assess impact of migration in the city.

2.8 Conclusions

Urban sprawl is an ongoing process hence the need for informed and sound management guidelines to manage the ever-increasing urban areas. Urban sprawl quantification and modelling gives policy-makers important information that is relevant in urban planning, management and prediction of future development. Changes in

urban growth augmented by proxies of urban growth such as a change in vegetation, impact on CBAs and change in LST. Gaining knowledge of urban growth and prediction will help in creating management guidelines. There is need to test how change in urbanisation in the CoT has affected growth in urban areas, change in vegetation cover and change in LST. With urban growth, there is a need to monitor if there are some variations in urban growth between low-density, medium-density and high-density area to establish areas that have a high degree of urban change. There is also a need to quantify the encroachment of urban areas into CBAs.

There are many methods, that are used to extract information from remote sensing imagery and of these methods, the supervised maximum likelihood classifier has been commonly used in most of the urban studies. Studies have also utilised different change detection techniques and there are many varieties with the post-classification change detection methods being the most popular of them all. These are used to quantify and assess urban growth. In this study landscape, metrics were identified as the best post-classification change detection techniques to assess and quantify urban growth. There is a need to model the future land cover in the study area. There are numerous prediction models that were used in urban studies and CA-Markov has proved to the most suitable algorithm used to predict urban land cover change. There is need to consider some proxies such as LST and vegetation, which show the impact of urban growth on these proxies. Land Surface Temperature (LST) is high in impervious surfaces (urban) and bare soils as compared to vegetated areas. Therefore, as urban areas increase, there is a hypothesis that LST will also increase and vegetation cover reduces. Urban dynamics are complex as there is vegetation growth within urban areas due to tree to planting. With the increase in population in the CoT there is need to assess the impact of urban growth on temperature and on vegetation cover. There are CBAs, which are areas that earmarked for conservation. They form part of the spatial development framework and are used as biodiversity informants, which are by land use advisors to help in environmental impact assessments. There is also to assess to the impact of urban growth on these CBAs in the CoT.

To achieve this GIS and remote sensing technology were used to identify areas of urban change. Advances in the technologies and algorithms are contributing immensely to the provision of accurate and detailed land cover maps, which are of importance to decision-makers. There are many successes in using remote sensing to quantify and predict land cover change in urban areas.

CHAPTER THREE

3 AN ASSESSMENT OF URBAN SPRAWL USING REMOTE SENSING AND LANDSCAPE METRICS: A CASE STUDY OF COT, SOUTH AFRICA.*[*]

3.1 Abstract

Urbanisation is a phenomenon that is of major concern in both developing and developed countries. Uncontrolled urbanisation leads to formal and informal settlements, industrialisation, improvement of transport networks and economic growth. Monitoring, quantifying and mapping urban sprawl as well as establishing the contributors of land cover change are crucial in designing strategies and policies for effective and sustainable land use management. This study determines the spatio-temporal characteristics of urban sprawl in the CoT from 1984 to 2015 using Landsat satellite imagery. Supervised maximum likelihood classification mapped the land cover for the CoT from 1984 to 2015 using archival Landsat TM, ETM+ and OLI datasets. Post-classification change detection techniques coupled with landscape metrics helped to assess and quantify trends and patterns of urban sprawl. Change detection and analysis revealed that over the 31 years of study between 1984 and 2015 there was an increase in built-up areas in the CoT by 109% between 1984 and 2015. Landscape metrics also confirmed the increase in built-up areas in the CoT.

Keywords: Built-Up Areas, GIS, Remote sensing, Landscape Metrics, Urban Sprawl, CoT

---

[*] Submitted to the Egyptian Journal of Remote Sensing and is currently under review.

3.2 Introduction

Urbanisation is a global phenomenon that has led to significant land cover change in both urban and rural areas. Urbanisation is a socio-economic worldwide phenomenon, which is increasing at an alarming rate (Ji *et al.*, 2006, Chikowore and Willemse, 2017). Urbanisation is basically the increase in urban dwellers mainly as a result of natural population increase and migration (rural-urban, urban-urban or international) of people into the city in search of employment, specialised services and better living conditions (Ji *et al.*, 2006, Chikowore and Willemse, 2017). Cities in the developing countries are also susceptible to urbanisation, controlled and uncontrolled urban growth, inner city decay, increase in pollution and traffic congestion (McGranahan *et al.*, 2009, Mubea *et al.*, 2011, Lee and Chang, 2011, Kityuttachai *et al.*, 2013). Urbanisation leads to irreversible land transformation, which has an impact on the landscapes leading to urban sprawl, urban morphology and loss of biodiversity (decrease of natural habitats) (Sudhira *et al.*, 2003a, Kamusoko and Aniya, 2007, Kamusoko and Aniya, 2009, Liu *et al.*, 2011, Shafizadeh Moghadam and Helbich, 2013, Abebe, 2013). Numerous studies on urban sprawl were carried out in both developed and developing countries and there is a clear indication that urbanisation and urban sprawl are increasing exponentially (Sudhira *et al.*, 2003b).

South African cities were also affected by urbanisation and its challenges, which has led to formal and informal urban growth (Mubiwa and Annegarn, 2015). The CoT as an economic hub experienced urbanisation, due to the migration of people to the political capital for better living conditions, education and employment (Pieter and Mark, 2006, Chikowore and Willemse, 2017). City of Tshwane is struggling to cope with the demand of housing and additional infrastructure and services. In the CoT, there are four major universities (The University of Pretoria, The University of South Africa, Tshwane University of Technology and Sefako Makgato Health Life University),which are also accelerating urban growth as they have established educational and accommodation facilities for their students. There is high demand for housing which has led to the emergence of informal settlements, backyard houses and increase in formal housing from both government and private sector (Lemanski, 2009, Turok and Borel-Saladin, 2016, Le Roux and Augustijn, 2017).

Monitoring urban sprawl is a method of studying the temporal differences in an area by observing it remotely at different times (Jensen and Cowen, 1999, Jensen and Im, 2007). Remote observation of urban areas is now a major application of GIS and remote sensing (Jensen and Cowen, 1999, Jensen and Im, 2007). GIS and remote sensing techniques provide a decision support system that enables researchers, urban planners and resource managers to have a historical perspective of the earth, detect and quantify urban land cover changes which will inform their decision-making process (Sudhira *et al.*, 2003a, Sudhira *et al.*, 2003b, Sudhira *et al.*, 2003c, Sudhira *et al.*, 2005, Sudhira and Ramachandra, 2007). GIS and remote sensing have proved to be reliable and cost-effective tools that can be used to assess these spatio-temporal land cover changes compared to the socio-economic indicators such as population growth because of its synoptic view, multi-temporal (repetitive) observations, real-time acquisition and multi-spectral characteristics (Maktav *et al.*, 2005, Hegazy and Kaloop, 2015).

Quantification of urban sprawl can be done landscape metrics and there are two main types of landscape metrics which are composition and configuration metrics (Gustafson, 1998, Herold *et al.*, 2005). Landscape metrics used in the research include CA, NUMP, TE, MPE, ED, PSSD, MSI, AWMPD, MPAR and AWMSI. CA is the size of the urban area in a given year, which was expected to continually increase due to of urbanisation (Mcgarigal *et al.*, 2002, McGarigal *et al.*, 2009). NUMP is the number of isolated or discrete urban patches in the urban area (Mcgarigal *et al.*, 2002, McGarigal *et al.*, 2009).

Number of Patches (NUMP) value is expected to increase in the case of nucleated urban development and to be low if the urban patches merge into a homogeneous patch (Seto and Fragkias, 2005, McGarigal *et al.*, 2009). Total Edge (TE) is a measure of the total perimeter of all the urban patches (Seto and Fragkias, 2005). Mean Patch Edge (MPE) is the average amount of edge per patch (McGarigal *et al.*, 2009).

To measure the relative size of urban patches four indices were used and these are mean patch size (MPS), Edge Density (ED), Patch Size Standard Deviation (PSSD) and Patch Size Coefficient of Variation (PSCOV) (Seto and Fragkias, 2005). MPS is a

function of number patches and size of the total size of the area covered by the urban patches (Luck and Wu, 2002, Kowe *et al.*, 2015). It measures shape complexity and MSI is greater 1 except for circular and grid patches. The value can increase or decrease with time (Seto and Fragkias, 2005). Edge density was calculated to quantify the total edge relative to the total size of the urban area (Kowe *et al.*, 2015). This value of ED increase in a nucleated urban area and decrease when urban patches merge into homogenous patches (Seto and Fragkias, 2005, Kowe *et al.*, 2015). Patch Size Standard Deviation (PSSD) – is determines the standard deviation of patch areas in hectares, it calculates the spread of the patch size. Patch Size Coefficient of Variation (PSCOV) is a measure that shows the standardised spread of the sizes of the urban patch (Seto and Fragkias, 2005, Vaz, 2014). This measures the coefficient of variation (CoV) of urban patch sizes (Seto and Fragkias, 2005, Vaz, 2014). To measure the complexity or irregularity of the shape of urban areas was measured using the Area Weighted Mean Patch Fractal Dimension (AWMPFD), Mean shape index (MSI), Mean Perimeter – Area Ratio (MPAR). Area Weighted Mean Patch Fractal Dimension (AWMPFD)- shows the degree of complexity of the shapes of urban patches (Pili *et al.*, 2017). The more the complexity (irregularity) of the urban patch the more the AWMPD value (Seto and Fragkias, 2005). The value ranges between 1 and 2, the value closer to 1 is for regular shapes and closer to 2 is for highly irregular shapes (Seto and Fragkias, 2005).

There is a hypothesis that this metric will increase with nucleated urban patches but as the patches merge the urban area more and more regular (Seto and Fragkias, 2005). Mean shape index (MSI) measures shape complexity and MSI is greater than 1 except for circular and grid patches. It deals with the geometric complexity of an urban patch (Vaz *et al.*, 2017). This landscape metrics measures the ratio between the size of the edge of an urban patch and the perimeter of the simplest urban patch in the same urban landscape. Area-Weighted Mean Shape Index (AWMSI) the value of AWMSI is higher for urban patches with a complex and irregular in shape. Mean Perimeter – Area Ratio (MPAR) measures shape complexity of the urban (metres/ha) (Yu and Ng, 2007, Pili *et al.*, 2017). To assess the isolation of urban patched the Mean Proximity Index (MPI) was calculated. This determines the degree of isolation and fragmentation of patches.

The aim of this study was to assess and quantify spatial patterns of urban sprawl in the CoT using remote sensing and landscape metrics between 1984 and 2015.

3.3 Study Area

City of Tshwane (CoT) (Figure 3) is the administrative capital of the Republic of South Africa and located in the North of the Gauteng Province. The city was founded in 1855 by Marthinus Pretorius and renamed to Tshwane in 2000 (Raper, 2008, Van der Vyver, 2015). It merged with Metsweding District following the Gauteng Global City Region Strategy (Matlala, 2015). COT has 7 regions, 105 wards and 210 councillors and is the single largest municipality. CoT lies between latitudes 25°6’34.60” S to 26°4’41.12” S and longitudes 27°53’24.26E to 29°5’54.31” E. The city landmass of 629 618 ha, 2 921 490 people and 911 536 households based on the census data of 2011. The population of the CoT was, 1770330 in 1996, 2142,322 in 2001 and 2,921,488 2011 (STATSSA, 2012). COT experiences sub-tropical climate with hot and rainy summer and very cold and dry winter.

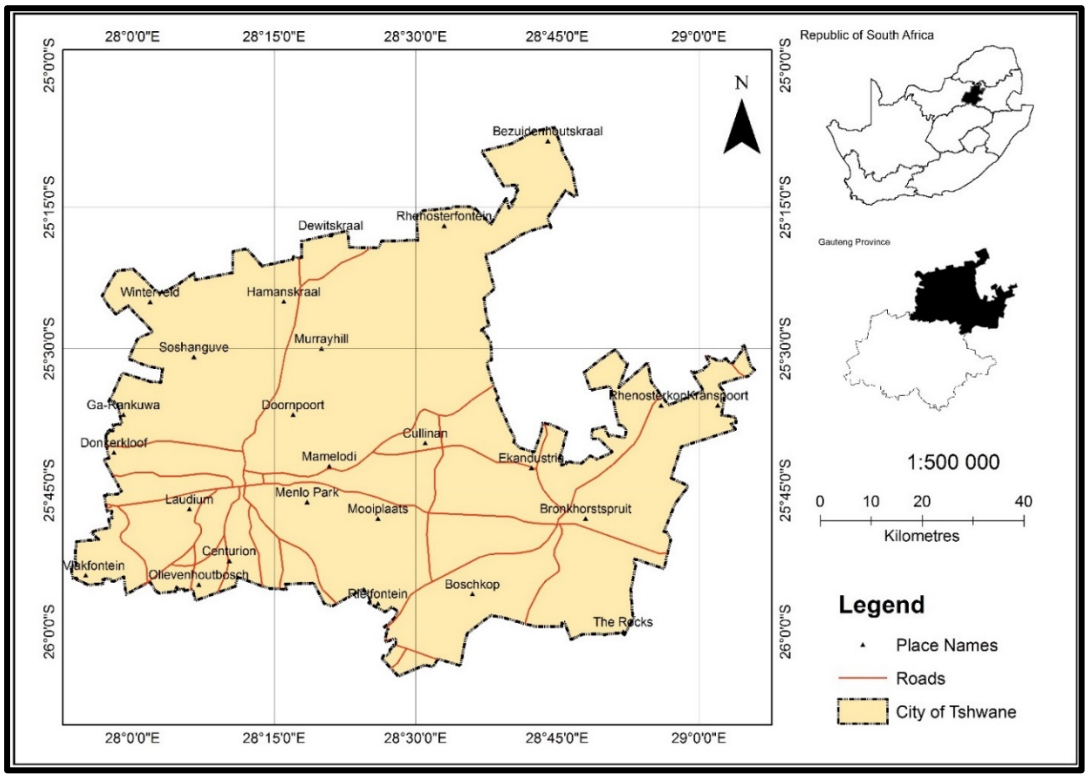

Figure 3: Location of the study areas in the Gauteng Province, in South Africa

3.4 Data and Methods

The flowchart (Figure 4) illustrates the methodology used to extract urban areas

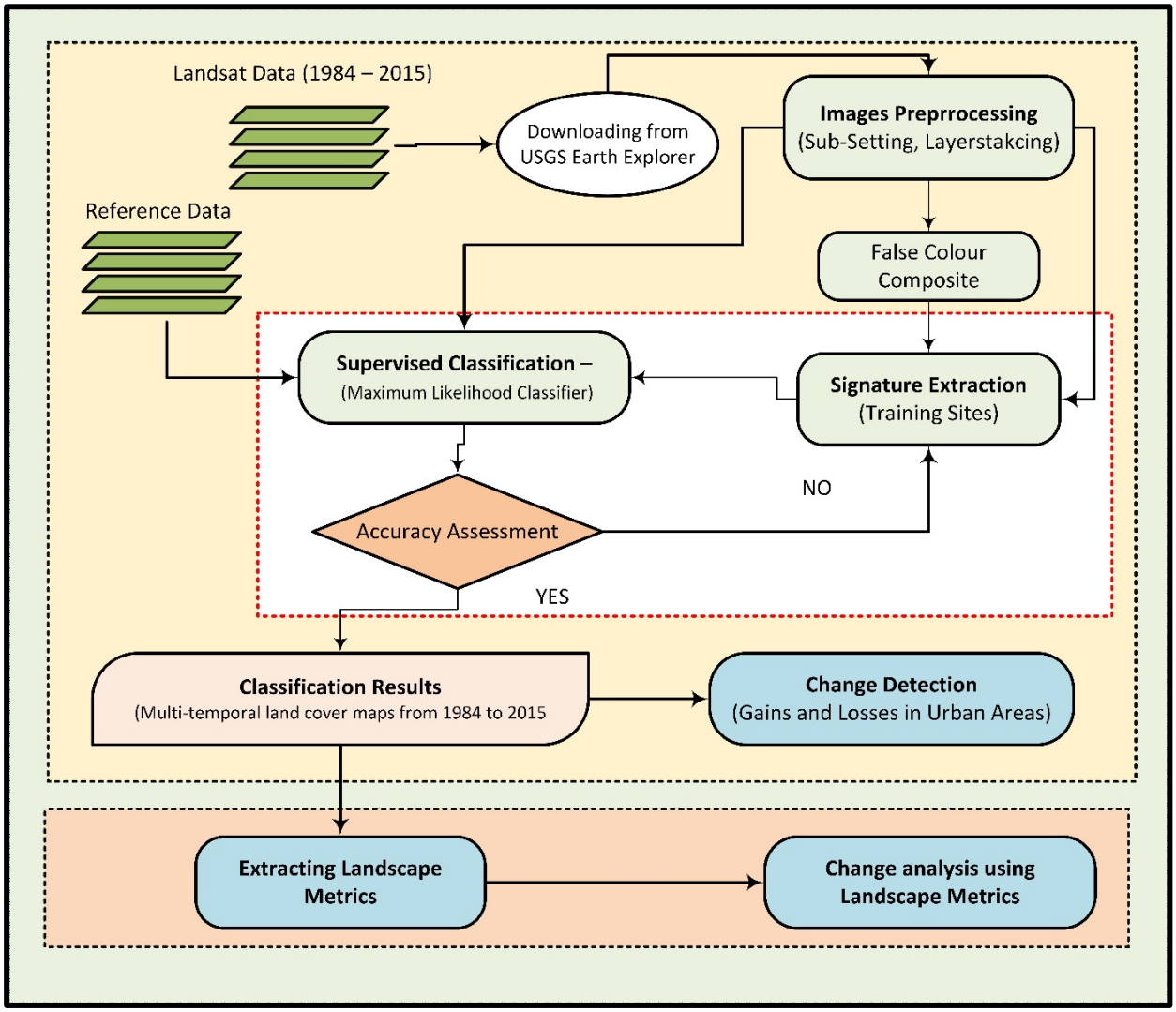

Figure 4: Methodology used to assess change in urban growth in the CoT using Landsat imagery between 1984 and 2015

3.4.1 Pre-processing

Cloud-free Landsat TM, ETM+ and OLI (170/077 and 170/078) satellite images downloaded from the USGS Earth Explorer, listed in Table 1 were used in this study. Landsat was launched in 1972 and the program has been acquiring information of the earth's surface for long time, so it is possible to have access to old imagery, which is

lacking in other sensors. These datasets were available free of charge which makes it cost-effective and efficient for multi-temporal monitoring and quantification of change in the earth surface. The remotely sensed data were geo-referenced and cropped to the study areas. The data were projected to the UTM (Universal Transverse Mercator) Zone 35 South coordinate system.

Table 1: Characteristics of the Landsat TM. ETM+ and OLI [*]datasets used in this study

Sensor	Path	Row	Resolution	Date
Landsat TM	170	077 & 078	30m	1984-05-27
Landsat TM				1991-05-25
Landsat TM				1995-08-08
Landsat TM				2006-07-18
Landsat TM				2009-05-26
Landsat ETM+				2000-10-16
Landsat OLI				2015-05-24

The two scenes (p170r077 and p170r078) were mosaicked into a single image for all the images from 1984 to 2015. All the bands in each image were resampled to 30m spatial resolution and were layerstacked in ERDAS Imagine 2014 (Intergraph, 2014). For Landsat TM and ETM+ Equation 3-1 was used to convert the from DN to radiance (Qin *et al.*, 2001).

$$L = (L_{\lambda max} - L_{\lambda min}) * \frac{Q_{\lambda DN} - Q_{\lambda min}}{Q_{\lambda max} - Q_{\lambda min}} + Lmin \qquad 3\text{-}1$$

where L= is the spectral radiance received by the sensor, $L_{\lambda max}$ is the maximum detected spectral radiance, $L_{\lambda min}$ is the minimum spectral radiance. Q_{DN} is the DN at a

[*] TM – Thematic Mapper, ETM+ - Enhanced Thematic Mapper Plus, OLI - Operational Land Imager

given pixel; $Q_{\lambda max}$ = is the maximum DN value (255) and $Q_{\lambda min}$ = is the minimum DN value (0) (Qin *et al.*, 2001).

For Landsat OLI Equation 3-2 was used to convert the from DN to radiance (Qin *et al.*, 2001).

$$L_\lambda = M_L Q_{cal} + A_L \qquad 3\text{-}2$$

Where: L_λ = TOA spectral radiance (Watts/(m^2 * srad * μm)), M_L = Band-specific multiplicative rescaling factor from the metadata A_L = Band-specific additive rescaling factor from the metadata, Q_{cal} = Quantized and calibrated standard product pixel values (DN).

3.4.2 Land Cover/ Use Classification

Multiple training sites were digitised on the false colour composite (FCC) of the Landsat, imagery and attributes were added based on expert knowledge. Supervised maximum likelihood classification (MLC) in ERDAS Imagine 2014 (Intergraph, 2014) was employed to classify all the Landsat imagery into four main classes, which are built-up areas, water, natural vegetation and agriculture using the South African classification system of 1996 (Thompson, 1996). The classified images were reclassified into two main classes, which are: urban areas and non-urban areas with the characteristics outlined in Table 2 using ERDAS Imagine 2014 (Intergraph, 2014) and ArcGIS.10.4 (ESRI, 2015). MLC is a probability approach, which makes use of training sites (sample areas) to determine classes of each cell in the image. Theoretical statistical distribution allows the uses of the Bayes MLC, which produces lowest probability of misclassifications (Lillesand *et al.*, 2007). The MLC used both variance and covariance of the class signature derived from training sites when allocating each cell to one of the classes in the signature file (Lillesand *et al.*, 2007).

Table 2: The land cover classes that were used in the study

Land cover class	Description
Built-up Area	Formal and Informal residential areas, administrative areas, industrial areas, transport networks, communication networks, excavations, construction sites
Non-built-up Area	vegetation, shrubs, bushes, grasslands, open landscapes, agricultural land, irrigated areas, mountains and riverine vegetation, rivers, water reservoirs,

3.4.3 Accuracy Assessment

Aerial photographs and topographic maps from National Geo-Spatial Information (NGI), South Africa were input in the assessment to determine if the land cover classification was accurate. The assessment was carried out using random ground control points generated using ERDAS Imagine 2014 (Intergraph, 2014). Each classified land cover map was compared against the reference data to assess the accuracy of the classification.

3.4.4 Delta Change Detection

Post-classification (Delta) change detection methods (cross-tabulation) using Terrset/Idrisi (Eastman, 2015) were used to monitor and quantify urban sprawl. These post-classification change detection techniques, which are pixel-based analysis allow the determination of quantity and spatial distribution of land cover changes (Lillesand *et al.*, 2007). Gains and losses in the built-up areas were determined using the Land Change Modeller, in Terrset/Idrisi (Eastman, 2015).

3.4.5 Quantifying Urban Sprawl Using Landscape Metrics

After the remote sensing classification and analysis landscape metrics of each map from 1984to, 2015 were calculated. Twelve landscape metrics were computed using the Patch Analyst extension in ArcGIS (ESRI, 2015) which is a product of the FRAGSTATS software (McGarigal and Marks, 1995, Mcgarigal *et al.*, 2002, McGarigal

et al., 2009). Landscape metrics were chosen to calculate three main characteristics of the urban areas and these are an absolute size, relative, complexity and isolation. To calculate absolute size of urban features these Class area (CA), Total Edge (TE), Mean Patch Edge (MPE) and Number of Patches (NUMP) in the Patch Analyst extension in ArcGIS (ESRI, 2015).

3.5 Results and Discussions

The land cover maps of 1984 (Figure 5), 1986 (Figure 6), 1991 (Figure 7), 1995 (Figure 8), 2000 (Figure 9), 2006 (Figure 10), 2009 (Figure 11) and 2015 (Figure 12) based on supervised classification and visual interpretation showed changes in urban areas between the years. Overall classification accuracy for 1984, 1986, 1991, 1995, 2000, 2006, 2009 and 2015 were 82.3%, 83.4%, 82.5%, 81.6%, 81.7%, 81.3%, 85.7% and 85.8% respectively.

Increase in urban areas was shown with the increase in the impervious surfaces (built-up areas), which was apparent on the land cover maps (Figure 5-11). These land cover maps (Figure 5-11) visually revealed urban sprawl in the CoT and its clear built-up areas were expanding outwards into non-built-up environments. Based on the results from 1984 to 2015, there was a notable change in urban areas as it increased from 80557.54 ha in1984 to 168475.14 ha in 2015 (Table 3). From 1984 to 2015, urban areas increased by 87917.60 ha (109.14%) (Table 4) and a rate of 3.25 ha per annum (Table 4) There was an increase in urban areas from 1984 to 2015, the proportion of urban areas in 1984 was 12.77% and it increased to 26.70% in 2015 (Table 3). Between 1996 and 2011 population increased by 1 151 158 at a rate of approximately 76 700 people per annum which was 4.34%. Increase in impervious surfaces has a positive correlation with the population growth over the years. The highest rate of urban sprawl occurred during the period between 1984 and 1986. In the period the urban areas increased by 24.61% (199823.74 ha). That was followed by the period between 1991 and 1995 with an increase of 10.18% (10222.20 ha) and the least urban growth occurred between 2005 and 2009 with an increase of 4.33% (6352.63 ha) as depicted in Table 4. For the whole period of study there was a 109.14% (87917.60.52 ha)

increase in urban areas and the overall rate of increase was 3.52% (2836.05 ha) as shown in Table 4.

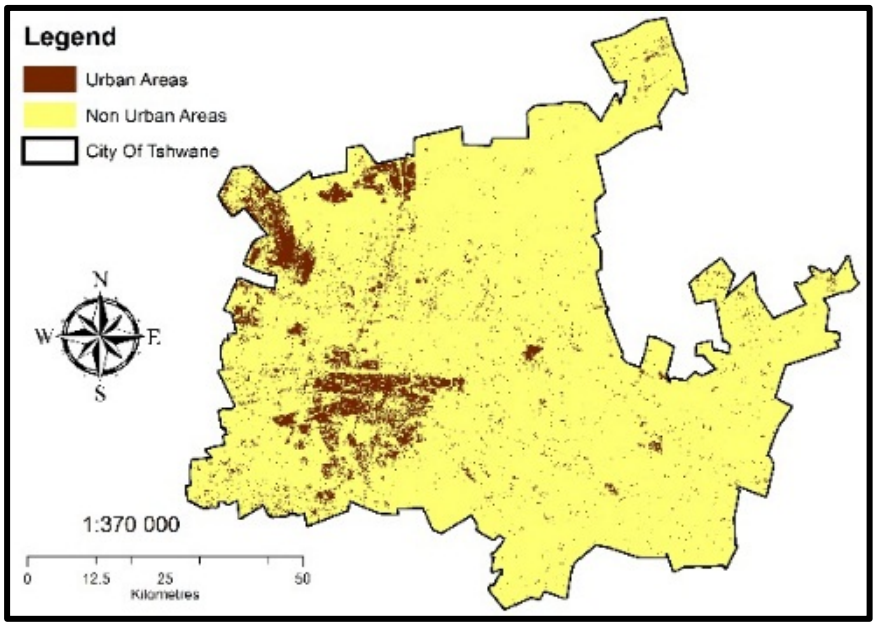

Figure 5: Land cover maps showing urban and non-urban areas of the CoT derived from the supervised classification of Landsat TM image of 1984.

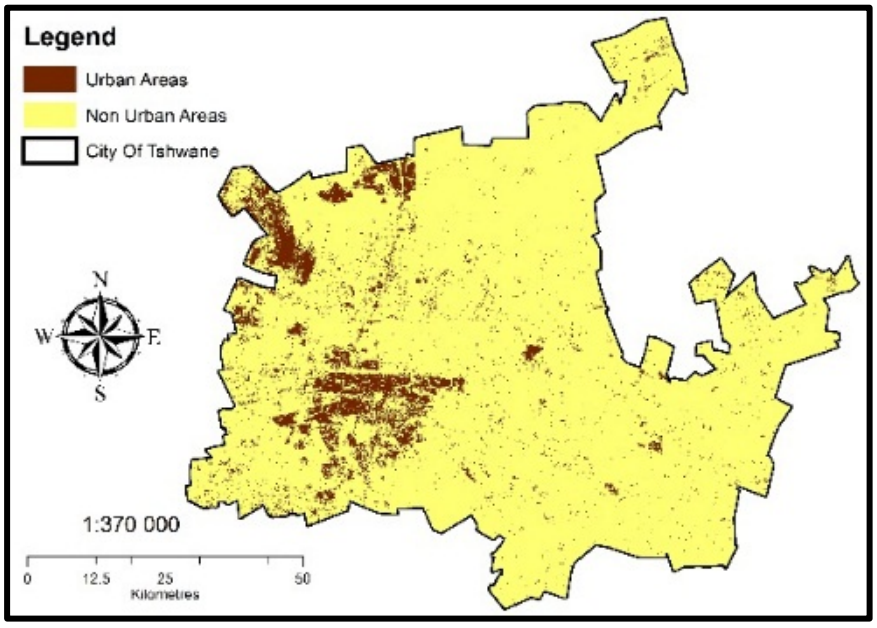

Figure 6: Land cover maps showing urban and non-urban areas of the CoT derived from the supervised classification of Landsat TM image of 1986

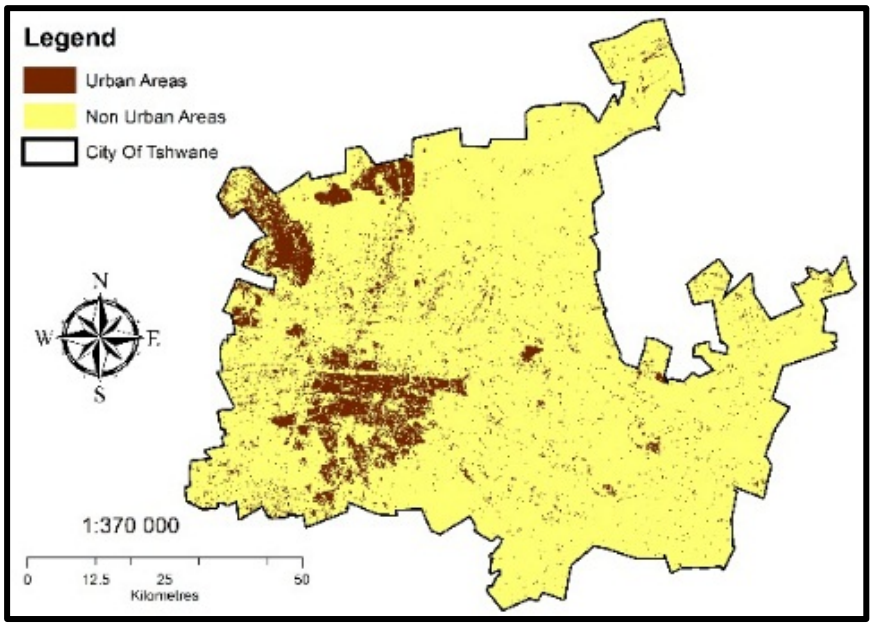

Figure 7: Land cover maps showing urban and non-urban areas of the CoT derived from the supervised classification of Landsat TM image of 1991

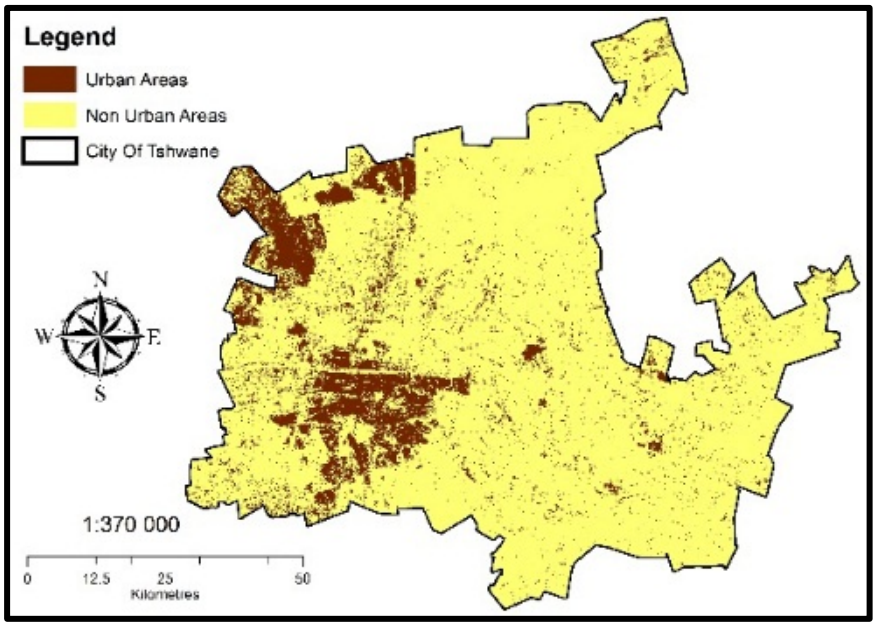

Figure 8: Land cover maps showing urban and non-urban areas of the CoT derived from the supervised classification of Landsat TM image of 1995

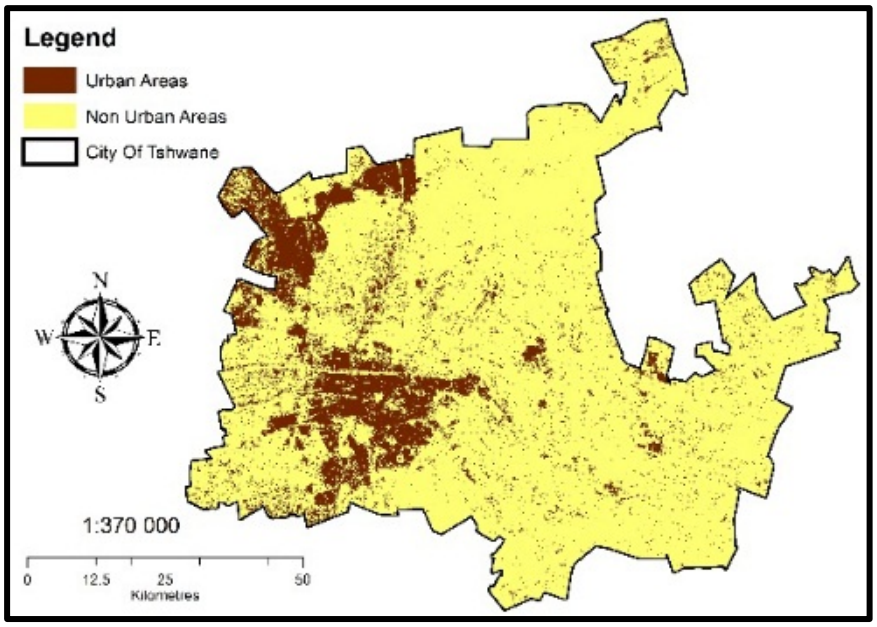

Figure 9: Land cover map showing urban and non-urban areas of the CoT derived from the supervised classification of Landsat 7 image of 2000

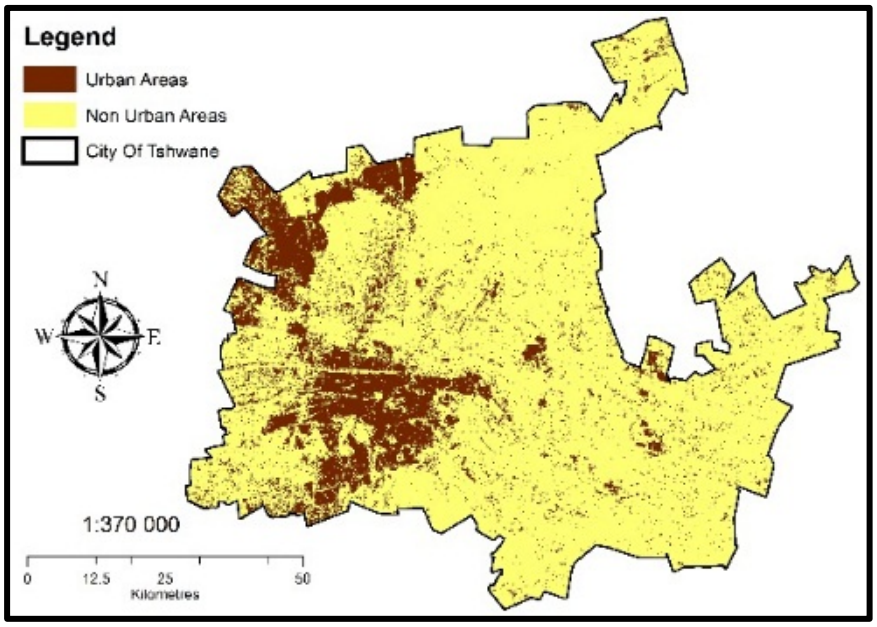

Figure 10: Land cover maps showing urban and non-urban areas of the CoT derived from the supervised classification of Landsat TM image of 2005

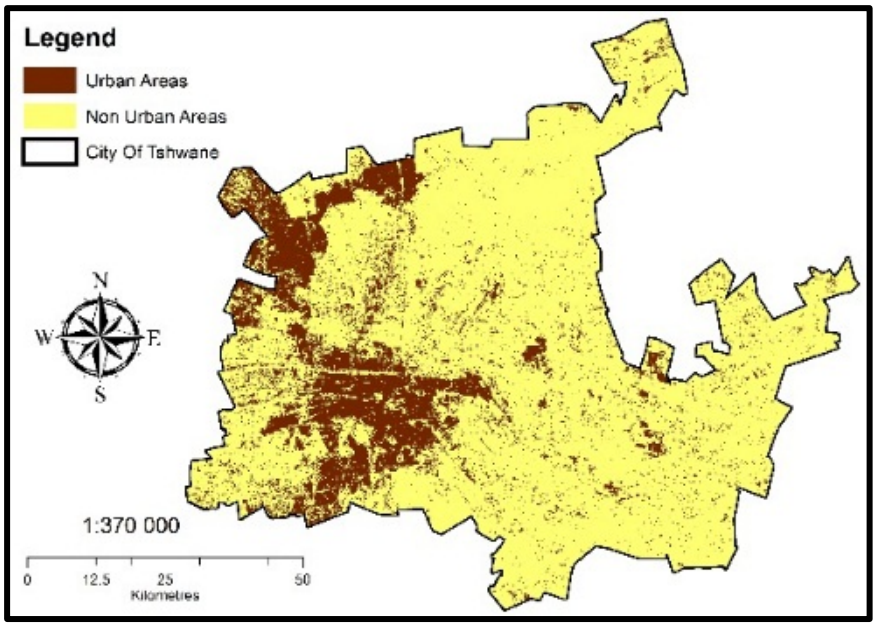

Figure 11: Land cover maps showing urban and non-urban areas of the CoT derived from the supervised classification of Landsat TM image of 2009.

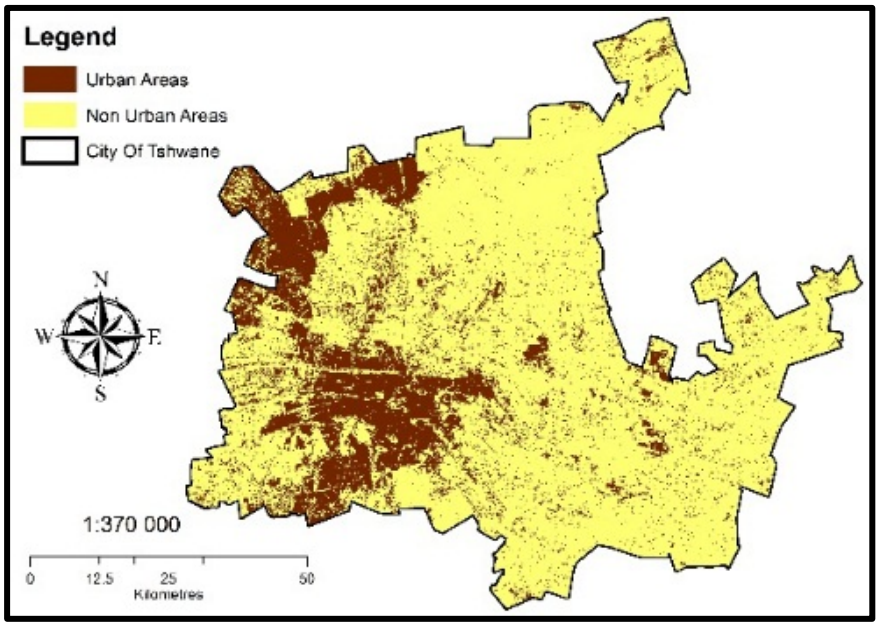

Figure 12: Land cover maps showing urban and non-urban areas of the CoT derived from the supervised classification of Landsat 8 image of 2015

Table 3: Built-up and non-built-up areas in ha for each year from 1984 to 2015

Year	1984	1986	1991	1995	2000	2006	2009	2015
Non- Urban Areas	550456.56	530632.82	520410.62	507167.33	494342.60	484450.27	478097.64	462538.96
Urban Areas	80557.54	100381.275	110603.48	123846.77	136671.50	146563.83	152916.46	168475.14
Percentage (%) Urban Areas	12.77	15.91	17.53	19.63	21.66	23.23	24.23	26.70

Table 4: Change in land cover between different years based on the land cover maps from 1984 to 2015

Period	From	1984	1986	1991	1995	2000	2006	2009	1984
	To	1986	1991	1995	2000	2006	2009	2015	2015
Time Span (Years)		2	5	4	5	6	3	6	31
Gains		19823.74	10222.20	13243.30	12824.73	9892.33	6352.63	15558.68	87917.60
Rate of Change in Ha		9911.87	2044.44	3310.82	2564.95	1648.72	2117.54	2593.11	2836.05
Change in Urban Areas (%)		24.61	10.18	11.97	10.36	7.24	4.33	10.17	109.14
Rate Per Year (%)		12.30	2.04	2.99	2.07	1.21	1.44	1.70	3.52

3.5.1 Change in Urban Areas Using Landscape Metrics

Most of the landscape metrics show a positive trend while a few of these indices show a negative trend. There was a continuous increase in the number of patches (NUMP) which were 40253 in 1984 and increase to 44848 in 2015 (Table 5). NUMP is an index used to indicate the aggregation or disaggregation in the landscape, so there were a number of discontinuous built-up areas that occurred as a result of urbanisation. Urbanisation brought about an 11% increase in the number of isolated areas between these two dates (1984 and 2015). This was similar to a study in Setubal and Sesimbra in Portugal where there was 17.54% increase in the number of patches (NUMP) between 1990 and 2000 (Araya and Cabral, 2010). In some cases, there was a reduction in the number of patches due to the agglomeration of built-up patches into bigger urban areas and this occurred in Sancaktepe District of Istanbul Metropolitan City (Kowe *et al.*, 2015).

Another determinant of urban sprawl is the size of the patches, as urbanisation increases sizes of patches also increase. In this study patch size coefficient of variance (PSCOV), patch size standard deviation (PSSD), mean patch sizes (MPS), Total Edge and mean patch edge were the indices that were used as determinants of the size of urban patches. Patch size coefficient of variance (PSCOV) which reveals the variance in patch size distribution increased from 4954.69 in 1984 to 11858.76 in 2015 (Table 5). In some urban areas such as Goa, India (Vaz *et al.*, 2017) and Athens Metropolitan Region (Greece) (Pili *et al.*, 2017) there was a decreasing trend first followed by an increasing trend in PSCOV. There was an increase in the mean patch sizes (MPS) between 1984 and 2015 from 2.00 ha to 3.76 ha (Table 5). This 88% increase in MPS was similar to the results in Istanbul by Kowe *et al.* (2015) which had a 135.60% increase in mean patch size. This showed that with urbanisation, size of patches will increase with the agglomeration of some of the urban patches.

This also corresponds with the PSSD, which also increased from 99.16 in 1984 to 445.48 in 2015 and this was similar to the study done in Mumbai (Vaz, 2014). Total Edge increased from 20893860 to 28473120 between 1984 and 2015, together with MPE, which was 519.06 in 1984 and the value increased to 634.88 in 2015. There was

a significant decrease in ED during the study period from 259.366 to 169.005 in 1984 and 2015 respectively. 259.37, 237.09, 223.65, 209.46, 194.14, 185.49, 179.81 and 169.01 for 1984, 1986, 1991, 1995, 2000, 2005, 2009 and 2015 respectively. There was an increase by total edge by 36.28% between 1984 and 2015 and this showed the increase in total length of the edge of the urban patches because of urban growth. This was similar to the study done in Portugal between 1990 and 2000 where a 26.93% increase in edge length was noticed (Araya and Cabral, 2010). Due to agglomeration of urban patches, there was a decrease in edge length the Sancaktepe District of Istanbul Metropolitan City (Kowe *et al.*, 2015) and in the Twin Cities Metropolitan Area (Paudel and Yuan, 2012).

An increase in the Area Weighted Mean Shape Index (AWMSI) was observed with values of 9.25, 10.03, 11.63, 12.69, 14.66, 16.09, 23.90 and 25.75 for 1984, 1986, 1991, 1995, 2000, 2005, 2009 and 2015 respectively (Table 5). The value of AWMSI in this study grew from 9.25 to 25.75, which means the urban patches were complex and irregular in shape. This increase was consistent with the increase in urban growth and these results correspond with the results by Kowe .*et al.*(2015) in Istanbul and Paudel and Yuan (2012) in Twin Cities Metropolitan Area. Changes of AWMSI were attributed to the merging or converting of small patches of non-built-up into built-up areas during the urban growth process (Paudel and Yuan, 2012).

Mean Shape Index (MSI) increased from 1.30 to 1.32 from 1984 to 2015. Mean shape index (MSI) assess the shape complexity of urban patches and in the case of the CoT MSI was greater than 1, which mean the shape of urban patches, have a high geometric complexity. This was similar to the study done in the urban coastal areas in Mumbai were MSI increase from 1.37 to 1.44 between 1973 and 2001 (Vaz, 2014). there was a decrease in MSI in Beijing (Yang *et al.*, 2018), Latvia (Rendenieks *et al.*, 2017) and in Goa, India (Vaz *et al.*, 2017) which was attributed to the amalgamation of urban patches.

Area Weighted Mean Patch Fractal Dimension (AWMPFD) determines the shape complexity of urban patches and describes how patch perimeter increase in patch areas was 1.40 in 1984 and it increased to 1.44 in 2015. Nevertheless, AWMPFD

remained 1.4 in 1984, 1986 and 1991 and 1.41 in 1995 and 2000 (Table 5). This landscape metrics (AWMPFD) was used in quantifying and measuring the degree of irregularity in the pattern of urban land cover change and the same results were also found in Sancaktepe District of Istanbul Metropolitan City where a 12.7% increase in AWMPFD was noticed between 2002 and 2009 (Kowe *et al.*, 2015).

Another index showing a decreasing trend was the Mean Perimeter - Area Ratio (MPAR) that was 670.28, 664.60, 664.71, 664.39, 663.93, 664.20, 664.28 and 661.64 in 1984, 1986, 1991, 1995, 2000, 2005, 2009 and 2015 respectively. In Athens Metropolitan Region (Greece) MPAR increased progressively first and later on decreased (Pili *et al.*, 2017) and in the CoT there was a decreasing trend.

Urban Sprawl in the CoT has been on going before the change of government in 1994 and it showed that more rapid urban growth occurred between 1984 and 1991. There has been a notable change in urban areas between 1984 and 2015 as 87917.60 ha of land transformed from non-built to built-up (Table 4). The rate of urban growth between 31 years was 3.52% per year and 109.14 between 1984 and 2015 (Table 4).

Interpretation of urban growth in the CoT over a period of 31 years allows researchers to have a deeper understanding of the urban growth patterns as it helps to identify the drivers or contributors of urban sprawl and their impact on the livelihoods of people living in urban areas. Apart from the above-mentioned causes CoT and other cities were experiencing change due to changes in the transport systems (Zhao, 2010). In the CoT changes in the transport was realised through the construction of the Gautrain Railway Link and the widening of some of the roads (Van der Westhuizen, 2007, Joubert, 2009) and this is one of the drivers of land cover change. Industrialisation is another cause of urban sprawl (Zhao, 2010) leading the establishment of different industrial zones for example Rosslyn. Such an increase in urban growth is common in areas located in a metropolitan city,' such as Lisbon (Araya and Cabral, 2010). For Lisbon, urban growth was associated with the availability of resources, services, infrastructures and proximity to the coast (Araya and Cabral, 2010). For the CoT, the growth in urban can also be attributed to resources, change of apartheid laws,

developments for the 2010 world cup, new policies being enacted which encouraged development.

Facts established from these urban dynamics assessments reveal both the desirable and undesirable changes that were a result of urbanisation. These changes serve as a very significant tool in sustainable decision-making and policy formulation. Based on the observations, urban sprawl has a negative impact on infrastructure and the sustainable management of urban areas.

Landscape metrics aided in assessing spatio-temporal change in urban growth and change in landscape characteristics at varying spatial scales. The PSSD index reveals the degree of absolute patch size variability. It is a function of the mean patch size and the difference in patch size between patches. This metric is a challenge to interpret without assessing the patch size, as the absolute variation is dependent on the mean patch size. Other landscape metrics such as AWMSI, MSI, MPAR, MPFD and MPE in Table 5 revealed an increase in impervious surfaces between 1984 and 2015. Landscape metrics make it easier to quantify the spatio-temporal trends and patterns in built-up areas. The built-up areas evidently increased at the expense of non-urban areas in the CoT.

Table 5: Landscape metrics calculated from the urban area the recoded built-up areas map[*]

Name of Indices / Year	AWMSI	MSI	MPAR	AWMPFD	TE	ED	MPE	MPS	NUMP	PSCoV	PSSD
1984	9.25	1.30	670.28	1.40	20893860	259.37	519.06	2.00	40253	4954.69	99.16
1986	10.03	1.31	664.60	1.40	23799420	237.09	549.63	2.32	43301	5041.71	116.88
1991	11.63	1.31	664.71	1.40	24736950	223.65	557.30	2.49	44387	5807.35	144.71
1995	12.69	1.31	664.39	1.41	25941060	209.46	572.75	2.73	45292	6264.20	171.29
2000	14.66	1.31	663.93	1.41	26533080	194.14	586.28	3.02	45257	7322.51	221.13
2006	16.09	1.31	664.20	1.42	27186750	185.49	599.99	3.24	45312	7784.40	251.79
2009	23.90	1.31	664.28	1.43	27495450	179.81	606.87	3.38	45307	11390.04	384.43
2015	25.75	1.32	661.64	1.44	28473120	169.01	634.88	3.76	44848	11858.76	445.48

[*] AWMSI, MSI - Mean Shape Index, MPAR - Mean Perimeter - Area Ratio, AWMPFD - Area Weighted Mean Patch Fractal Dimension, TE – Total Edge, ED – Edge Density, MPE, MPS - Mean Shape Index, NUMP - Number of Patches, PSCoV – Patch Size Coefficient of Variance, PSSD - Patch Size Standard Deviation,

3.6 Conclusions

This study attempted to provide an understanding of the urban sprawl of the CoT. It quantified the extent and degree of urban sprawl by defining certain landscape metrics. Remote sensing and GIS techniques were applied in the monitoring and quantification of the impacts of urbanisation. The spatial and attribute data of urban areas in the CoT were attained using landscape metrics. Patchiness, shape index and built-up density landscape metrics were calculated and that helped in the understanding of the spatial trends and patterns of urban sprawl. There was a 109.14% increase in built-up areas between 1984 and 2015. Proportion area covered by urban patches to the total area was 12.77% in 1984 and it increased to 26.70% in 2015. This was augmented by an increase in the NUMP, which increased by 11% between the two dates (1984 and 2015). This revealed a significant increase in built-up areas. These changes in urban areas were evident on the land cover maps. There is increase in the complexity of the shape of urban patches, which was revealed by MSI, AWMSI and the AWMPFD landscape metrics. Absolute size, relative size, complexity and isolation revealed there was an increase in urban area between 1984 and 2015. Over the 31-year study period, there has been a remarkable increase in urban sprawl as illustrated by the classified maps, landscape metrics and cross-tabulation results.

This study demonstrated how multi-temporal remote sensing imagery coupled with landscape metrics and change analysis techniques can be employed in assessing and quantifying spatio-temporal patterns of urban sprawl in the CoT. Landscape metrics has proved to be a useful tool that can be used to describe urban structure. Decision-making in urban areas can be carried out based on these landscape metrics as they show the patterns and trends of urban growth. As such, spatial metrics could provide quantitation spatio-temporal information to decision-makers in informing them about containing human modifications on the landscape, particularly in controlling some unauthorized developments and constructions, which were possible explanations for the irregular urban growth pattern indicated by the use of AWMSI and AWMPFDI.

It was observed and concluded that while it is possible for the spatial configuration to change (as evidenced by a change in the number of patches, MPS and total edge), the diversity (relative abundance of land cover types) can, however, remain relatively stable over time. The increase in the urban expansion would cause an increase in landscape diversity.

There is need to explore the use of remotely sensed data with higher resolution. The high-resolution satellite will improve the quality of the land cover maps and will accurately map all the urban classes such as informal settlements, linear features such as roads and backyard suburbs, unlike Landsat imagery. These high-resolution images will help in revealing trends and patterns in the densification of urban areas due to backyard houses and informal settlement.

CHAPTER FOUR

4 SPATIAL MODELLING OF URBAN SPRAWL IN THE CITY OF TSHWANE, SOUTH AFRICA. *

4.1 Abstract

Rapid urban sprawl in both developed and developing countries is due to accelerated industrialisation, increase in transportation accessibility and urbanisation. Urban sprawl is characterised by the transition of non-built-up areas into built-up areas mainly in the urban fringes. Recent advances in geospatial techniques and models have allowed researchers and decision-makers to predict future urban dynamics. In this study, remote sensing, GIS and CA-Markov modelling techniques were employed to predict urban sprawl in the CoT in South Africa. The CA-Markov Model was applied on classified land cover maps of 1986 and 2005 to predict land cover of 2009, land cover of 1986 and 2009 to predict land cover of 2013 and lastly land cover of 1986 and 2013 to predict land cover of 2030. Predicted land cover maps of 2009 and 2013 were validated against the respective classified images. The kappa indices of agreement (KIA) for each of the two images (2009 and 2013) were 0.92 and 0.90 respectively. This study reveals that GIS, remote sensing and CA-Markov can be used as land cover change assessment tools to model, monitor, quantify and map urban sprawl and can potentially be used together to evaluate impacts of proposed urban management and planning policy in urban areas. There was an anticipated increase in urban growth in the CoT and urban modelling will assist in the future planning and management of the city as it informs decision-makers.

Keywords: CA-Markov, Transitional Areas, Transitional Probability, Kappa Index, Spatial Pattern, Validation, Prediction, GIS

---

* Submitted to the South African Geographical Journal and is currently under review.

4.2 Introduction

Outward expansion of urban environments in developed and developing countries is due to accelerated industrialisation, increase in transport networks and urbanisation (Mubea *et al.*, 2011, Lee and Chang, 2011). There are projections that by 2030 about 60% of the population will be living in urban areas (Omar *et al.*, 2013). Urbanisation is a human-induced problem that has caused significant global land cover changes (Deep and Saklani, 2014). This will accelerate urban growth thereby leading to the outward expansion of urban areas (urban sprawl) (Lee and Chang, 2011). Urban sprawl is a subject of global concern and can be defined as the encroachment of urban areas into the urban fringe leading to the decrease in natural vegetation, open spaces and agricultural land (Araya and Cabral, 2010, Lee and Chang, 2011). Urban sprawl is a major contributor of land-use and land-cover change as it induces the increase of built-up areas (impervious surfaces) (Sudhira *et al.*, 2004, Araya and Cabral, 2010, Deep and Saklani, 2014). Urban sprawl has led to the loss in agricultural land and natural vegetation in both developing and developed countries (Araya and Cabral, 2010, Lee and Chang, 2011, Omar *et al.*, 2013, Deep and Saklani, 2014).

The CoT Municipality in South Africa, like any other African city, has been affected by urban growth and reduction in non-urban environments (Mubiwa and Annegarn, 2015). Some of the cities that were affected by urban sprawl in South Africa include Port Elizabeth (Odindi *et al.*, 2012), Rustenburg (Mudau *et al.*, 2014), Johannesburg (Abutaleb *et al.*, 2013, Ngie *et al.*, 2013, Mubiwa and Annegarn, 2015) and eThekwini (Otunga *et al.*, 2014). Cities in Africa were urban sprawl occurred are Nairobi, Kenya (Mubea *et al.*, 2011), Tripoli, Libya (Alsharif and Pradhan, 2014, Al-sharif and Pradhan, 2014) Cairo, Egypt and Kampala, Uganda (Abebe, 2013) among others.

There is need to quantify, monitor and predict spatial patterns, trends and characteristics of urban sprawl for sustainable management land use management (Araya and Cabral, 2010, Kityuttachai *et al.*, 2013). Remote sensing, GIS techniques and spatial statistics can be applied in mapping, quantifying and predicting land cover change patterns and trends (Sudhira *et al.*, 2003a, Sudhira *et al.*, 2003b, Sudhira *et al.*, 2003c, Sudhira and Ramachandra, 2007, Araya and Cabral, 2010). These

methods are better than the traditional and time-consuming techniques (Kityuttachai *et al.*, 2013). GIS and remote sensing have proved to be powerful, cost-effective and efficient tools to quantify, monitor and predict land cover change using multi-temporal and multi-spectral spatial datasets (Araya and Cabral, 2010, Kityuttachai *et al.*, 2013, Omar *et al.*, 2013). Predicting urban sprawl evaluates future urban land cover transitions and establishes the relationship between driving forces of urban change (Omar *et al.*, 2013). Urban sprawl prediction aid urban planners in designing decision support systems to evaluate alternative management scenarios and to formulate land cover policies that are effective for the sustainable management of urban areas (Kityuttachai *et al.*, 2013, Omar *et al.*, 2013).

There are various prediction algorithms for different applications and they differ in their levels of complexity (Subedi *et al.*, 2013, Omar *et al.*, 2013). These models can be categorised into two main types, which are stochastic and process-based models. Stochastic models include Markov, logistic regression and cell automaton (Abebe, 2013). The only process-based model is the dynamic ecosystem model (Abebe, 2013). The popular predictive models are the CA, Markov and the combination of the CA and Markov Chain (CA-Markov) (Reveshty, 2011, Ahmed and Ahmed, 2012). Cell Automaton Markov (CA-Markov) is a robust spatially explicit hybrid model, which is an integration of logistic regression model, Markov chain and cellular automata (CA) (Xie *et al.*, 2007, Subedi *et al.*, 2013, Deep and Saklani, 2014). It was designed as an improvement to the performance of standard logistic regression models in predicting urban areas and it combined the strength of Markov and CA (Pontius and Malanson, 2005, Araya and Cabral, 2010, Vermeiren *et al.*, 2012, Deep and Saklani, 2014). The amalgamation of Markov, logistic regression and cellular automaton algorithms gives CA-Markov a better modelling benefit over other prediction models (Kamusoko *et al.*, 2009). Hence the CA-Markov is classified the best model in simulating future land use changes (Kamusoko et al., 2009, Subedi et al., 2013, Omar et al., 2013).

CA-Markov model was used to predict and analyse land cover change between 2012 and 2018 in Pudong, Shanghai City (Xie *et al.*, 2007). Urban prediction was also done in Tripoli, Libya to predict the land cover maps of 2020 and 2015 and it produced an accuracy of 85% and there was an increase in urban areas and reduction in

agricultural areas (Al-sharif and Pradhan, 2014). In Setubal and Sesimbra, Portugal urban changes were predicted using CA-Markov, landscape metrics, the resultant kappa index 0.87 and 0.83, for location and quantity respectively (Araya and Cabral, 2010). In Mashdad City CA-Markov algorithm coupled with multi-criteria evaluation (MCE) were used to predict urban changes and the results revealed an increase in urban areas and after validation, the kappa index was above 09 for the quantity and location (Tajbakhsh *et al.*, 2016).

In South Africa, there have been some initiatives to predict land cover using remote sensing and these were executed at municipal level and at provincial scales, with some being academic research done by different research institutions (Wray and Cheruiyot, 2015). CoT, as a fast-growing city in Africa and is one of South Africa's three administrative cities, was chosen as a case study to quantify, monitor and map future land cover scenario due to intensive urbanisation. The aim of this paper was to predict future urban land cover scenarios in the CoT using GIS and remote sensing techniques.

4.3 Study Area

CoT (Figure 13 popularly known as the City of Pretoria is the administrative capital of the Republic of South Africa and located in the North of the Gauteng Province. The city was founded in 1855 by Marthinus Pretorius and renamed to Tshwane in 2000 (Raper, 2008, Van der Vyver, 2015). It merged with Metsweding District following the Gauteng Global City Region Strategy (Matlala, 2015). COT has 7 regions, 105 wards and 210 councillors and is the single largest municipality. CoT lies between latitudes 25°6'34.60" S to 26°4'41.12" S and longitudes 27°53'24.26E to 29°5'54.31" E. The city landmass of 629 618 ha, 2 921 490 people and 911 536 households based on the census data on 2011. The population of the CoT was 1 770 330 in 1996, 2,142,322 in 2001 and 2,921,488 in 2011 (STATSSA, 2012). COT experiences sub-tropical climate with hot and rainy summer and very cold and dry winter.

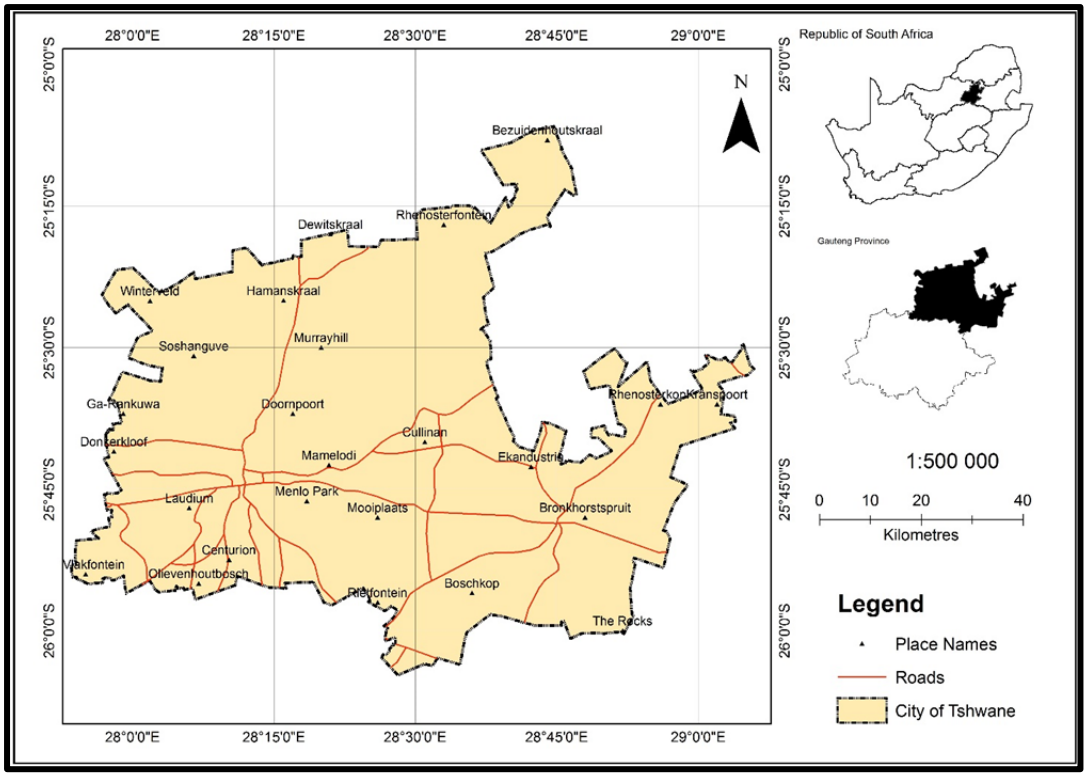

Figure 13: The study area CoT Municipality) situated in Gauteng Province, South Africa.

4.4 Data and Methods

Land cover patterns were mapped using the archival data from the Landsat TM and OLI (p170r 077 and p170r078) images of 1986, 2005, 2009 and 2013 (Table 6) was downloaded from the USGS Earth Explorer's Earth Explorer web portal. Ancillary datasets such as 1:50 000 topographic maps and aerial photographs were used in the pre-processing for geometric correction and accuracy assessment. The digital number (DN) of the two Landsat scenes that covers the study areas were converted to reflectance. For Landsat TM and ETM+ Equation 4-1 was used to convert the from DN to radiance (Qin *et al.*, 2001).

$$L = (L_{\lambda max} - L_{\lambda min}) * \frac{Q_{\lambda DN} - Q_{\lambda min}}{Q_{\lambda max} - Q_{\lambda min}} + Lmin \qquad 4\text{-}1$$

where L= is the spectral radiance received by the sensor, $L_{\lambda max}$ is the maximum detected spectral radiance, $L_{\lambda min}$ is the minimum spectral radiance. Q_{DN} is the DN at a

given pixel; $Q_{\lambda max}$ = is the maximum DN value (255) and $Q_{\lambda min}$ = is the minimum DN value (0) (Qin *et al.*, 2001)

For Landsat OLI Equation 4-2 was used to convert the from DN to radiance (Qin *et al.*, 2001).

$$L_\lambda = M_L Q_{cal} + A_L \qquad 4\text{-}2$$

Where: L_λ = TOA spectral radiance (Watts/ (m^2 * srad * μm)), M_L = Band-specific multiplicative rescaling factor from the metadata A_L = Band-specific additive rescaling factor from the metadata, Q_{cal} = Quantized and calibrated standard product pixel values (DN).

Table 6: Characteristics of the satellite images that were used in this study

Year	Sensor	Spatial Resolution	Radiometric Resolution	Path and Row
May 1986	Landsat TM	30m	8 bit	p170r077 & p170r078
May 2005				
May 2009				
May 2013	Landsat 8 (OLI)		11 bit	

Supervised classification using the maximum likelihood classifier in ERDAS Imagine (Intergraph, 2014) was used to classify all the Landsat images based on the South African classification systems (Thompson, 1996) into four main classes which are urban areas (built-up), natural vegetation, agriculture and water. The classified maps were reclassified into two main classes which are urban (built-up) and non-urban (non-built-up) and their description is in Table 7.

Table 7: The land cover classes that were used in the study

Land cover class	Description
Built-up Area	Formal and Informal residential areas, administrative areas, industrial areas, transport networks, communication networks, excavations, construction sites
Non-built-up Area	vegetation, shrubs, bushes, grasslands, open landscapes, agricultural land, irrigated areas, mountains and riverine vegetation, rivers, water reservoirs,

Markovian Transition Estimator (Markov) a Module in Terrset/Idrisi (Eastman, 2015) was used to generate transitional areas and transition probabilities (Table 8, Table 9, Table 10, Table 11, Table 12 and Table 13) in the specified times (Araya and Cabral, 2010). Transitional probabilities explain the probability that each land cover class will change to the other class and the transitional areas matrix is the number of pixels that are expected to change from one land cover class to another at the specified time. Cell Automaton Markov a Module in Terrset/Idrisi (Eastman, 2015) was run using the transitional probabilities, transitional areas and transition suitability image collection generated by the Markovian Transition Estimator to predict the land cover of 2009 and 2013 respectively. CA-Markov and Markov was run using the four classes (Natural Vegetation, Agriculture, Water and Urban Areas) and after the predictions, the maps were reclassified into two classes (built-up and non-built-up).

These two projected images of 2009 and 2013 were validated against the classified images of 2009 and 2013 respectively. The validation process involved a comparative analysis or cross-tabulation of the predicted land cover map against the reference map. After validation, the prediction map of 2030 was produced using the classified image of 1986 and 2013. The predicted map of 2030 was used to calculate the predicted extent of built-up and non-built-up areas by 2030. The flow-chart of predicting urban growth in the CoT is illustrated in Figure 14.

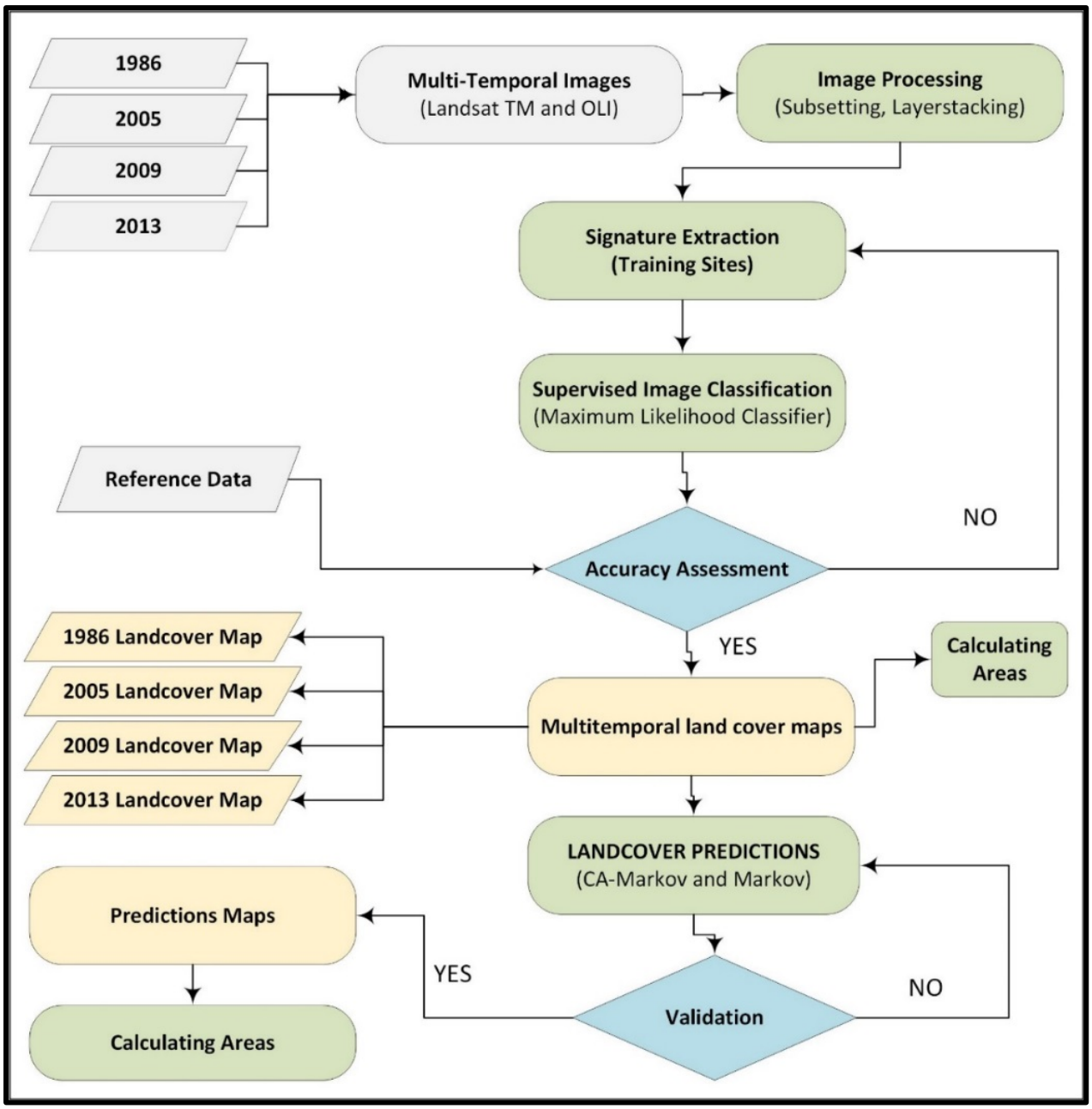

Figure 14: Methodology used to predict future scenarios in urban growth in the CoT.

Table 8: Transitional probabilities that were used to predict land cover for 2009 using 1986 and 2005 land cover maps

	Probability of changing to :			
	Water	Natural Vegetation	Agriculture	Urban Areas
Water	0.9439	0.0161	0.0065	0.0335
Natural Vegetation	0.0004	0.8508	0.1335	0.0153
Agriculture	0.0000	0.0000	0.9680	0.0320
Urban Areas	0.0000	0.0000	0.0000	1.0000

Table 9: Transitional areas (pixels) that were used to predict land cover for 2009 using 1986 and 2005 land cover maps

	Expected to transition to			
	Water	Natural Vegetation	Agriculture	Urban Areas
Water	18917	322	130	672
Natural Vegetation	1665	3501657	549567	63072
Agriculture	0	0	3862135	127838
Urban Areas	0	0	0	1490809

Table 10: Transitional probabilities that were used to predict land cover for 2013 using 1986 and 2009 land cover maps

	Probability of changing to :			
	Water	Natural Vegetation	Agriculture	Urban Areas
Water	0.9455	0.0105	0.0147	0.0293
Natural Vegetation	0.0004	0.8290	0.1577	0.0129
Agriculture	0	0.0000	0.9696	0.0304
Urban Areas	0	0	0	1.0000

Table 11: Transitional areas (pixels) that were used to predict land cover for 2013 using 1986 and 2009 land cover maps

	Expected to transition to			
	Water	Natural Vegetation	Agriculture	Urban Areas
Water	18127	201	281	562
Natural Vegetation	1480	3106014	590688	48506
Agriculture	0	0	4099799	128597
Urban Areas	0	0	0	1622529

Table 12: Transitional probabilities that were used to predict land cover for 2030 using 1986 and 2009 land cover maps

	Probability of changing to :			
	Water	Natural Vegetation	Agriculture	Urban Areas
Water	0.7582	0.0429	0.0652	0.1337
Natural Vegetation	0.0003	0.6063	0.3020	0.0915
Agriculture	0	0	0.8745	0.1255
Urban Areas	0	0	0	1.0000

Table 13: Transitional areas used to predict land cover for 2030 using 1986 and 2013 land cover maps

	Expected to transition to			
	Water	Natural Vegetation	Agriculture	Urban Areas
Water	10678	604	919	1883
Natural Vegetation	974	2036024	1014033	307167
Agriculture	0	0	3747969	537910
Urban Areas	0	0	0	1959237

4.5 Results and Discussions

4.5.1 Land cover Maps

The initial step was to extract land cover maps from Landsat images. Land cover maps of 1986 (Figure 15), 2005 (Figure 16), 2009 (Figure 17) and 2013 (Figure 18) with only two main classes (built and non-built areas) were generated. Accuracy assessment of these classifications was done using aerial photographs and topographical maps from National Geo-Spatial Information (NGI), South Africa. Overall classification accuracy of the CoT for 1986, 2005, 2009 and 2013 were 83.4, 81.3%, 85.7% and 82.15% respectively. Built-up and non-built-up areas (Table 14 and Table 15) were tabulated and land cover analysis showed that there was an increase in built-up areas by 83.57% between 1986 and 2013 and correspondingly there was a reduction of non-urban areas. There were 529239.34 ha on non-urban areas, which were reduced to 445347,122 ha in 2013.

Table 14: The extent of built-up and non-built-up areas in ha of each year from 1986 to 2013 in the CoT derived from remote sensing images.

Total Areas (Ha)				
Year	1986	2005	2009	2013
Built-up (Urban)	10038127	146563,84	152916,46	184273,49
Non-built-up Area	529239,34	483056,77	476704,15	582698,72

There was a 248.52% (83892, 21ha) increase in urban area between 1986 and 2013 with a rate of 3.10% increase per year (Table 15). The highest rate of change occurred between 1986 and 2015 was 46.01% (19919.34 ha) with a rate of 2.42% percent per year (Table 15).

Table 15: Change in land cover between different years based on the land cover maps from 1986 to 2013

Period	From	1986	2005	2009	1986
	To	2005	2009	2013	2013
Time Span (Years)		19	4	4	27
Growth Rate (%) Per Year		2.42	1.08	5.13	3.10
Built-Up Areas (%)		46,01	4,33	20,51	83,57
Built-Up Areas (Ha)		46182,564	6352,621	31357,03	83892,21

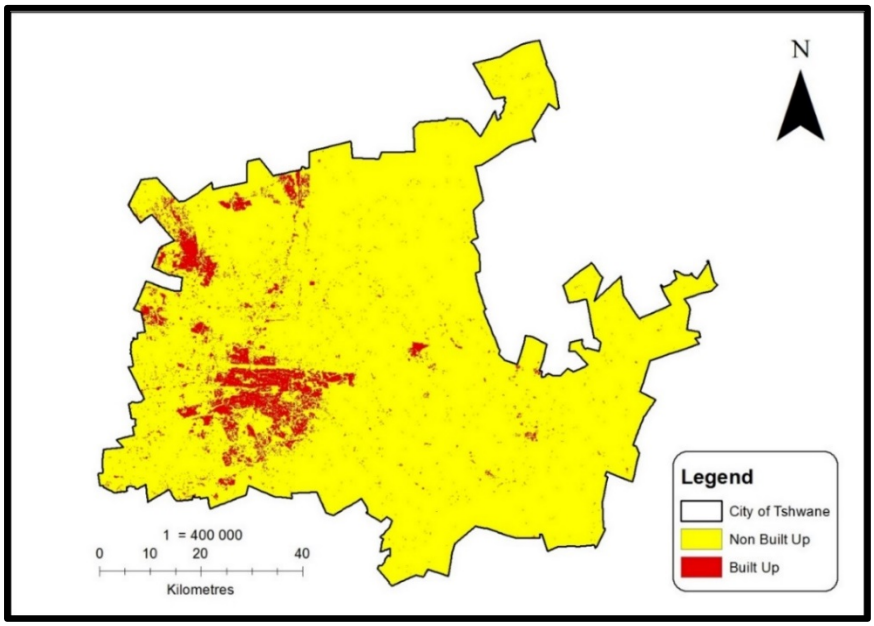

Figure 15: CoT reclassified land cover map of 1986, derived from the maximum likelihood classification of the Landsat TM image of 1986

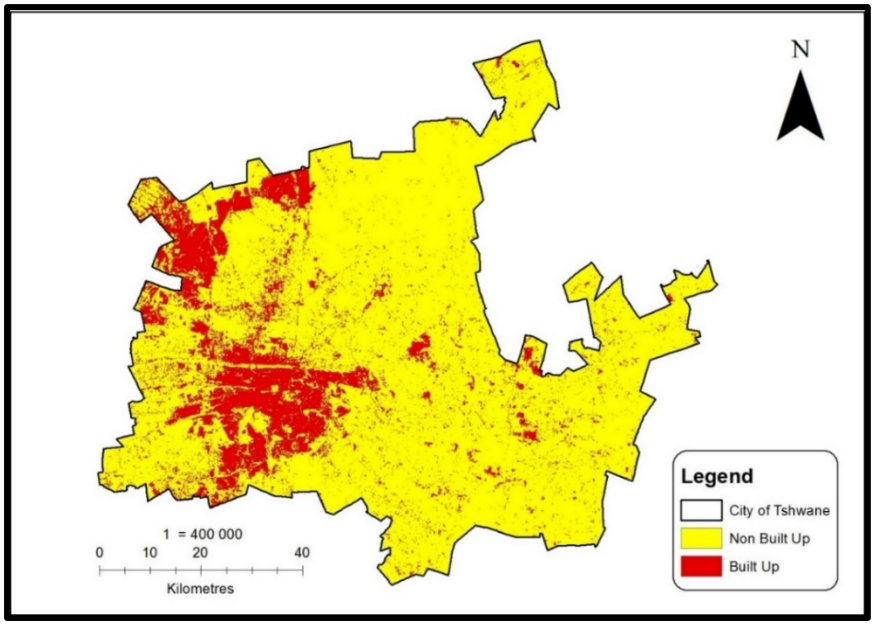

Figure 16: CoT reclassified land cover map of 2005, derived from the maximum likelihood classification of the Landsat TM image of 2005

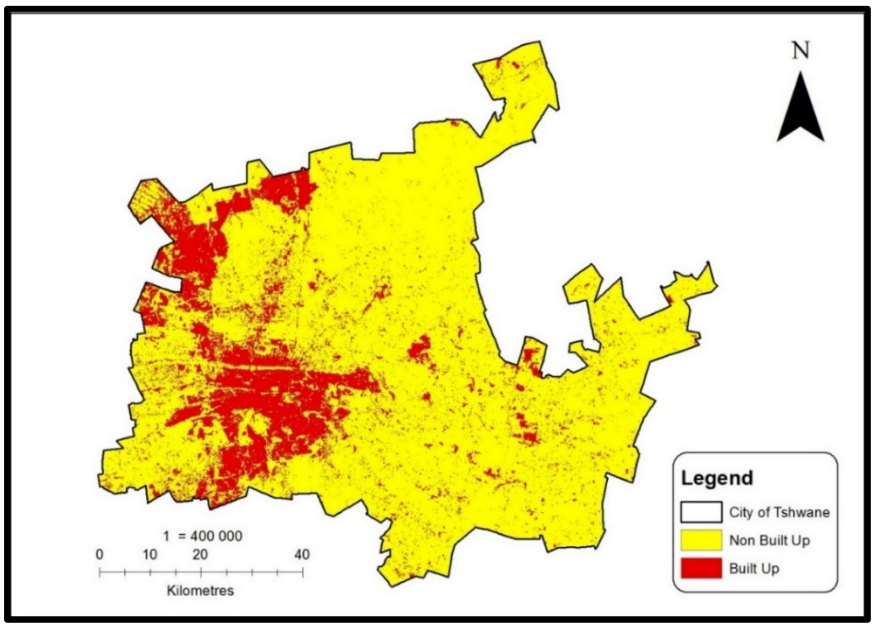

Figure 17: CoT reclassified land cover map of 2009, derived from the maximum likelihood classification of the Landsat TM image of 2009.

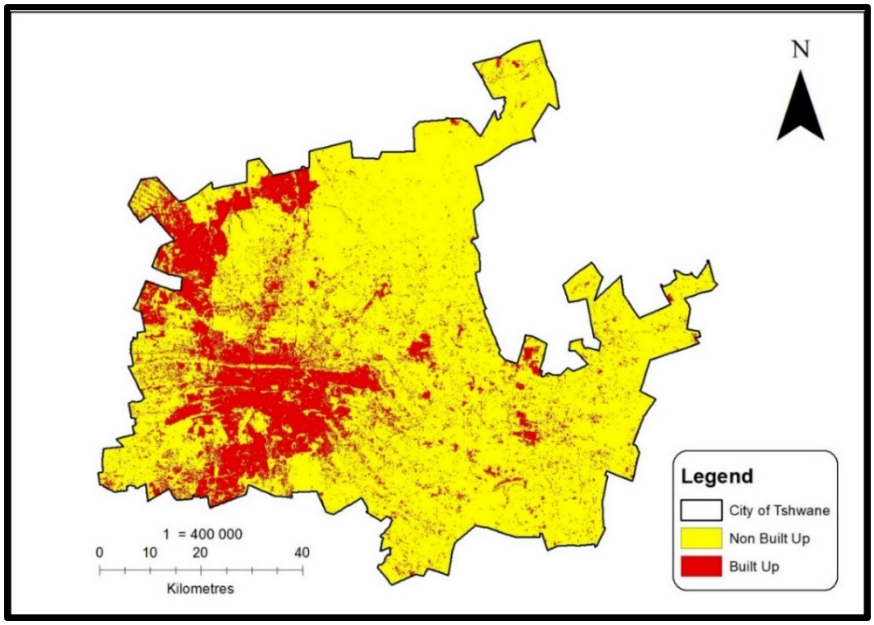

Figure 18: CoT reclassified land cover map of 2013, derived from the maximum likelihood classification of the Landsat 8 image of 2013.

4.5.2 Urban Prediction and Validation

Land cover of 2009 (Figure 19) and 2013 (Figure 20) were predicted using the CA-Markov algorithm and the associated transitional parameters and this was validated with the classified images of the respective years. Visual interpretation of the prediction results shown in Figure 19 and Figure 20 reveals that predicted maps were similar to the classified maps of 2009 (Figure 17) and 2013 (Figure 20). These predicted land cover maps were validated against the classified land cover maps. The reason for validating the predicted images against the reference images or actual datasets was mainly to monitor if the actual data fit the predicted output. Validation results (Table 16) give out a statistical analysis that showed how the two maps agree in terms of the quantity and spatial location of cells in each class. An analysis was also made using the kappa variations between the predicted and reference map. Kappa index of agreement is expressed in percentages and the closer they are to 100%, the stronger the agreement between the predicted and reference map. Validation also calculates specialised Kappa measures that differentiate between errors of quantity and errors of location between the two quantitative land cover maps. There was a kappa Index of agreement ($K_{standard}$) of 0.92 and 0.90 for 2009 and 2013 respectively

(Table 16). Kappa for no information (K_{no}) which gives the overall accuracy of the predicted was 0.93 and 0.91 for 2009 and 2013. Kappa location was 0.99 and 0.96 for 2009 and 2013 respectively (Table 16) The results of the urban prediction in this study was similar to the Mashad city using the CA-Markov and has a Kappa index on quantity and location of 0.92 and 0.95 (Tajbakhsh *et al.*, 2016).

The results of this study (Table 16) was also similar to the study that was carried out by Araya and Cabral (2010). in Stuabal and Sesimbra in Portugal which has a $K_{location}$ of 0.84 and $K_{quantity}$ of 0.83 (Araya and Cabral, 2010). There were discrepancies between the real and predicted land cover map of 2009 and 2013 that can be attributed to classification errors. These discrepancies (disagreements) between the predicted map and reference maps were due to location and quantity. Disagreements due to location was zero and 0.2 for 2009 and 2013 and the disagreement due to quantity was 0.04 for both 2009 and 2013. There were agreements due to chance, quantity and location between the predicted and reference map. Agreement due to chance was 0.25 for both 2009 and 2013, agreement due to quantity was 0.11 for 2009 and 2013 and agreement due to location was 0.58 and 0.57 for 2009 and 2013 (Table 16). Comparison between the results from the CA-Markov model to the actual classified imagery showed similarities and that the images were reliable and acceptable. The two images (predicted and classified) matched in both the location of the cells and quantity.

Land cover map of 2030 (Figure 21) was predicted and the visual representations showed that there was an increase in urban areas. Based on the prediction urban area is likely to increase from 184273.49 ha to 235800.31 ha (Table 17). The main developments were likely to occur in the former township because of the government initiative to provide housing to the low-income earners. There was an anticipated increase in urban areas of 51526.82 ha between 2013 (Table 17) and the predicted 2030. This was similar to the study carried out Dhaka, Bangladesh (Ahmed and Ahmed, 2012), Stuabal and Sesimbra in Portugal (Araya and Cabral, 2010), Anzali, Iran (Nouri *et al.*, 2014) and Mashad city (Tajbakhsh *et al.*, 2016).

.

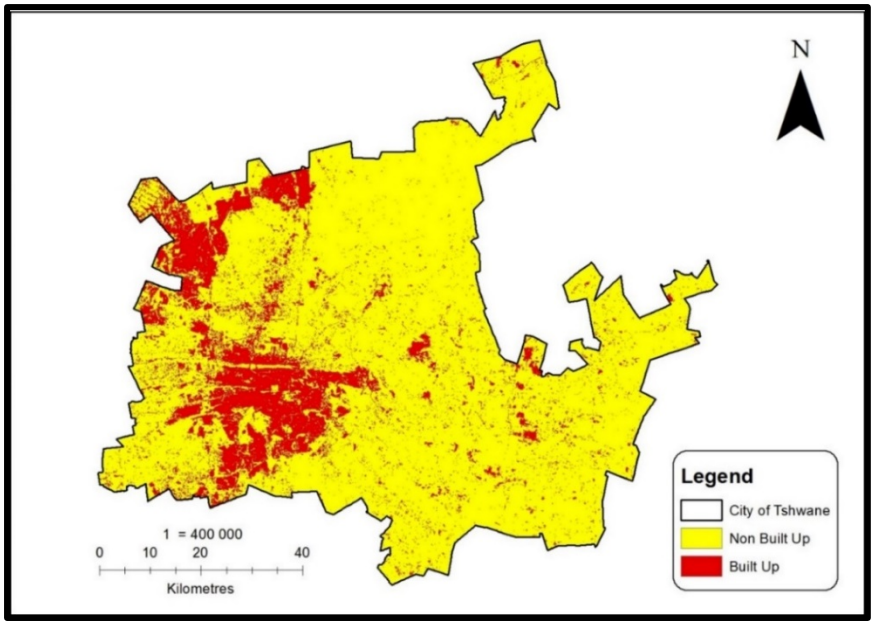

Figure 19: Predicted land cover map of 2009 for the CoT derived from the CA-Markov Prediction Model using transitional areas and probabilities.

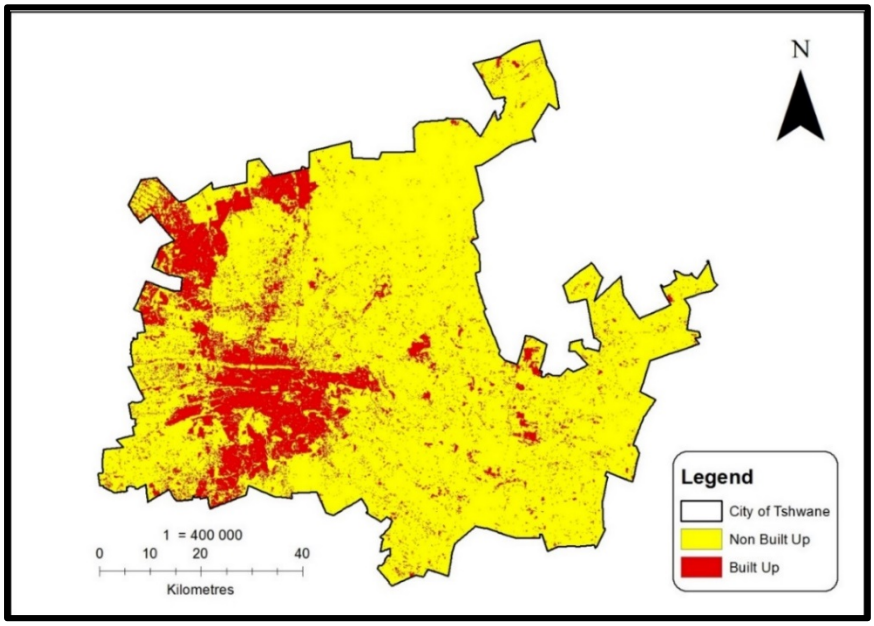

Figure 20 Predicted land cover map of 2013 for the CoT derived from the CA-Markov Prediction Model using transitional areas and probabilities.

Table 16: Validation summary of agreements and kappa indices derived from classified maps and predicted ones of 2009 and 2013

Parameters	2009	2013
Agreement due to chance	0.250	0.2500
Agreement due to quantity	0.11187	0.1096
Agreement due to location at the grid cell level	0.5825	0.5745
Disagreement due to location at the grid cell level	0.0086	0.0230
Disagreement due to quantity	0.0403	0.0.429
Kappa for no information	0.9349	0.9122
Kappa for grid-cell level location	0.9855	0.9615
Kappa for stratum-level location	0.9855	0.9615
Kappa Index of Agreement (Kappa Standard)	0.9226	0.8971

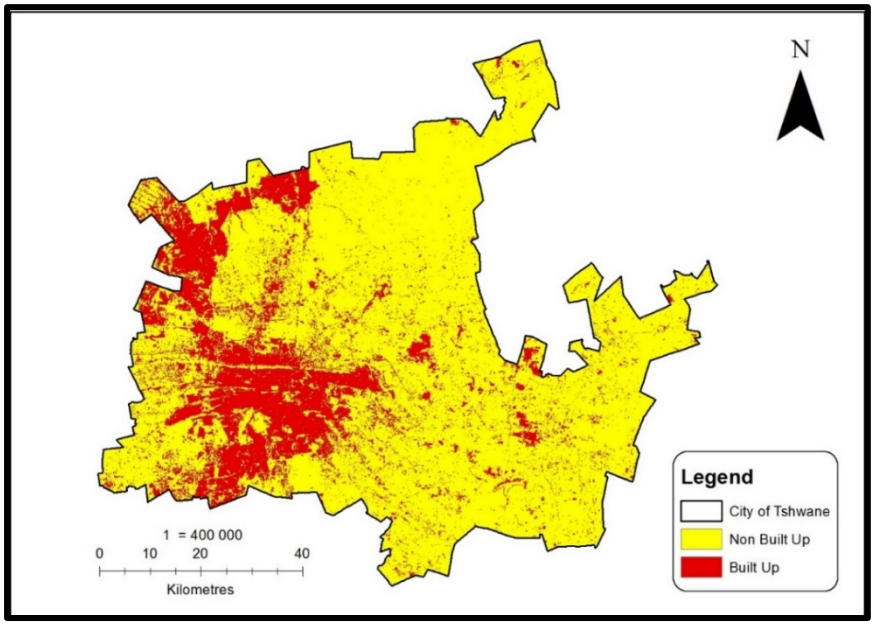

Figure 21: The 2030 Predicted Map for CoT derived from CA-Markov Analysis using transitional probabilities and a land cover map of 2013

Table 17: The areas of urban and non-urban areas for the three year 2009 (classified), 2013 (classified) 2030 (predicted) and change between the years.

Land cover class	Area in Ha		
	2009	2013	2030
Built-up Areas	152916,46	184273,49	235800,31
Non-built-up Areas	476704,15	445347,122	393820,30

4.6 Conclusions

The area covered by the urban areas was calculated to show the urban characteristic and trends in the CoT. GIS allowed the integration of the data into the models enabling us to find relations in the outputs. There was an anticipated increase in urban areas in 2030, which shows the capability of CA-Markov in predicting future land cover scenarios. Validation of the performance of the prediction models was necessary as it indicates that CA-Markov simulation provides results that were good for planning purposes. The validation values derived from the predicted images of 2009 and 2013 show that CA-Markov models can be used to analyse and predict urban sprawl in the CoT. There is a need to be cautious about using the CA-Markov in long-term predictions, as they will give unreliable results. Prediction models can be used to detect areas where urban sprawl is most likely to occur (critical “hot spots”).

This study revealed an integrated approach of remote sensing, GIS and modelling. Markov-CA model proved to be a very useful module that is needed in simulating future scenarios of urban growth and may be used to provide policy options for sustainable urban management and planning. CA-Markov models can be used as part of the spatial decision support system that will aid researchers and spatial planners in mapping future land cover change scenarios and can be beneficial in planning and policy formulation. For future urban prediction, there is a need to consider using high-resolution images such as SPOT as was done in Anzali in Iran (Nouri *et al.*, 2014).

CHAPTER FIVE

5 AN ASSESSMENT OF URBAN SPRAWL IN THE COT, SOUTH AFRICA USING ARCHIVAL SPOT IMAGERY.*

5.1 Abstract

Gaining an understanding of the extent and dynamics of urban sprawl is crucial in sustainable land use management and spatial planning. Information on urban sprawl is an important input for predicting future urban land cover changes. The influx of people into urban areas due to migration and natural population increase has led to rapid increase in urban areas and encroachment of urban-like environments into non-urban areas. One of the observable effects of urbanisation is the controlled and uncontrolled urban sprawl and morphological change of urban areas. The aim of this study was to assess and monitor the similarities and differences in urban sprawl dimensions, patterns and trends in the three main suburban areas (former townships, medium-density and low-density urban settings) in the CoT, which are: Eastern Townships (former townships), Pretoria Moot (former suburbs) and Pretoria East Suburbs (former suburbs) using high-resolution satellite imagery. SPOT images of 2008, 2012 and 2015 were classified using the supervised MLC and results were used to quantify and assess spatio-temporal variations in urban sprawl in the three study areas. Change analysis revealed an increase in urban sprawl between these three regions in the CoT. There was a high rate of increase in built-up areas in the high-density areas as compared to the medium and the low-density areas. There was a 38%, 25.00% and 13.80% increase in built-up areas in the Eastern Townships, Pretoria Moot and Pretoria East respectively between 2008 and 2015. Increase in urban growth led to 17.19%, 11.71% and 25.55% reduction in the CBAs in Pretoria Moot, Pretoria East and Eastern Townships respectively.

---

* Submitted in the CITIES Journal and is currently under review

Keywords: urban Sprawl, SPOT, GIS, land cover change, comparison, landscape metrics

5.2 Introduction

Urbanisation can be regarded as the increase in urban dwellers and is mainly as a result of socio-economic problems and population increase (Bhatta *et al.*, 2010, Aithal and Ramachandra, 2013). These socio-economic challenges have led to internal and international migration (Abutaleb *et al.*, 2013, Chikowore and Willemse, 2017). Urbanisation is one of the anthropogenic causes of agricultural and natural habitats in both developed and developing countries (Esch *et al.*, 2012, Abutaleb *et al.*, 2013, Jiang *et al.*, 2016). Conversion of arable and non-arable land into urban environments is occurring at an alarming rate (Aithal and Ramachandra, 2013). Establishment of urban environments attracts a lot of attention because of its size, complexity, socio-economic, cultural and political relevance which call for sustainable management and development in order for economic, social and ecological sustainability and stability (Esch *et al.*, 2012). Africa has been affected by political problems, which led to an exodus of people from other countries into South Africa in search of greener pastures (Lucas, 2015, Osman *et al.*, 2016, Marschall, 2017). Repressive apartheid laws in South Africa restricted the movement of non-white races from one region to another and its abolishment in 1994 with the dawn of democracy led to increased urban to urban, rural to urban migration (Seekings, 2000, McLennan *et al.*, 2016). South African townships have different political history, as suburbs were meant for whites during the apartheid era but nowadays they are for the affluent in society (Seekings, 2000, McLennan *et al.*, 2016). Townships were designed for black and other non-white races but this has changed since the dawn of democracy and reconciliation in 1994 (Seekings, 2000).

Unsustainable urbanisation led to controlled and uncontrolled urban sprawl, Urban sprawl is the advance of urban-like environments into non-urban areas (agricultural land, natural vegetation and natural habitats among others) (Aithal and Ramachandra, 2013). Urbanisation has negative effects on the environment and causes loss of both arable and non-arable land (Ya *et al.*, 2010). The conversion of non-urban areas into

impervious surfaces (urban areas) coupled with challenges in urban environments such as increased pollution (water, air and land) and pressure on the available resources are affecting proper ecosystem functioning (Ya *et al.*, 2010). Some of the problems attached to urbanisation include the sprouting of informal settlements, back-yard suburbs, traffic congestion and lack of parking space (THDA, 2012, Turok and Borel-Saladin, 2016).

In response to the pressure on the available resources, decision-makers are widening and expanding transport networks for example the Gautrain Project in Gauteng (Du Plessis, 2010, Walters, 2013, Wood, 2014), building of formal houses for the poor for example. RDP houses and approving private developers to develop more property for housing people (Munyati and Motholo, 2014). To reduce congestion in the central business districts, town planners have introduced growth centres as a way to decentralise some of the services in the CBD thereby creating nucleated settlements. These growth centres are also subject to urbanisation, which will subsequently lead to urban sprawl. Responses from decision-makers need well-informed decisions and this can only be done if there is accurate information about the urban environments such as remotely sensed data. Knowledge of urban sprawl is very important in sustainable urban management and planning. In developing countries, there is a lack of accurate information to analyse the spatio-temporal dimension and characteristics of urban growth (Esch *et al.*, 2012, Abebe, 2013). The information is necessary for the effective spatial and urban planning strategies (Esch *et al.*, 2012).

Advances in GIS and remote sensing technology have provided researchers and decision-makers with the ability to assess and monitor trends and patterns of urban sprawl (Abutaleb *et al.*, 2013, Abebe, 2013). Remote sensing technologies have been widely used to study urban sprawl in many countries both developed and developing (Abutaleb *et al.*, 2013). Recently, there were studies on urban sprawl using remote sensing and GIS (Aithal and Ramachandra, 2013, Shafizadeh Moghadam and Helbich, 2013, Ramachandra and Aithal, 2013, Ramachandra *et al.*, 2014). In Kolkata, India remote sensing was used to analyse change in urban areas (Bhatta, 2009). In the Gulf of Mexico in Mexico, there was a significant increase in urban areas (Xian *et al.*, 2012). There was a trend of rapid urbanisation in China, which led to rapid urban

growth and is causing the government to enact policies to increase urban growth (Xu and Min, 2013, Jiang *et al.*, 2016), Tainan City, Taiwan (Lee and Chang, 2011), Sansa City, Yemen (Al-shalabi *et al.*, 2013) and many other countries. The positive trend of urban area growth with the increase in population is evident in many studies done in both developing and developed countries (Mundia and Aniya, 2006, Taubenböck *et al.*, 2009, Vermeiren *et al.*, 2012, Abebe, 2013, Taiwo *et al.*, 2014, Alsharif and Pradhan, 2014).

In South Africa, some significant studies were done to assess urban growth using remote sensing and GIS technologies (Odindi and Mhangara, 2011, Odindi *et al.*, 2012, Mudau *et al.*, 2014, Mubiwa and Annegarn, 2015). In Port Elizabeth Landsat images of 1990, 1995 and 2000 were used to assess change in urban areas and there was a 13.3% increase in built-up areas (Odindi and Mhangara, 2011, Odindi *et al.*, 2012, Mubiwa and Annegarn, 2015). In Rustenburg, SPOT 5 satellite imagery of 2007 and 2012 was used to monitor and quantify urban growth and there was a 25.5% increase in urban areas between the years (Mudau *et al.*, 2014). The same trend was found in the Gauteng Region with the study done for the Gauteng City Region Observatory (GCRO) (Mubiwa and Annegarn, 2015). In eThekwini SPOT imagery was used to show the increase in impervious surfaces which affected the green spaces.(Otunga *et al.*, 2014). In Stellenbosch, remote sensing and spatial statistics were used to assess urban sprawl hot and cold spots (Musakwa and Van Niekerk, 2014).

Due to the pressure in the central business district, the CoT decentralised its services and created growth centres, surrounding it. Those growth centres have residential areas (formal and informal), shopping malls, industrial areas and transport networks. There are townships and suburbs in the CoT and each of these areas are suffering from urbanisation, which is accelerating urban sprawl. City of Tshwane has experienced a rapid population growth from 2 142 322 people in 2001 to 2 921 488 people in 2011 (STATSSA, 2012). Urban growth has led the impervious surfaces to encourage into areas that are earmarked for conservation, which are known as Critical Biodiversity Areas (CBAs) and Ecological Support Areas (ESAs) (Pence, 2008, Pence, 2014, GRARD, 2014). These are terrestrial and aquatic areas that need protection

because of the landscape, fauna, flora or historical significance (Carroll, 1992). These areas are protected in order to meet the biodiversity targets as determined by the systematic conservation planning (Maree and Vromans, 2010, Pence, 2014, GRARD, 2014). Systematic conservation planning is critical in identifying areas where unique biodiversity needs to be conserved in order to reduce global loss of biodiversity (Ralston *et al.*, 2009). There are ESAs, which are earmarked to safeguard the CBAs for example. if a river is classified as a CBA there is need to set a buffer surrounding it to prohibit any form of activity close to it to avoid siltation and pollution among other effects (Ralston *et al.*, 2009, Maree and Vromans, 2010, Pence, 2014, GRARD, 2014). Areas classified as CBAs and ESAs are regarded as highly sensitive areas, which are *"no-go"* areas for any development. They are used as biodiversity informants needed to support land use planning and decision-making (Ralston *et al.*, 2009, Maree and Vromans, 2010, Pence, 2014, GRARD, 2014). With the increase in urbanisation, are the guidelines from CBAs maps followed as the urban areas grows? Is there any difference of how settlements are established between high, medium and low-density areas? Is there any difference in how the CBAs are preserved in the former townships and in the former suburbs?

This study is focusing on analysing temporal and spatial variations of urban sprawl in suburbs (medium and low-density) and townships (high-density) in the CoT using high-resolution remote sensing imagery. The objective of this study is therefore, to quantify and compared urban expansion in the low, medium and high-density areas in the CoT from 2008 using SPOT 5 and 6 satellite images. The study additionally assessed the impact of urban growth on CBAs.

5.3 Study Area

The CoT (Figure 22) is popularly known as the City of Pretoria is the administrative capital of the Republic of South Africa and located in the North of the Gauteng Province. The city was founded in 1855 by Marthinus Pretorius and renamed to Tshwane in 2000 (Raper, 2008, Van der Vyver, 2015). It merged with Metsweding District following the Gauteng Global City Region Strategy (Matlala, 2015). COT has 7 regions, 105 wards and 210 councillors and is the single largest municipality. CoT

lies between latitudes 25°6’34.60” S to 26°4’41.12” S and longitudes 27°53’24.26E to 29°5’54.31” E. The city landmass of 629 618 ha, 2 921 490 people and 911 536 households based on the census data of 2011. The population of the CoT was 1 770 330 in 1996, 2,142,322 in 2001 and 2,921,488 in 2011 (STATSSA, 2012). COT experiences sub-tropical climate with hot and rainy summer and very cold and dry winter.

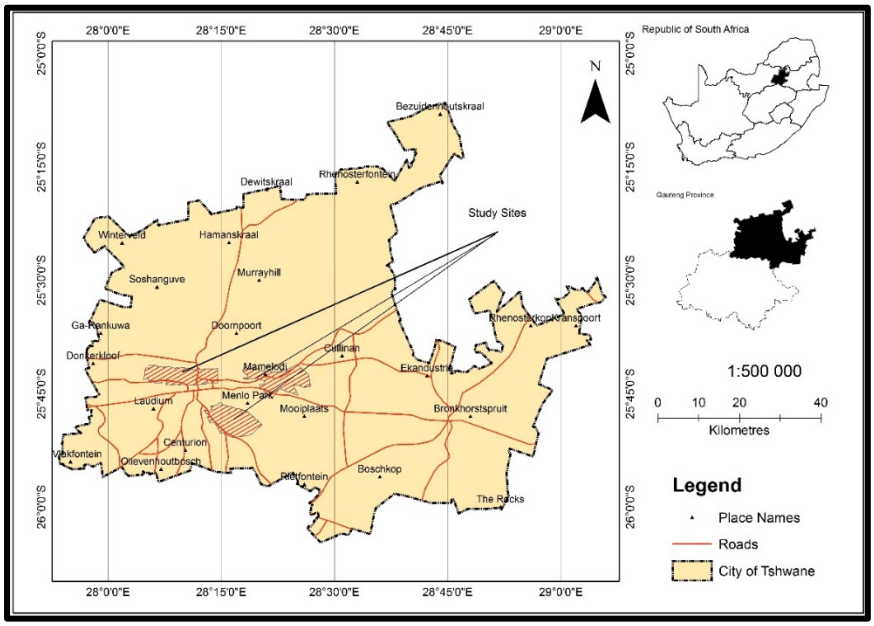

Figure 22: The study area CoT Municipality) situated in Gauteng Province, South Africa.

5.4 Data and Methods

The flowchart (Figure 23) illustrates the methodology used to extract urban areas using the SPOT satellite imagery. The SPOT 5 and SPOT 6 (Table 18) remote sensing imagery that was acquired from ASTRIUM (ASTRIUM, 2017) through the South African National Space Agency were used in this study. The properties of the imagery used in this study is in Table 18. Pre-processing of the satellite imagery (layer staked, image enhancement and clipping into the three study was carried out using ERDAS Imagine (Intergraph, 2014). The satellite images for the three different years (2008, 2012 and 2015) and for three different study sites were classified using the supervised MLC in ERDAS Imagine (Intergraph, 2014). Supervised MLC is better than

unsupervised classification as it allows integration of expert knowledge and spectral information in the extraction of land covers classes (Congalton, 1991, Weng, 2012). The supervised MLC is based on the simple probabilistic classifier by Naive Bayes where pixels are assigned classes based on the probability of belonging to a particular class as determined by user-defined trained sites (Sisodia *et al.*, 2014). The results according to Sisodia *et al.* (2014) MLC are more robust classification method with few chances of classification errors. Land cover maps were classified into four main classes, which are water, natural vegetation, agriculture and urban areas (impervious surfaces), which were later reclassified into two classes (built-up and non-built-up areas). The accuracy of all the classified images was above 85% for all classifications and its shows the classification was accurate.

After image classification, the size (area) of the built-up areas was calculated to determine the areas covered by impervious surface. The size of built-up areas was computed and compared amongst the three sites (spatially) and the three years (temporal). Two research questions were considered: How did urban growth in the chosen sites affected natural habitat? What was the impact of urban growth on the areas earmarked for conservation (CBAs)? The study assessed the impact of urban growth on CBAs and ESAs. Size (area) of CBAs) and ESAs that were affected by urban growth were calculated and compared among the years and the three places.

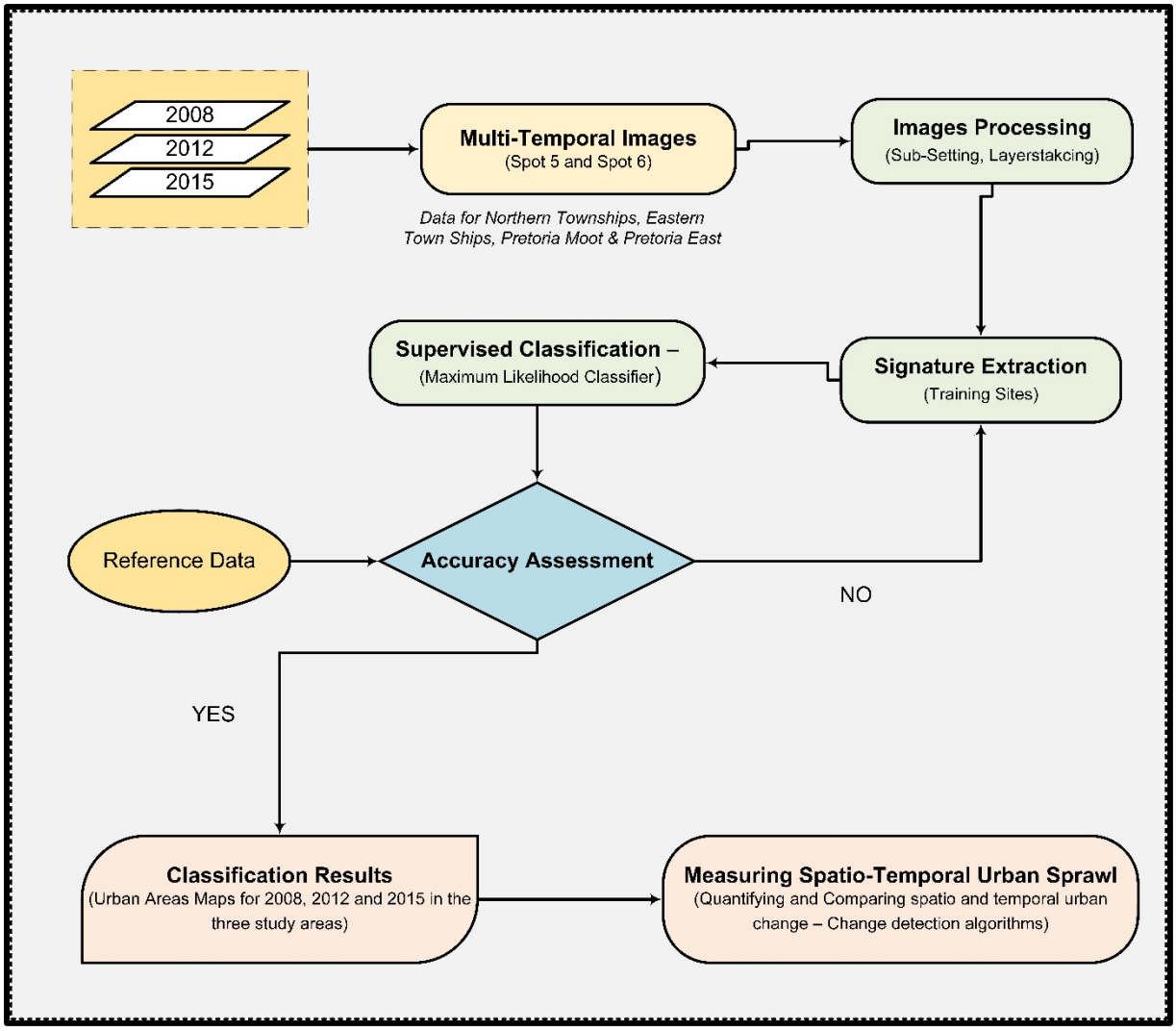

Figure 23: The methods used to extract and analyse spatio-temporal change in urban areas in different sites (low, medium and high-density areas).

Table 18: Characteristics of the SPOT 5 and SPOT 6 satellite images that were used in this study

	SPOT 5	SPOT 6
Launch Date	3 May 2002	9 September 2012
Orbital Altitude	822Km	694km
Swath	60*60km (nadir)	60*60km (nadir)
Radiometric Resolution	8 Bits	12 bits
Spatial Resolution	Pan: 2.5m from 2 x 5m scenes, Pan: 5m (nadir),MS: 10m (nadir), SWI: 20m (nadir)	Panchromatic - 1.5m, Multispectral-6.0m (B,G,R,NIR)
Spectral Resolution	Pan: 480-710 nm, Green: 500-590 nm, Red: 610-680 nm, Near IR: 780-890 nm, Shortwave IR: 1,580-1,750 nm	Panchromatic (1.5m), Multispectral 6.0m (B,G,R,NIR)
Temporal Resolution	2-3 Days	1-3 Days

5.5 Results and Discussions

In the eastern townships, which are composed of high-density areas (both formal and informal housing) there was an increase in built-up areas. There was a noticeable land cover change from 2008 (Figure 24), 2012 (Figure 25) and 2015 (Figure 26). There were 2997.08 ha of built-up areas in 2008, 3668.87 ha in 2012 and it increased to 4137.07 ha in 2015 as shown in Table 19 and Figure 36. The rate of increase in built-up between 2008 and 2015 was 5.43% per annum (Table 19) and the urban areas increased by 38% (1139.99 Ha) (Table 19) from 2008 to 2015. There was a notable increase in the impervious surface as depicted in Figure 24, Figure 25 and Figure 26.

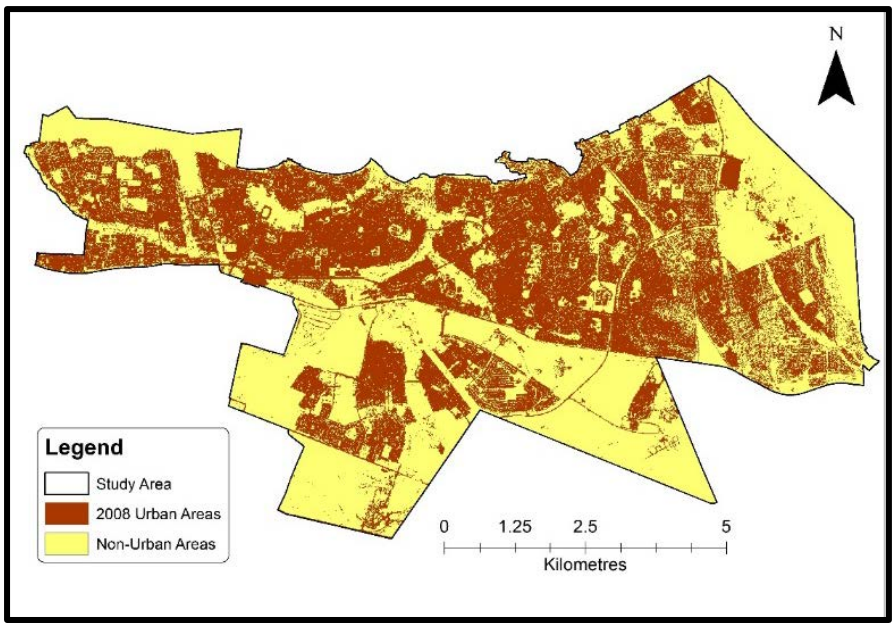

Figure 24: Built-up areas in the Eastern Townships in 2008 derived from a supervised classification of the SPOT 5 Satellite imagery of 2008.

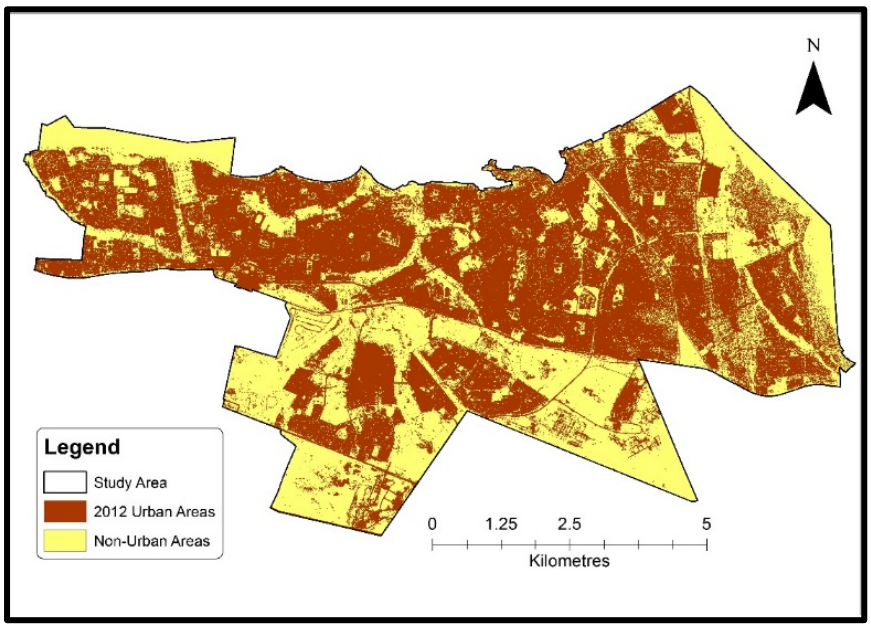

Figure 25: Built-up areas (Urban areas) in the Eastern Townships in 2012 derived from a supervised classification of the SPOT 5 Satellite imagery of 2012.

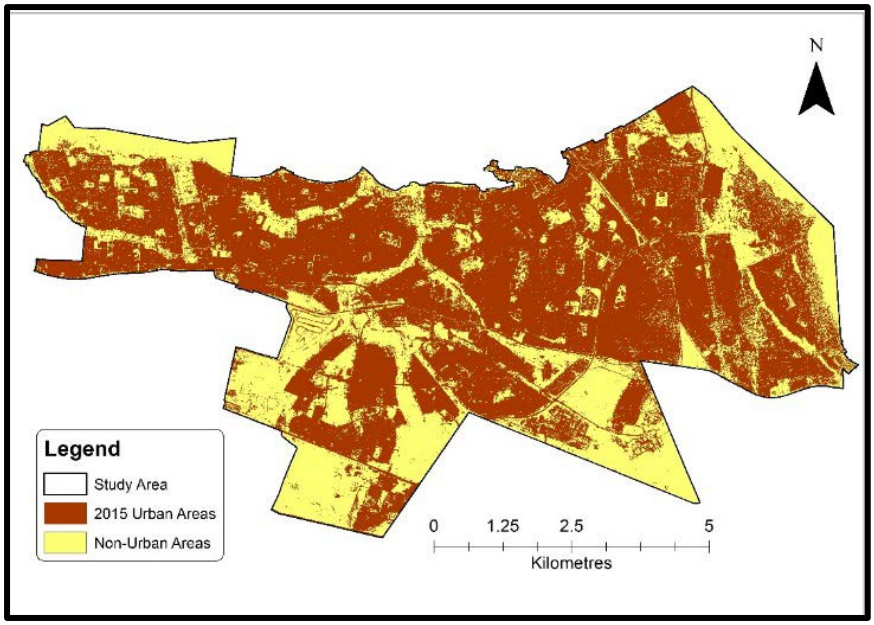

Figure 26: Built-up areas in the Eastern Townships in 2015 derived from a supervised classification of the SPOT 6 Satellite imagery of 2015.

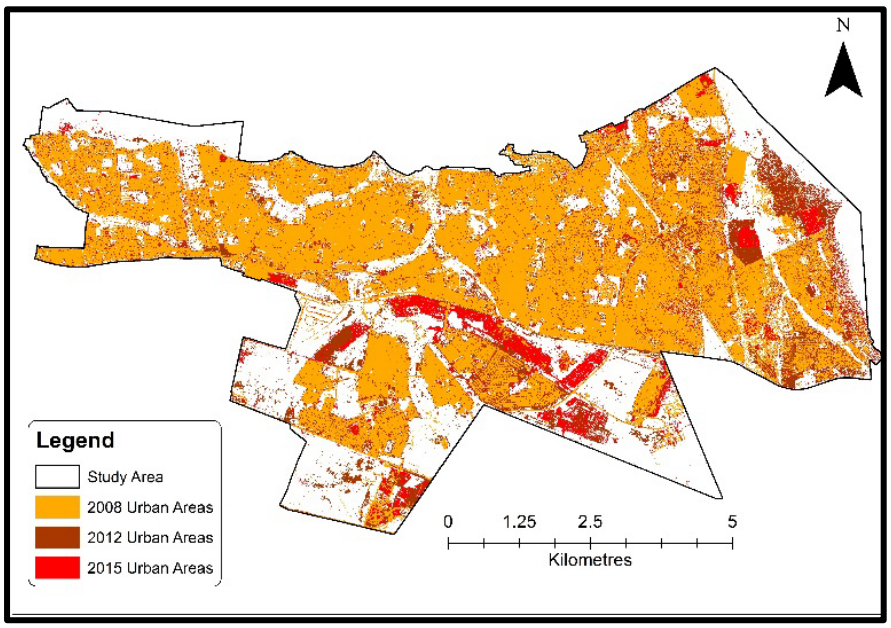

Figure 27. Changes in Built-up areas from 2008 to 2015.

In the Pretoria Moot area, there were 2747.85 ha in 2008, 3159.92 ha in 2012 and 3441.30 ha in 2015 as shown in Table 19, Figure 28, Figure 29 and Figure 30. The rate of increase in built-up between 2008 (Figure 28) and 2015 (Figure 30) was 3.61% per annum (Table 19) and the percentage increase between the two years (2008 and

2015) was 25% which was 693.72 ha (Table 19). There was an increase in the impervious surface as depicted in Figure 31.

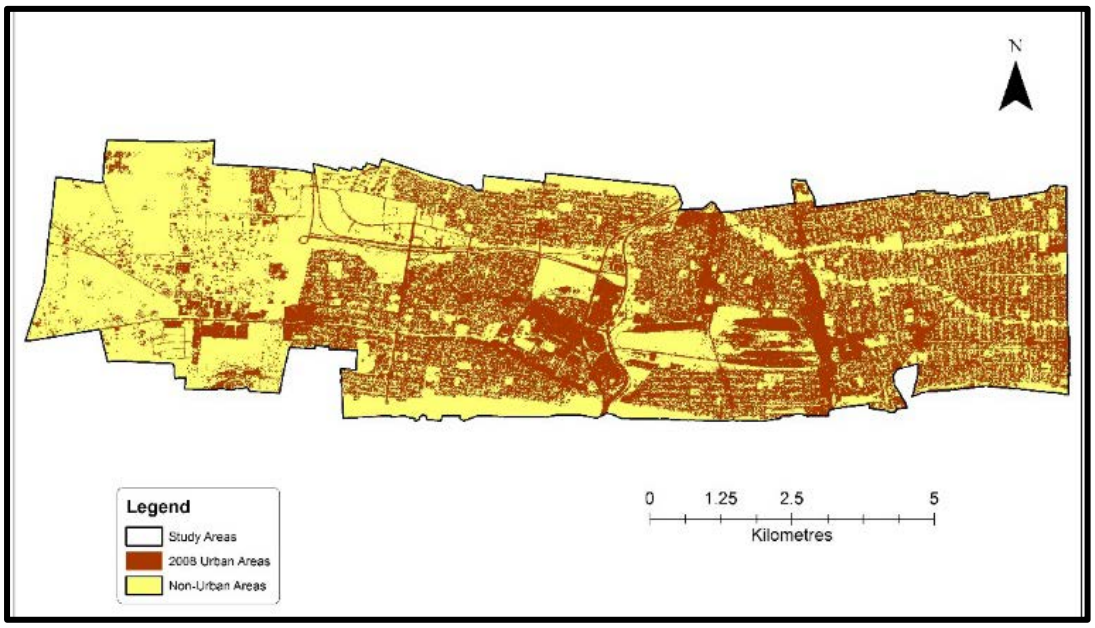

Figure 28: Built-up areas in Pretoria Moot in 2008 derived from a supervised classification of the SPOT 5 and SPOT 6 Satellite imagery of 2008.

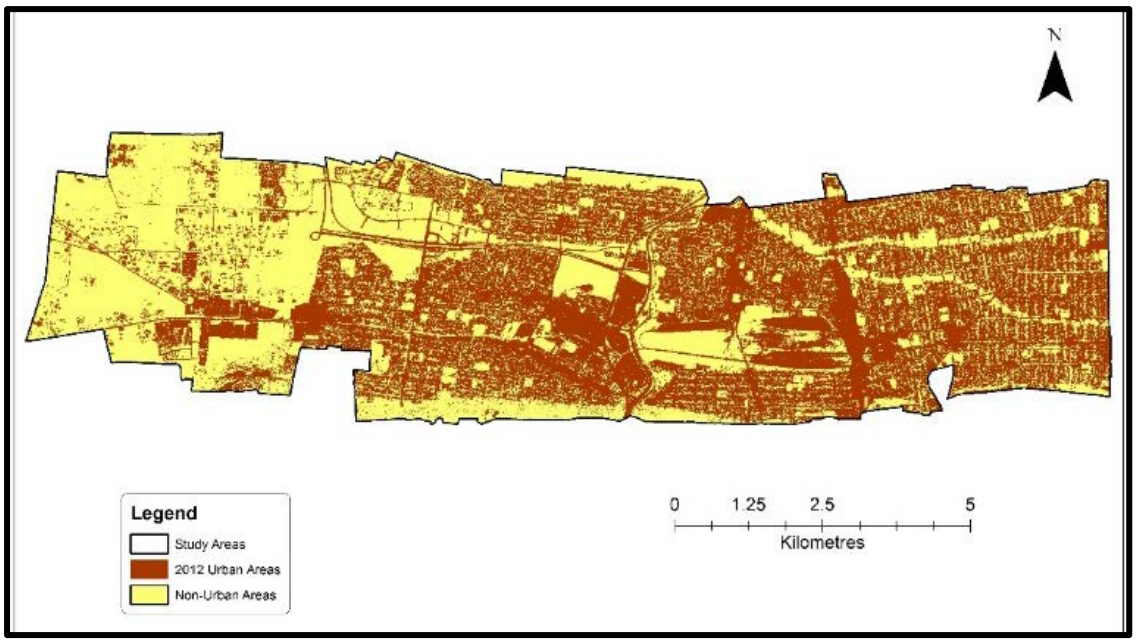

Figure 29: Built-up areas in Pretoria Moot in 2012 derived from a supervised classification of the SPOT 5 and SPOT 6 Satellite imagery of 2012.

Figure 30: Built-up areas in Pretoria Moot in 2015 derived from a supervised classification of the SPOT 5 and SPOT 6 Satellite imagery of 2015.

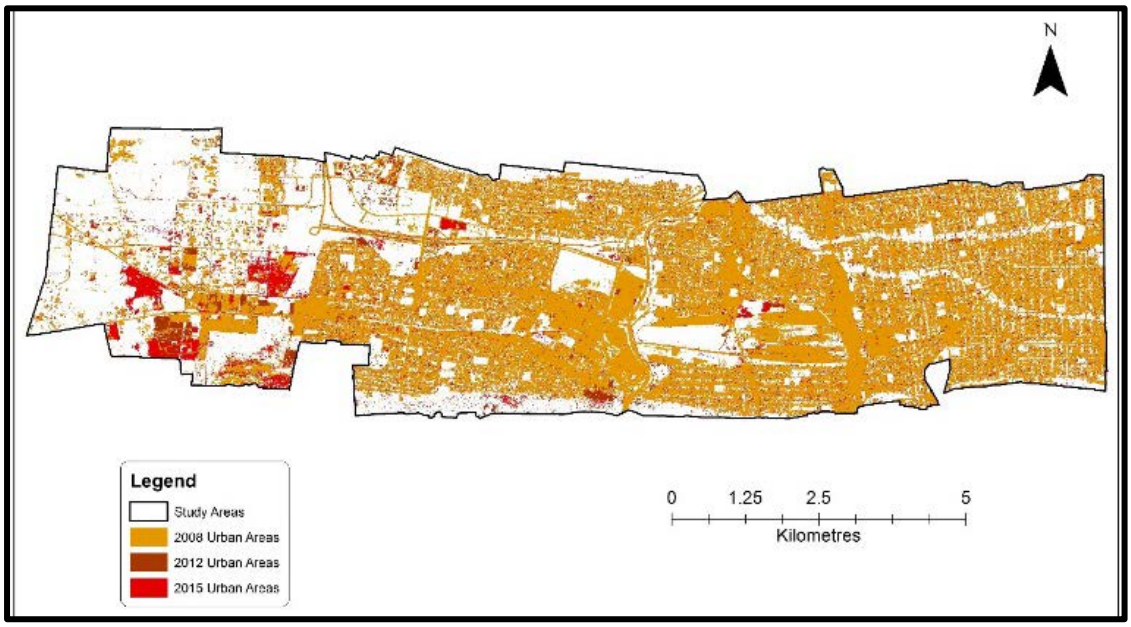

Figure 31: Changes in Built-up areas from 2008 to 2015.

As for the low density areas in Pretoria East, the size of built-up areas remained constant at 3499.10 ha in 2008 (Figure 32) and 2012 (Figure 33) and it increased to 3981.82 ha in 2015 (Figure 34) as shown in Table 19. The rate of increase in built-up areas between 2008 and 2015 was 5.43% (Table 19) and the percentage increase between the two years was 13.80% which was 482.72 ha (Table 19). There was no significant change in the increase in impervious surface and Figure 35 shows few patches, which depict an increase in impervious surfaces.

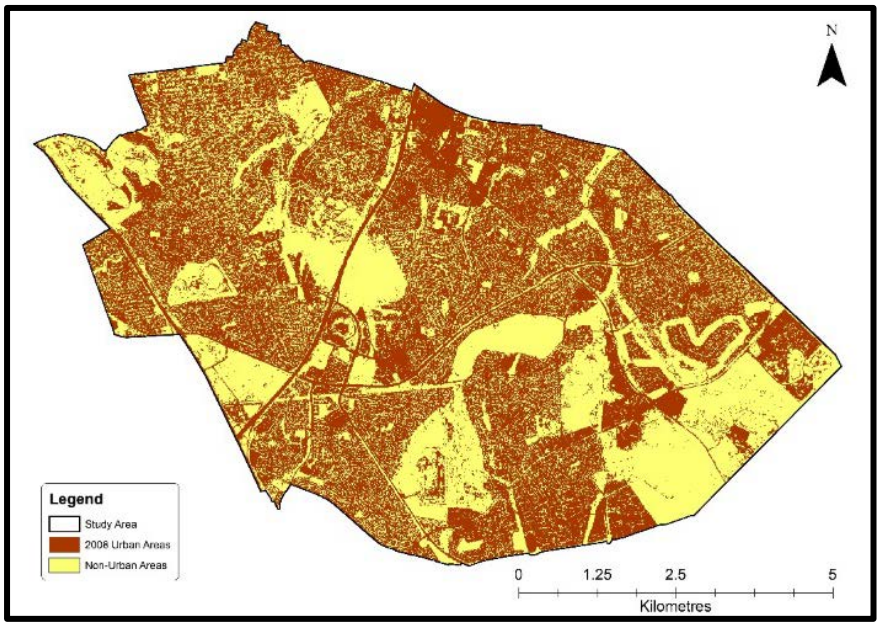

Figure 32: Built-up areas in Pretoria East in 2008 (derived from a supervised classification of the SPOT Satellite imagery of 2008.

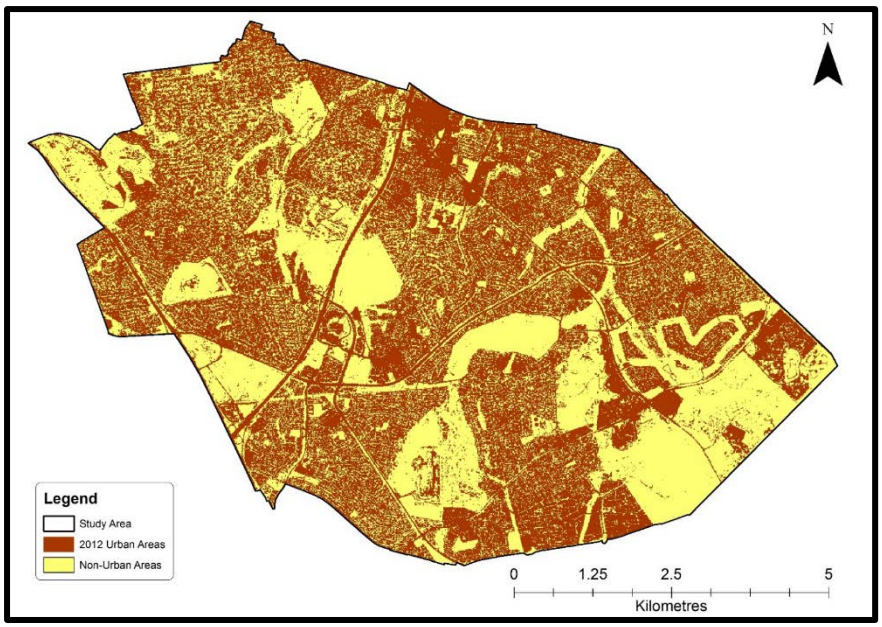

Figure 33: Built-up areas in Pretoria East in 2012 derived from a supervised classification of the SPOT Satellite imagery of 2012

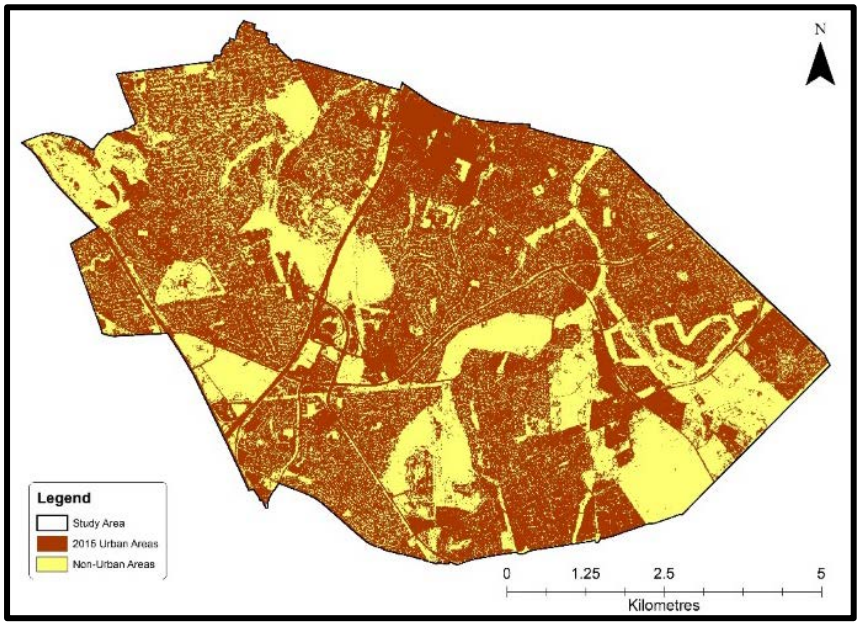

Figure 34: Built-up areas in Pretoria East in 2015 derived from a supervised classification of the SPOT Satellite imagery of 2015

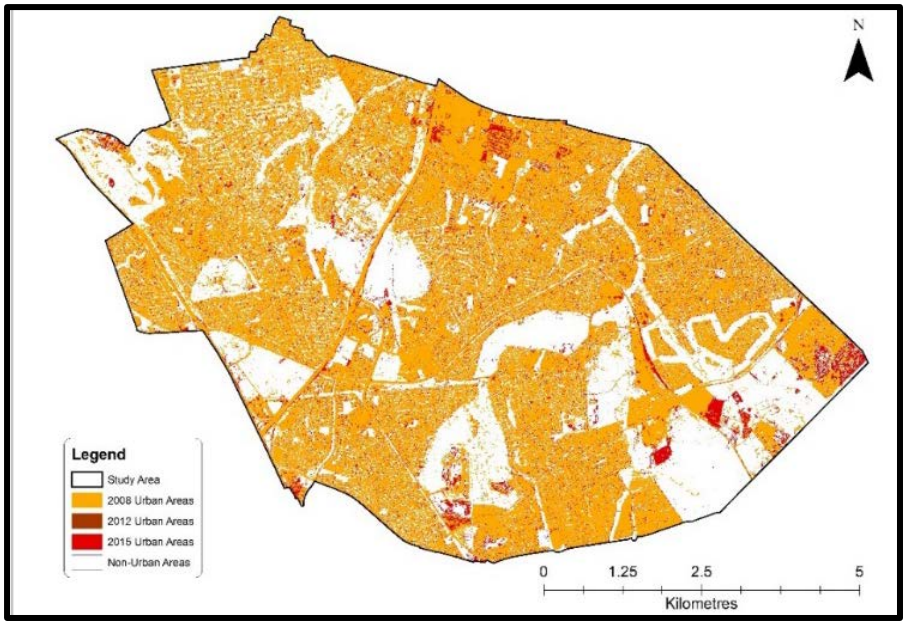

Figure 35: Changes in Built-up areas between 2008 and 2015 in Pretoria East.

Table 19: Areas and rate of change of Built-up areas in Pretoria East, Pretoria Moot and Eastern Township from 2008 to 2015 derived from a supervised classification of SPOT images.

		Eastern Townships	Pretoria East	Pretoria Moot
Area Covered by urban areas	2008 (Ha)	2997.08	3499.10	2747.58
	2012 (Ha)	3668.87	3499.10	3159.92
	2015 (Ha)	4137.07	3981.82	3441.30
Change in Urban Areas	2008 -2012 (Ha)	671.79	0	412.34
	2008 -2012 (%)	22.41%	0	15%
	2012 -2015 (Ha)	468.20	482.72	281.38
	2012 - 2015 (%)	12.76	13.80	8.90%
	2008 - 2015 (Ha)	1139.99	482.72	693.72
	2008 - 2015 (%)	38%	13.80%	25%
	Rate of Change (2008-2015)	5.43%	1.97%	3.61%

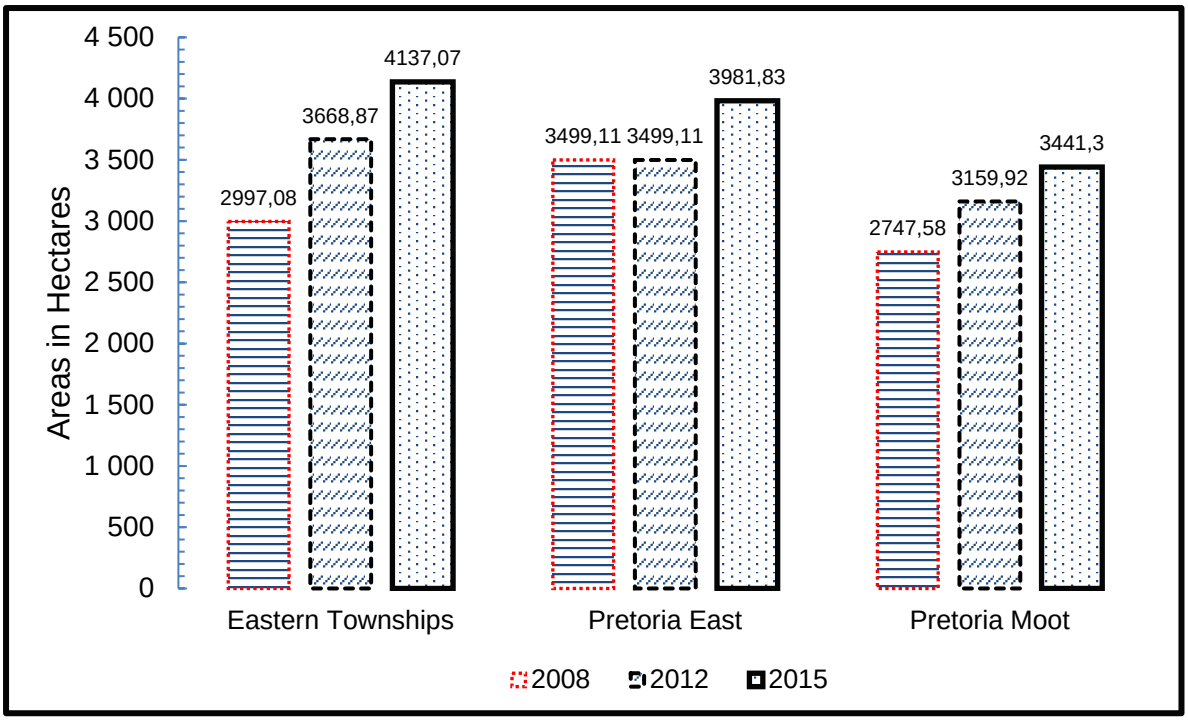

Figure 36: Spatio-temporal change in Built-up areas in Eastern Townships, Pretoria East and Pretoria Moot from 2008 to 2015 derived from supervised classification of the SPOT images.

High degree of land cover change was evident in the high-density areas as compared to the low-density and the medium-density areas. Low-density areas were already developed and in the high and medium-density areas, there was still available space, which can be used for development. The rate of change into built-up areas in Pretoria East was not as high as compared to the Pretoria Moot and Eastern Townships. Changes in Eastern Townships were mainly because there were new residential settlements (RDP houses and property development by private developers) and there were increases in informal settlements along the railway line in Nellmapius, Lusaka and Mahube in Mamelodi. There was an increase in informal settlements along the mountains in Mahube and Lusaka and they have invaded the mountainous areas in their vicinity. In Pretoria Moot, there was development due to RDP houses close to Mountain View. There were development of informal settlements in Gomora and house development from private developers in Kirkney and in Andeon. There were

few changes in Pretoria East other than the increase in the informal settlements in Moreleta Park.

One of the main drivers of land cover change in the CoT was informal settlements. The establishments of these informal settlements led to the invasion of pristine areas set aside to maintain conservation targets (CBAs and ESAs). There were informal settlements in all the study areas, which were Gomora in the Pretoria Moot, Mahube in Eastern Townships, Lusaka in the Eastern Townships and new informal settlement developing along the railway lines in Nellmapius (Eastern Townships). Urban renewal projects such as roads, new buildings and formal housing such as RDP houses have accelerated increase in the built-up areas between the years and in all the different areas. In the townships, house owners were extending their houses to create backyard suburbs and informal non-permanent structures in their stands to augment their income.

These results agree with the study done in Puerto Rico where there was a high urban sprawl in urban areas as compared to low-density areas (Martinuzzi *et al.*, 2007). In the same study it was argued that in low-density areas, there was a non-contiguous pattern of development which grows from urban areas in main urban centres in linear features such as roads (Martinuzzi *et al.*, 2007). In the study by Jat *et al*. (2008) there was high percentage of impervious surfaces in area high-density areas as compared to low-density areas (Jat *et al.*, 2008). In Nairobi, Kenya the growth of urban environments has been accompanied by severe loss of forests and encroachment of urban-like conditions into those forests and agricultural areas (Mundia and Aniya, 2005). The study suggested that economic growth and proximity to transportation routes were the main factors that lead to urban growth in Nairobi (Mundia and Aniya, 2005).

5.5.1 CBAs in Pretoria East, Pretoria Moot and Eastern Townships

With the increase in urban areas in the CoT, some of the areas earmarked as CBAs were transformed. As depicted on the maps, Figure 37, Figure 38 and Figure 39 there were areas, classified as CBAs, which were transformed into built-up areas. In the low-

densities (Figure 38) only 11.71% (Table 20) of the areas that were earmarked for conservation (CBA) to meet the conservation targets which were transformed into impervious surfaces. In the medium-density areas (Figure 37), 17.19% (Table 20) of the CBAs and their ESAs were transformed into built-up areas. The high-density area suffered transformation of the natural habitat due to urbanisation. Eastern Township (Figure 39) experienced a loss of 15.55% (Table 20) of CBAs.

Some of the areas, which were once CBAs but have been transformed, are circled in red in Figure 37, Figure 38 and Figure 39. In the high-density and medium-density suburbs, some of the highly sensitive areas were transformed into built-up areas (formal and informal settlements). This study showed how vulnerable non-urban and sensitive areas were to future and unplanned land use development in medium and high-density areas. The information generated from this study can be used as an informant to responsible authorities in decision-making and can help identify challenges faced by cities and towns because of the continual and unprecedented increase in urbanisation.

This was also a concern in Taipei according to the research done by Huang *et al.* (2009) where landscapes transformed from forestry to urban area (Huang *et al.*, 2009).

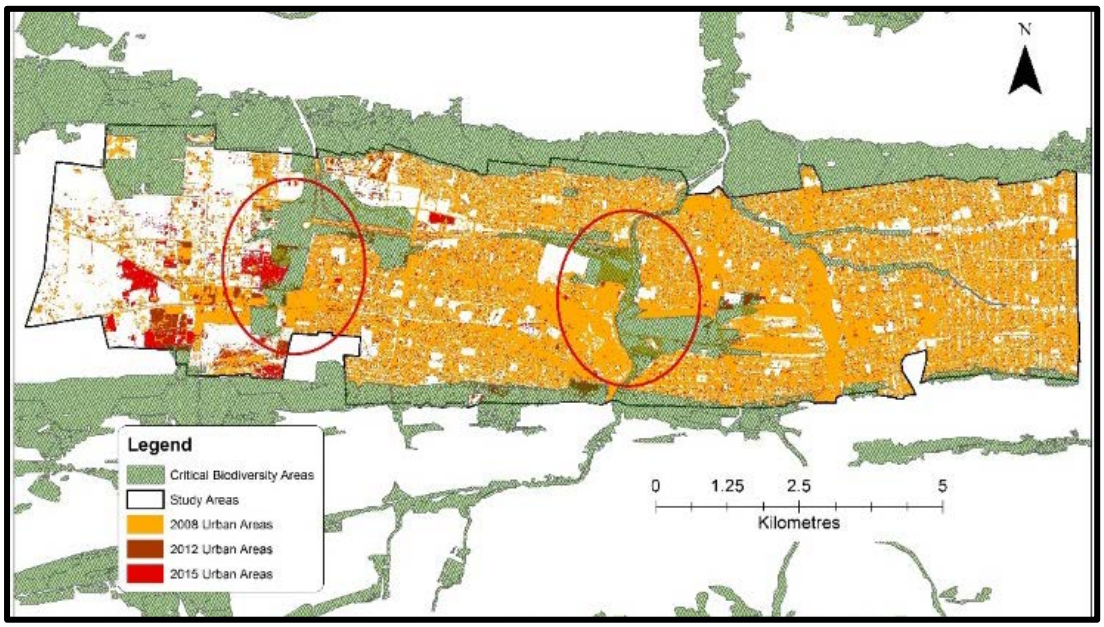

Figure 37: Maps of Pretoria Moot showing Built-up areas and the CBAs. Areas encircled in red earmarked for conservation but were transformed due to urbanisation.

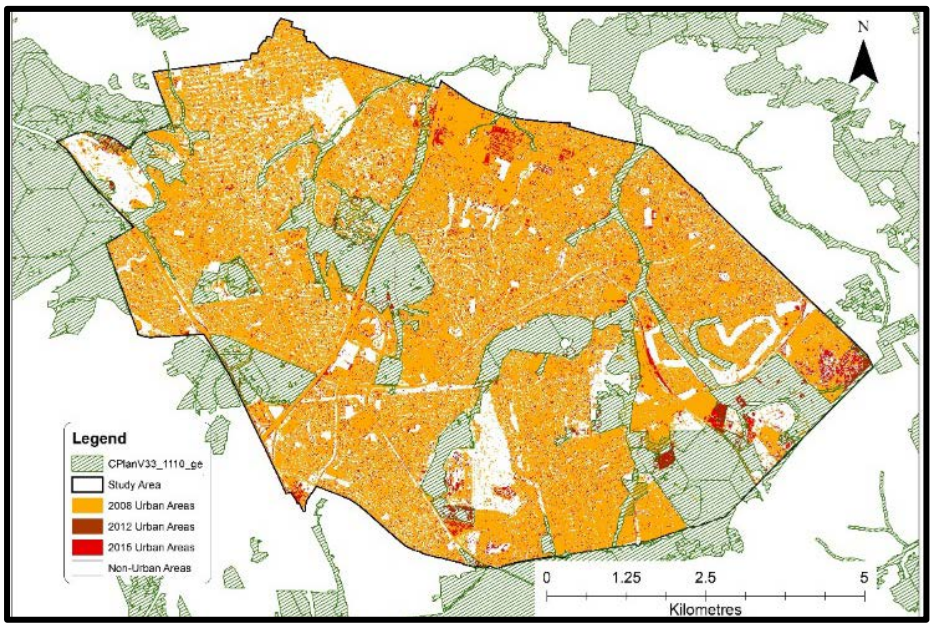

Figure 38: Maps of Pretoria East showing Built-up areas and the CBAs. Areas encircled in red earmarked for conservation but were transformed due to urbanisation.

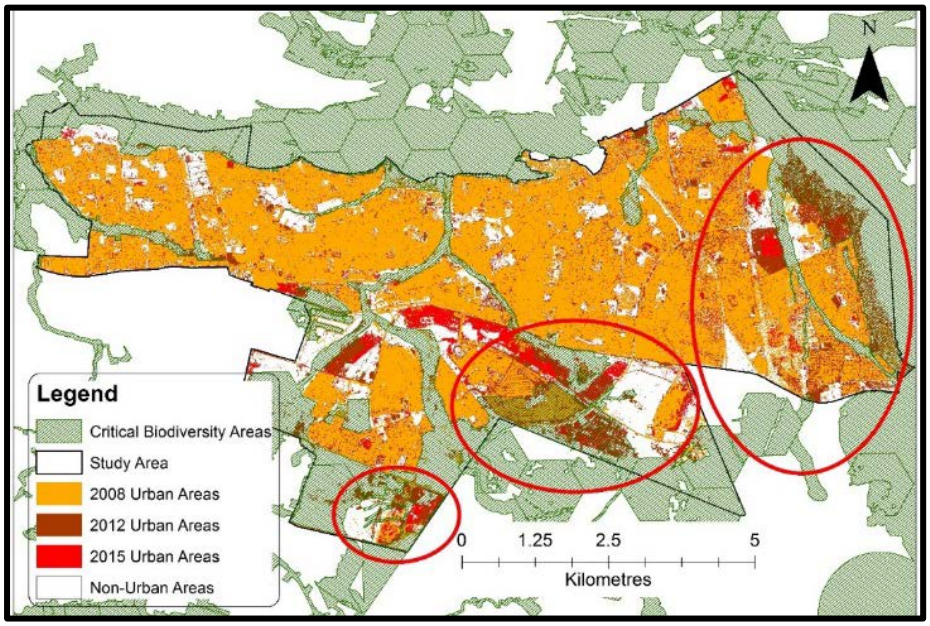

Figure 39: Maps of Eastern Townships showing Built-up areas and the CBAs. Areas encircled in red earmarked for conservation but were transformed due to urbanisation

Table 20: Table showing the proportion of CBAs that were transformed into impervious surfaces

	Pretoria Moot	Pretoria East	Eastern Townships
Transformed CBA (Ha) -2015	169.62	135.15	436.23
Areas CBA (Ha) - 2015	986.79	1154.08	1707.64
% Transformed CBA (%) - 2015	17.19	11.71	25.55

5.6 Conclusions

There was generally a higher increase in built-up areas in high-density areas as compared to low-density and medium-density areas. The main drivers of urban change in any environment in Pretoria whether low-density, medium-density or high-density was the increase in housing because of urbanisation. There was unprecedented urban growth in the townships than in low-density suburbs but the emergence of informal settlements, as low-income workers in the low-density areas prefer to stay close to workplaces, hence the establishment of these informal settlements.

In addition, some of the areas that were classified as CBAs, which are regarded as “no-go” areas or highly sensitive areas have also been affected by the growth of these urban areas. Now, these settlements are permanent features in the areas previously earmarked for conservation and there is a need for the responsible authorities to re-run the systematic conservation planning to establish new CBAs. For proper ecosystem functioning, there is a need for the enactment of laws that will protect unlawful invasion of areas that were earmarked for conservation. There is a need for continuous monitoring of urban areas using very high-resolution imagery such as QUICK BIRD, IKONOS, Worldview and other sensors with better spatial resolution other than SPOT that was used in this study. There is need to explore other very high

satellite sensors in assessing urban growth in low, medium and high-density. It will aid in showing the densification because of backyard houses and change in land cover.

CHAPTER SIX

6 MONITORING VEGETATION PHENOLOGY USING MODIS NDVI 250M IN THE COT, SOUTH AFRICA.*

6.1 Abstract

The unprecedented influx of people into urban areas has serious impacts on the horizontal and vertical growth of urban environments. One of the impacts of urbanisation is the encroachment of urban-like environments into non-urban areas. This is common in urban areas in both developed and developing countries and South Africa's CoT, which is the administrative capital, has been affected by urbanisation because of migration. One of the parameters or proxies used to quantify urban growth is vegetation cover. There is a consensus that with the increase in the population of urban dwellers vegetation cover will decrease. In order to measure the vegetation cover the MODIS NDVI data with a 250m spatial resolution was used to assess the impact of urban growth on vegetation. Time series plots of the MODIS NDVI was used to establish the patterns of vegetation cover in different sampling areas. Trends in vegetation were determined in newly developed residential areas, informal settlements, central business district and different vegetated areas. Sen's slope estimator, p-value and the Mann-Kendall statistics with a significance level (α) of 0.05 were used to analyse the spatial trends and variations in trends among different land cover types. The slope of the trends differs significantly but there is a general decline in vegetation cover. The temporal profiles revealed seasonal variations in vegetation (showing browning (low NDVI) in winter and greening (high vegetation) in summer from 2000 to 2016. Conclusively urban growth has an impact on the vegetation vigour. It is crucial to integrate MODIS NDVI 250m data and datasets from other sensors to assist in assessing the impact of urban growth on vegetation cover.

---

* Submitted in the South African Journal of Geomatics, currently under review

Keywords: Urban areas, Remote Sensing, MODIS, Phenology, Time Series Analysis, Mann-Kendall

6.2 Introduction

The influx of people into urban areas has led to urban sprawl which is the outward growth of urban-like environments into the non-urban environments (Cobbinah and Amoako, 2012, Turok and Borel-Saladin, 2016). United Nations (2014) has estimated that there will be an increase in global urban population by about 3 billion by the year 2050 which will be double the present urban population (United Nations, 2014). Urban sprawl is the encroachment of urban-like characteristics into non-urban environments (Cobbinah and Amoako, 2012). Its effects have attracted a lot of attention with urban developers and decision-makers. Urban sprawl entails transforming natural areas, agricultural areas into urban conditions and has a negative impact on the natural ecosystems (Grobler *et al.*, 2006, Zeng *et al.*, 2015).

The establishment of houses, industries and shopping complexes has its own impact on the environments (Grobler *et al.*, 2006). Urban dwellers, local authorities and land developers plant their own trees and grass (lawn) thereby establishing their own urban ecosystems. Construction and extension of road networks have accelerated the conversion of non-urban-like environments into urban areas (Walters, 2013, Wood, 2014). This includes the construction of Gautrain, the widening of the roads and the construction of the bus transit system for Areyeng buses in the CoT (Walters, 2013, Wood, 2014). With the increase in population, the responsible authorities are failing to cope with the increase in urban dwellers; there will be much pressure on the available resources (Turok and Borel-Saladin, 2016, Smit *et al.*, 2017). Rapid urban population growth has posed housing challenges (Munyati and Motholo, 2014, Turok and Borel-Saladin, 2016, Tiwari *et al.*, 2016). The government cannot provide decent housing, so people resort to make shift houses (shacks) and those in established houses also establish back-yard suburbs (Munyati and Motholo, 2014, Turok and Borel-Saladin, 2016, Tiwari *et al.*, 2016).

There are many informal settlements in different locations of the CoT and they are situated in different places, in low-density, medium-density and high-density areas

(THDA, 2012, Munyati and Motholo, 2014). As urban areas develop, they encroach into some of the areas are undeveloped areas thereby leading to habitat fragmentation (Grobler *et al.*, 2006). Nature reserves and parks in the CoT have a high-density of natural vegetation and the un-conserved areas have suffered from massive deforestation due to the need for firewood (Chishaleshale *et al.*, 2015). Some of natural vegetation still maintain thick bushes as compared to the natural areas in close proximity of residential areas especially the informal settlements where the source of energy is firewood (Grobler *et al.*, 2006, NPC, 2011).

There are some urban renewal projects, construction of malls and mining of stones in the city, which have brought about an increase in urban areas (Wen *et al.*, 2017). Therefore, the establishment of these facilities for example roads, malls, residential suburbs came with the growth of indigenous and exotic vegetation species as planted by the residents, local government or developers thereby establishing an urban ecosystem (Cobbinah and Amoako, 2012, Turok and Borel-Saladin, 2016). Some of the vegetation will grow to cover the established structures (roads, houses, offices, industries) (Chishaleshale *et al.*, 2015). In the CoT, most of the roads are full of the jacaranda trees and other non-invasive and invasive species which have high social, cultural, economic, landscape and ecological value in the city (Dickie *et al.*, 2014, Little, 2014).

The advent of remote sensing and GIS has provided a cost-effective unique tool, to assess and monitor qualitative and quantitative urban land cover change (Jat *et al.*, 2008, Bhatta *et al.*, 2010, Espindola *et al.*, 2017). With observational and repetitive capacity, remote sensing and GIS techniques are used in quantifying, monitoring and predicting urban land cover changes which are beneficial to decision-makers and planners (Jat *et al.*, 2008, Wen *et al.*, 2017, El Garouani *et al.*, 2017). There are many parameters used to quantify and monitor urban sprawl and one of them determines the greenness of the environment (Wen *et al.*, 2017, El Garouani *et al.*, 2017). Phenology (vegetation temporal variation) is a suitable indicator to assess land cover change. In order to assess seasonality there is a need for statistical tests such as Mann-Kendall statistics (Kendall, 1938, Mann, 1945) and Sen's slope (Sen, 1968) which assess the trends in vegetation change with time. There are transformational

vegetation indices that are utilised to measure vegetation vigour and the most popular is Normalised Difference Vegetation Index (NDVI). MODIS NDVI is rarely used to assess change in urban areas because of its low spatial resolution but its continuity allows assessing the continuous variations because of climate change and human changes. MODIS NDVI with a 250-metre spatial resolution data was utilised in Wuhan City to profile change in vegetation cover using the TIMESAT software (Tao *et al.*, 2016, Wen *et al.*, 2017). MODIS NDVI 250m data are used to compile temporal profiles mainly because of its capability to continuously monitor vegetation as compared to some medium, high and very high spatial resolution satellite sensors.

The objective of this study is to monitor and assess spatio-temporal dynamics in vegetation cover in the CoT using MODIS Normal Difference Vegetation Index (NDVI).

6.3 Study Areas

CoT (Figure 40) popularly known as the City of Pretoria is the administrative capital of the Republic of South Africa and is located in the North of the Gauteng Province. The city was founded in 1855 by Marthinus Pretorius and renamed to Tshwane in 2000 (Raper, 2008, Van der Vyver, 2015). It merged with Metsweding District following the Gauteng Global City Region Strategy (Matlala, 2015). COT has seven regions, 105 wards and 210 councillors and is the single largest municipality. CoT lies between latitudes 25°6’34.60” S to 26°4’41.12” S and longitudes 27°53’24.26E to 29°5’54.31” E. The city landmass of 629 618 ha, 2 921 490 people and 911 536 households based on the census data of 2011. The population of the CoT was 1 770 330 in 1996, 2,142,322 in 2001 and 2,921,488 in 2011 (STATSSA, 2012). COT experiences sub-tropical climate with hot and rainy summer and very cold and dry winter.

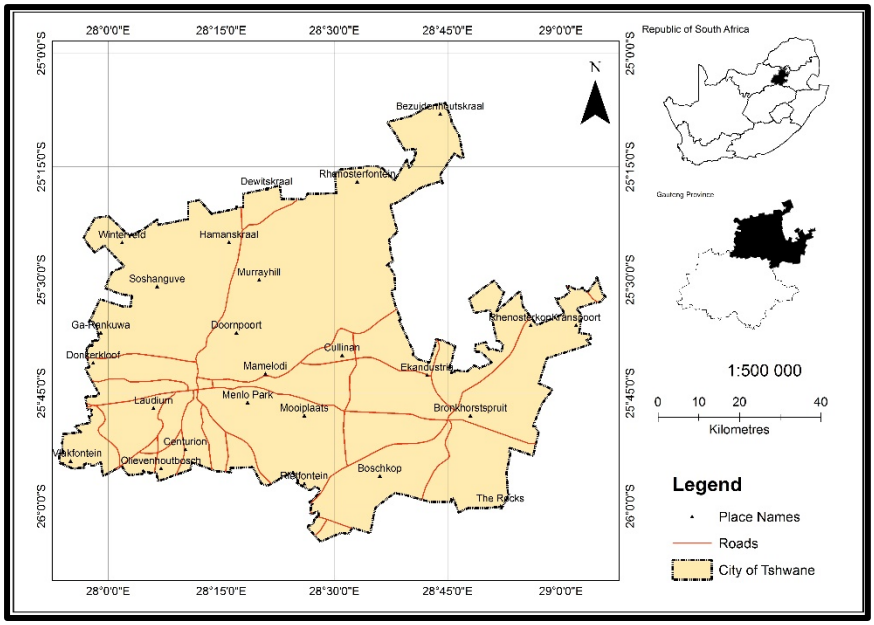

Figure 40: Map of the study area in the Gauteng Province, South Africa.

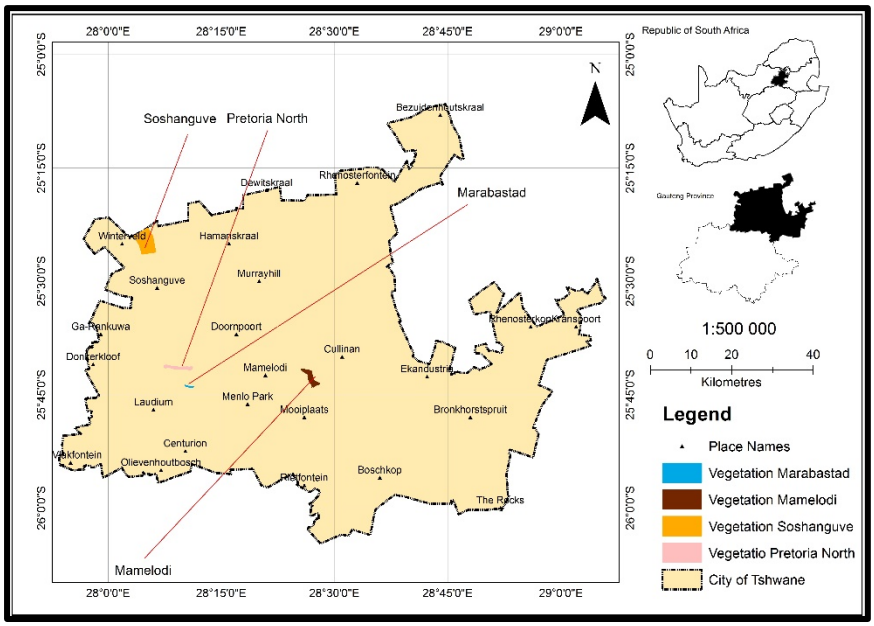

Figure 41: The study sites used to assess spatio-temporal variations in vegetation in undisturbed areas located in different locations

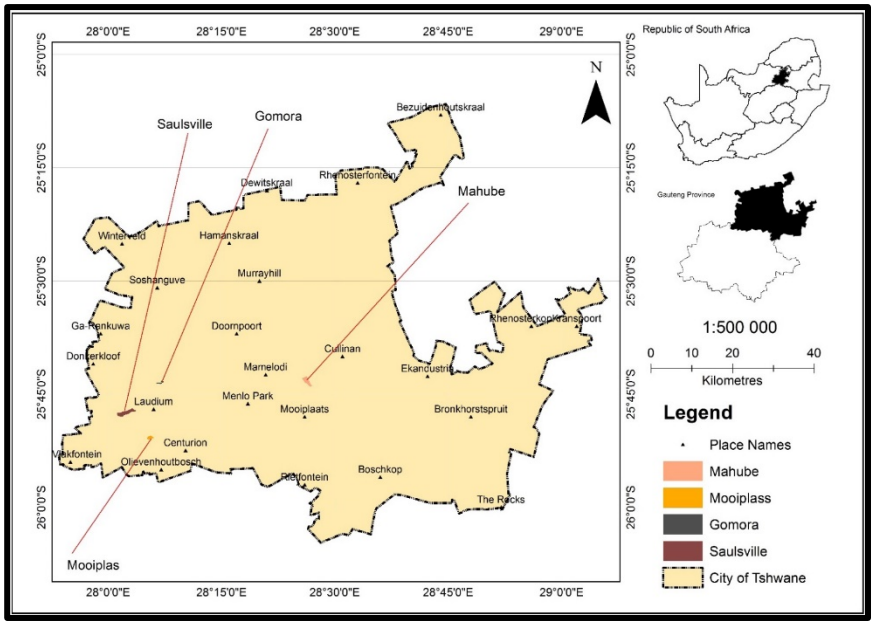

Figure 42: The study sites used to assess spatio-temporal variations in vegetation in informal settlements situated in different locations

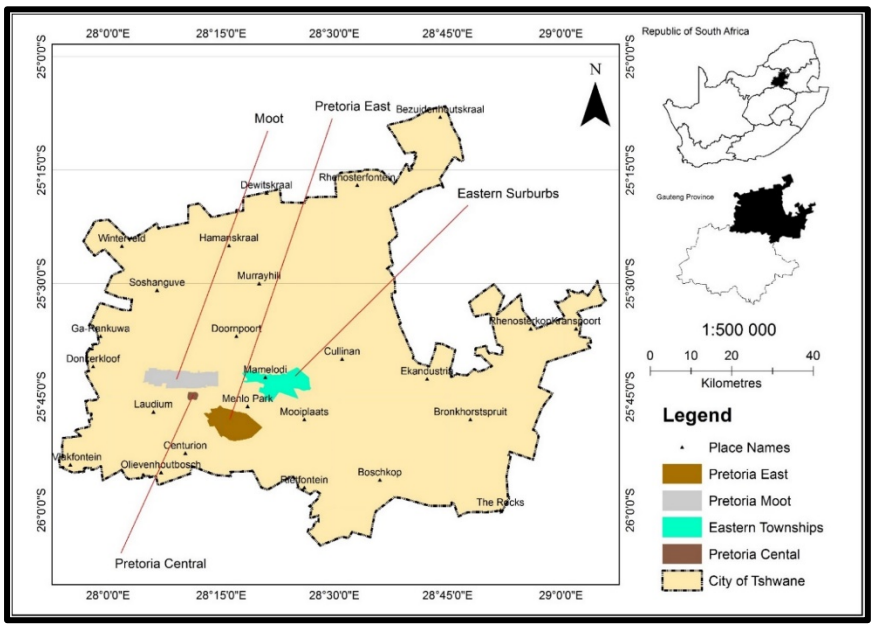

Figure 43: The study sites used to assess spatio-temporal variations in vegetation in undisturbed vegetation located in low-density, medium-density and high-density areas

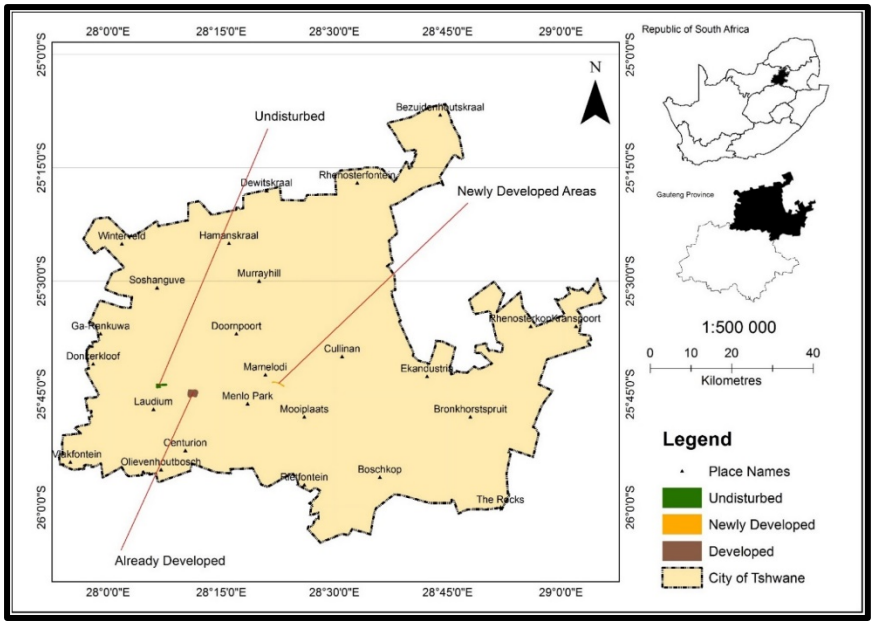

Figure 44: The study sites used to assess spatio-temporal variations in vegetation in already developed areas, undisturbed vegetation and newly developed areas.

6.4 Data and Methods

The remotely sensed data that was used in this study is the MOD13Q1 v005 product recorded by NASA's Terra satellite downloaded from the USGS data portal for a period from February 2000 to December 2016. Some of the products in the MOD13Q1 include the 250m EVI and NDVI data, reflectance data derived from the maximum value composite (MVC) which has a temporal resolution of 16 days. After downloading, the projection of the data was changed from Sinusoidal (SIN) projection to Universal Transverse Mercator using the MODIS Projection Tool. MODIS temporal data from 2000 to 2016 were layer stacked into a single file and thereafter clipped into the study area (Figure 40) using ERDAS Imagine (Intergraph, 2014). Phenological assessments were determined using a compound of 388 MODIS NDVI images from 2000 to 2016. Spatio-temporal profiling (times series analysis) to assess the phenology of vegetation was run using ENVI (ITT, 2007) in the whole study areas and in some portions of the study area. Mann –Kendall statistics and Sen's estimator was run on the NDVI datasets using XLSTAT (Addinsoft, 2017) to access the trend in vegetation in different land cover (Kendall, 1938, Mann, 1945). These were the main comparisons:

i. Time Series Analysis of the whole CoT (Figure 40).
ii. Time Series Analysis of natural vegetation area in low-density, medium-density and high-density areas (Figure 41).
iii. Time Series Analysis of different informal settlements (Figure 42).
iv. Time Series Analysis of high-density, medium-density and low-density areas (Figure 43).
v. Time Series Analysis of newly developed areas, natural vegetation and already developed areas (Figure 44).

6.5 Results and Discussion

Temporal variations in NDVI in the CoT and the temporal profile showed a sinusoidal curve with peaks in summer and low values in winter, which was the general characteristic of vegetation variation in the tropical regions (Figure 45) (Goldblati, 1978, Richard and Poccard, 1998). The minimum NDVI was 0.228, maximum NDVI was 0.629 and mean was 0.405 with the standard deviation was 0.114 (Table 21). The S-statistic was -232, Kendall's tau was -0.039, the p-value (two-tailed) was 0.497, the variance of 115781 and the Sen's slope was zero which means there was no trend as the vegetation content did not have much significant change. Once an urban area is established, the planners and property owners start to grow trees along the roads, in parks and in their respective properties. The p-value was greater than 0.05 which means there was a non-monotonic trend (Pohlert, 2016).

Table 21: The statistics of the change in NDVI in the CoT derived from the Mann Kendall statistical analysis

Variable	Minimum	Maximum	Mean	Std. deviation	Kendall's tau	S'	Var(S')	p-value (Two-tailed)	Sen's slope
CoT	0.228	0.629	0.405	0.114	-0.039	-232	115781	0.497	0.000

6.5.1 High, Medium and Low-density Suburbs

All these areas used for the analysis of high-density areas (Eastern Townships and Northern Townships), medium-density (Pretoria Moot) and low-density areas (Pretoria East) have a sinusoidal curve with high in summer and low in winter (Figure 46). The values of NDVI in low-density were more than that of the medium and high-density areas, with the one for the high-density areas being the lowest as depicted in Figure 46. The highest mean NDVI was 0.425 in Pretoria East (low-density area), followed by a mean NDVI of 0.415 in Pretoria Moot (Medium-density), 0.366 in the Eastern Townships (High-Density) and the lowest 0.353 in the Northern Townships (High-Density). The S-statistic was -232, Kendall's tau was -0.039 and the p-value (two-tailed) was 0.497. The Sen's Slope showed a negative value for the all the samples areas, which mean there was decreasing trend in vegetation (Table 22). The p-value was above 0.05 which mean the trend in vegetation cover in non-monotonic. The highest NDVI was in the low-density areas because there was less disturbance in vegetation cover. In the high-density areas, people cleared vegetated areas hence the low mean NDVI. The standard deviation was high in the high-density areas and low in the low-density area areas (Table 22). This was because in the high-density areas the vegetation was mainly disturbed unlike in the low-density areas. The Sen's Slope showed a negative value for the all the sampled areas, which mean there was decreasing trend in vegetation.

Table 22: The statistics of the change in NDVI in the low, medium and high-density areas in the CoT derived from the Mann Kendall statistical analysis using XLSTAT

Variable	Minimum	Maximum	Mean	Std. deviation	Kendall's tau	S'	Var(S')	p-value (Two-tailed)	Sen's slope
Eastern Townships	0.211	0.554	0.366	0.096	-0.095	-568	110981	0.089	-0.001
Northern Townships	0.196	0.573	0.353	0.106	-0.052	-310	117210	0.367	-0.001
Pretoria Moot	0.249	0.587	0.415	0.091	-0.075	-444	106880	0.175	-0.001
Pretoria East	0.274	0.567	0.425	0.074	-0.052	-308	106541	0.347	-0.001

6.5.2 Undisturbed Areas, Developed and Newly Developed suburbs

Variations of NDVI for the natural vegetation (undisturbed), for the Pretoria Central (which was already developed by 2000) and for the newly developed areas were shown in Figure 47 and they were revealed the sinusoidal variation with high vegetation vigour in summer and low in winter. The NDVI values in the natural vegetation (untransformed or undisturbed) was very high as compared to the already developed areas (Pretoria CBD). Even though Pretoria CBD (developed areas) showed high NDVI values in summer and low in winter the values were very low as compared to the untransformed areas. In the newly developed areas, the variations in NDVI values seem uniform but there was a significant drop in the summer values as shown in Figure 47. The time that coincides with these drops was the time when development in the areas started. Highest mean NDVI of 0.384 was in the undisturbed areas (natural vegetation), followed by 0.298 in newly developed areas and 0.242 in Pretoria Central (already established). The standard deviation differed between the areas with 0.110 in the undisturbed, 0.095 in newly developed areas and 0.46 in the already developed areas (Pretoria Central) (Table 23). Kendall's tau was -0.08 in the undisturbed areas, -0.154 in the already developed areas (Pretoria Central) and -0.223 in the newly developed areas (Table 23). The variance was high in newly developed

areas (140735) followed by Pretoria central (117093) and low in the undisturbed areas (113187) (Table 23). The main reason for the results was that there was an insignificant change in vegetation in the undisturbed areas as compared to the new developments and Pretoria Central. The Sen's slope in the newly developed areas was -0.03 in the new developments, -0.01 in Pretoria Central and zero in the undisturbed areas. The was a negative trend in vegetation both Pretoria Central and the new developments due to the reduction in vegetation cover but in the undisturbed area there was neither a positive or negative trend as the value was zero. The p-value for the undisturbed areas was greater than 0.05 which means there was a non-monotonic trend and its less than 0.05 in the New Developments and Pretoria Central which mean there was a monotonic trend according to Pohlert (2016).

Table 23: The statistics of the change in NDVI in the undisturbed areas, newly developed area and in the Pretoria Central derived from the Mann Kendall statistical analysis using XLSTAT.

Variable	Minimum	Maximum	Mean	Std. deviation	Kendall's tau	S'	Var(S')	p-value (Two-tailed)	Sen's slope
Undisturbed	0.212	0.581	0.384	0.110	-0.008	-46	113187	0.894	0.000
New developments	0.154	0.527	0.298	0.095	-0.223	-1328	140735	0.000	-0.003
Pretoria Central	0.151	0.349	0.242	0.046	-0.154	-914	117093	0.008	-0.001

6.5.3 Informal Settlements

There was no significant difference in the vegetation trend among the informal settlements that were used in the analysis. They all showed the high summer and low winter variations, which is a characteristic of vegetation in the tropical regions. The mean NDVI values for informal settlements was close to each other and the values were 0.345, 0.343, 0.369 and 0.328 for Mooisplaas, Mahube, Gomora and Saulsville respectively (Table 25). The mean NDVI was close to each other as they were all

ranging between 0.328 and 0.369. There was a high standard deviation of 0.116 in Mooiplaas, followed by 0.093 in Mahube, 0091 in Saulsville and the lowest was 0.088 in Gomora. Kendall's tau differed between the four places with the highest of -0.046 in Saulsville, -0.119 in Gomora, -0.182 in Mooiplaas and lastly -0.199 in Mahube (Table 24). P-values were 0.001, 0.02, 0.025 and 0.415 for Mahube, Mooiplaas, Gomora and Saulsville respectively. There were variance values of 1306641 in Mahube, 123117 in Mooisplaas, 114011 in Saulsville and 99369 in Gomora (Table 25). Sen's slope was -0.003 for Mooiplaas and Mahube and -0.001 for Gomora and Saulsville. There was a general negative trend in vegetation in the informal settlements, which signifies a decrease in vegetation due to the increase in impervious surfaces. In some informal settlements, people depend on wood as a source of energy hence the decrease in vegetation as they cut trees. The p-value was lower than 0.05 in the other informal settlements (Mooiplaas and Mahube) and higher than 0.05 in Gomora and Saulsville, which showed a non-monotonic trend (Pohlert, 2016).

Table 24: The statistics of the change in NDVI in informal settlements in the CoT derived from the Mann Kendall statistical analysis using XLSTAT

Variable	Minimum	Maximum	Mean	Std. deviation	Kendall's tau	S	Var(S')	p-value (Two-tailed)	Sen's slope
Mooiplaas	0.185	0.655	0.345	0.116	-0.182	-1084	123117	'0.002	-0.003
Mahube	0.193	0.543	0.343	0.093	-0.199	-1182	130641	0.001	-0.003
Gomora	0.213	0.588	0.369	0.088	-0.119	-706	99369	0.025	-0.001
Saulsville	0.188	0.540	0.328	0.091	-0.046	-276	114011	0.415	-0.001

6.5.4 Natural Vegetation in High-density and Low-density Areas

Figure 49 showed the variations in NDVI among areas, which were adjacent to high-density areas, low/medium-density and vegetation in protected areas. Besides the normal variation in all the areas (low winter and high summer) in Figure 49, there were

low NDVI values in areas that were situated in high-density areas as compared to those in low-density areas. The highest mean NDVI of 0.515 was found in the mountain close to Marabastad, followed by 0.456 in the Magaliesburg, 0.412 in Soshanguve with the lowest value of 0.378 in Mamelodi (Table 25). The area (Marabastad) with the highest Mean NDVI was an undisturbed forest and even it Sen's slope was at zero. Areas with Kendall's tau varies in all the four areas with values of -0.11, 0.048, -0.047 and -0.013 in Mamelodi, Soshanguve, Magaliesburg and Marabastad respectively (Table 25). There was a negative trend in NDVI in all the areas with natural vegetation except for the area close to Marabastad with a slope of zero gradient. For all the sampled areas the p-value was greater than 0.05 which mean it is a non-monotonic trend (Pohlert, 2016).

Table 25: The statistics of the change in NDVI in the Natural Vegetation in High, medium and low-density areas derived from the Mann Kendall statistical analysis using XLStat

Variable	Minimum	Maximum	Mean	Std. deviation	Kendall's tau	S'	Var(S')	p-value (Two-tailed)	Sen's slope
Magalisburg	0.277	0.672	0.456	0.102	-0.047	-282	104806	0.385	-0.001
Marabastad	0.275	0.736	0.515	0.116	0.013	-80	108317	0.810	0.000
Mamelodi	0.216	0.586	0.378	0.105	-0.110	-652	112929	0.053	-0.001
Soshanguve	0.213	0.693	0.412	0.134	-0.048	-288	115186	0.398	-0.001

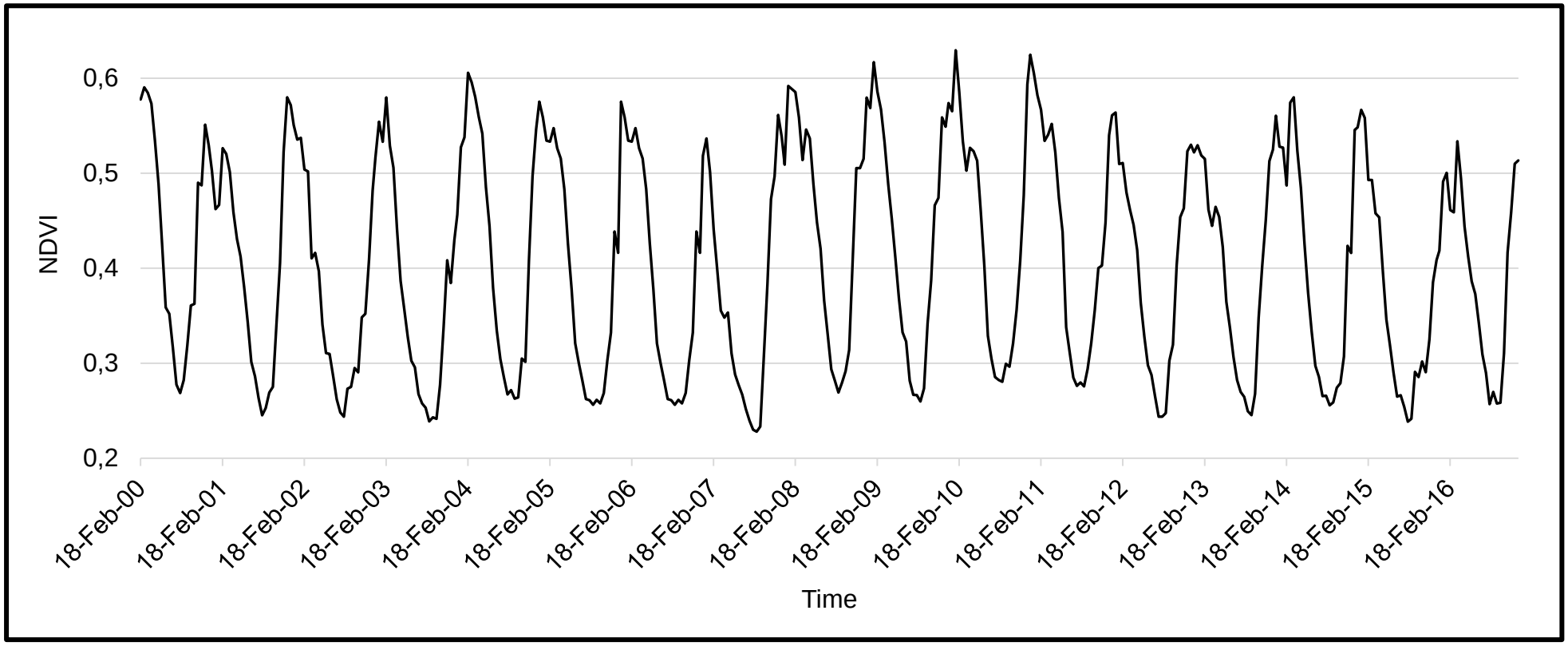

Figure 45: Variation in vegetation in the whole CoT based on the MODIS 250m NDVI data from February 2000 to December 2016.

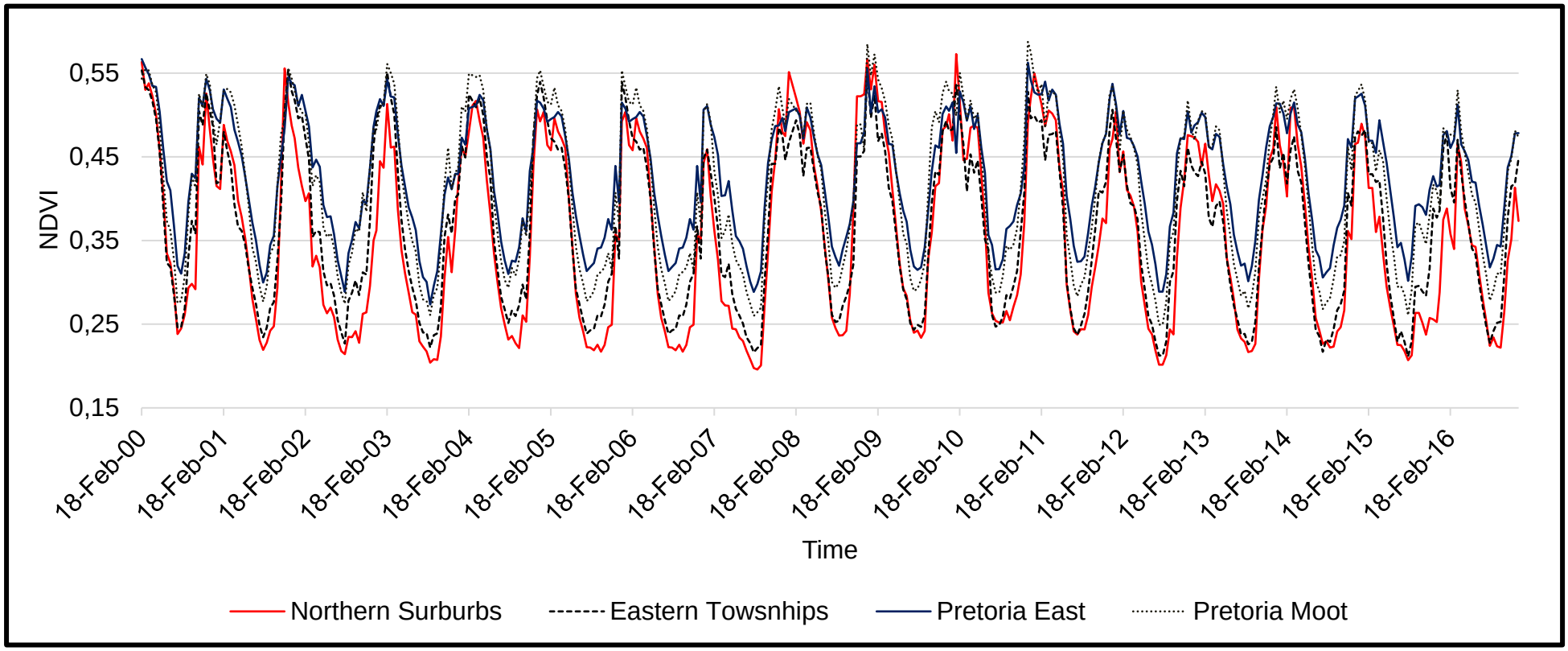

Figure 46: Variation in vegetation in the four areas (low, medium and high-density areas) in the CoT based on the MODIS 250m NDVI data from February 2000 to December 2016.

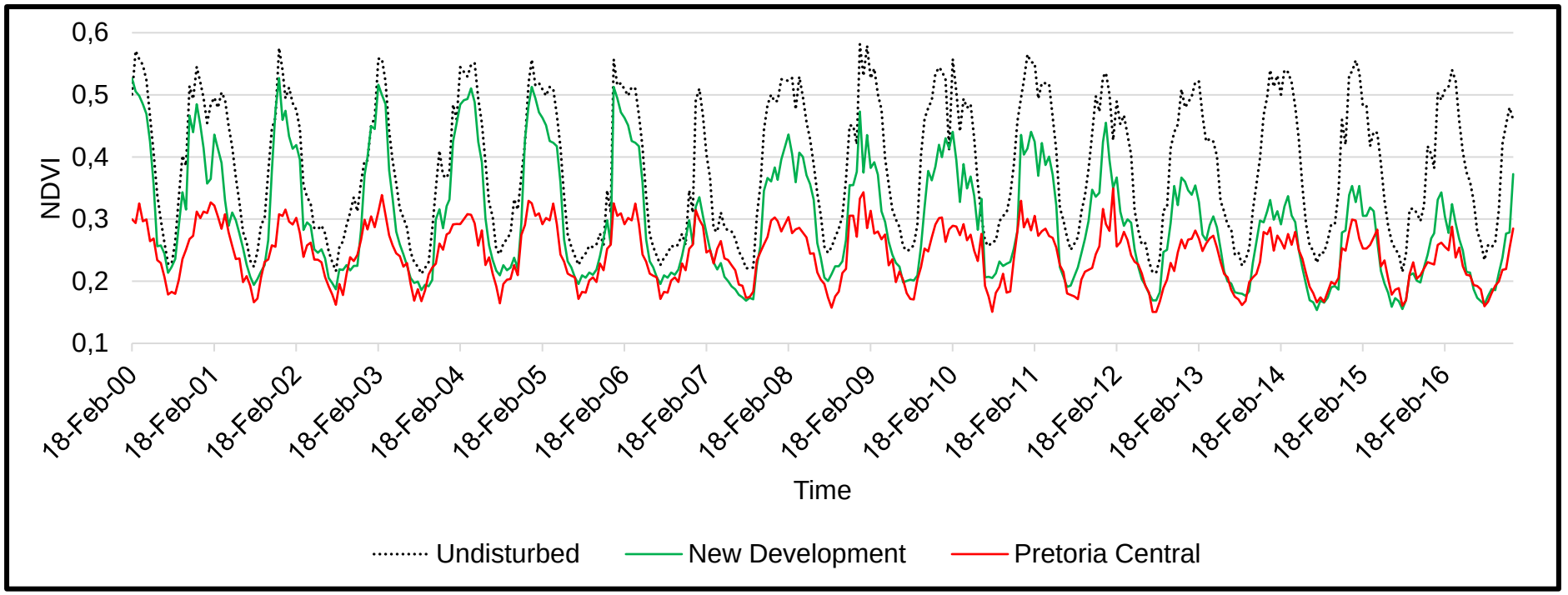

Figure 47: Variations in vegetation in the already developed area (Pretoria Central (CBD)), newly developed suburb and vegetated area (undisturbed) based on the MODIS NDVI data from February 2000 to December 2016

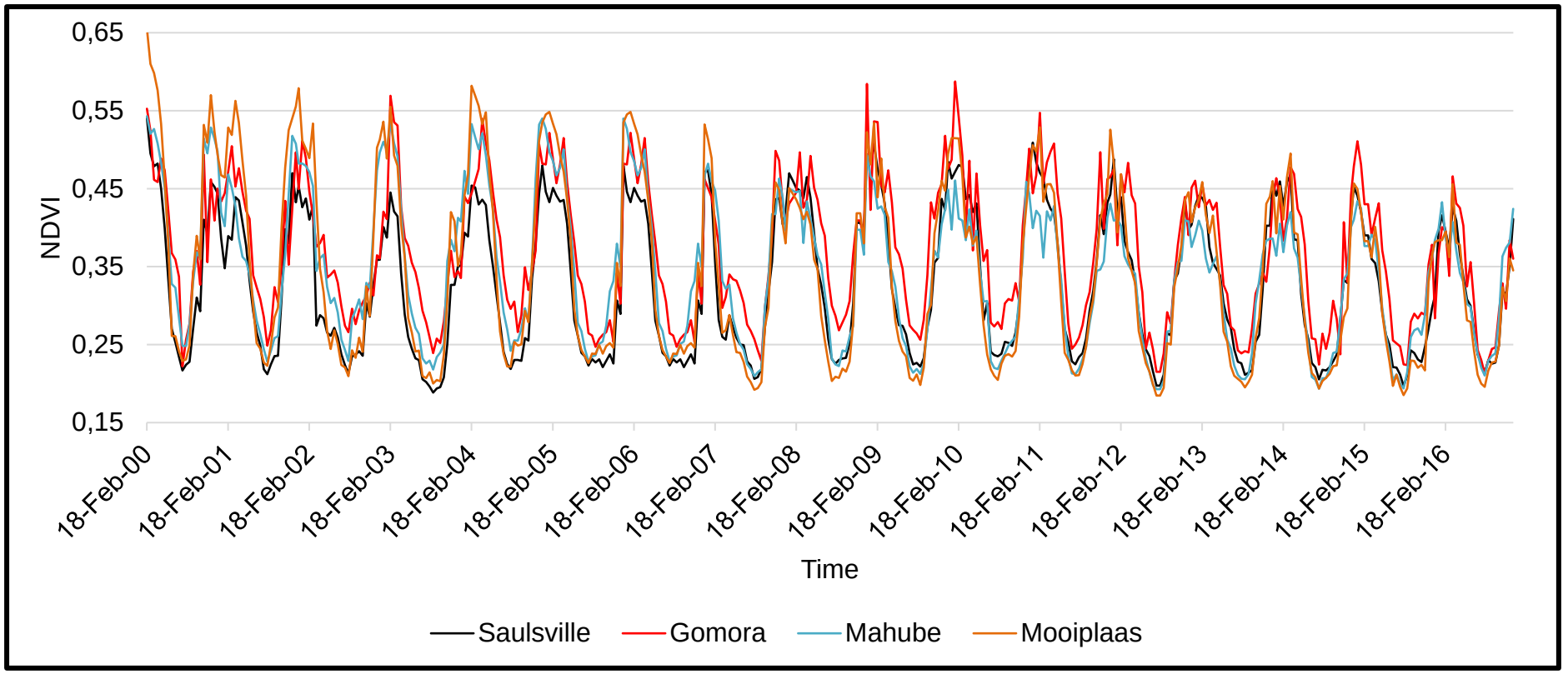

Figure 48: The variations of vegetation in different informal settlements in the CoT based on the MODIS NDVI data from February 2000 to December 2016.

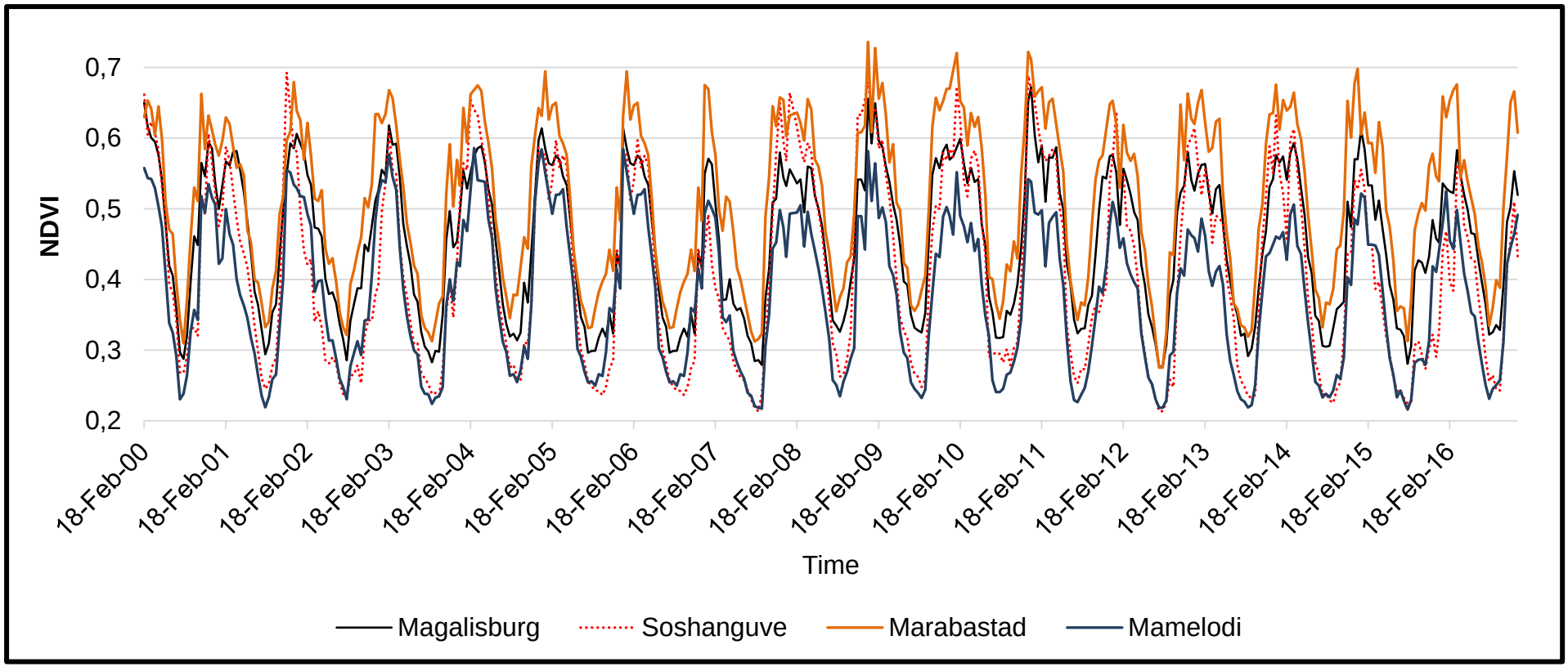

Figure 49: The variation in vegetation between open area adjacent to residential areas and one protected area based on the MODIS 250m NDVI data from February 2000 to December 2016.

In the temporal profiles, the greenings and browning were evident with high NDVI (greening) in summer and low NDVI (browning) in winter. Mann Kendall from most the sampled areas showed a p-value that was greater than 0.05, which mean there was no monotonic trend as the NDVI values are high in summer and low in winter (Pohlert, 2016). This agrees with the study done by de Jong *et al.* (2011) which revealed temporal variations in vegetation cover with high (greening) and low (browning). Vegetation trends were difficult to quantify hence the use of seasonal Mann–Kendall model to properly illuminate seasonality (de Jong *et al.*, 2011). According to de Jong *et al.* (2011), the Kendall was lower than 0.25 which indicates a weak trend hence the need to make use of the maps. The Sen's slope was negative for all the sample points, which means there a negative trend in vegetation cover. There a negative trend in the vegetation cover in the informal settlements and this was because in informal settlements, people depend on both firewood and electricity for their energy and there was no space to plant new trees. This agrees with a research done in the Cui Cuiabá informal settlements in Brazil where there was serious environmental degradation in both the terrestrial and aquatic ecosystems as a result of the informal settlements (Zeilhofer and Topanotti, 2008).

Vegetation is crucial in the reduction of environmental degradation in urban areas. Urbanisation has proved to be the main contributor to urban dynamics and has caused a global decline in vegetation cover (Odindi and Mhangara, 2012). In Port Elizabeth, based on the research by Odindi and Mhangara (2012) there was a general decline in green vegetation cover between 1990 and 2000 and this was attributed to urban expansion as very low vegetation was found in built-up areas (Odindi and Mhangara, 2012). This was also evident in some of the South African Cities such as eThekwini (Otunga *et al.*, 2014). It was found out that urbanisation leads to the excessive decline in the extent and density of vegetated areas (Odindi and Mhangara, 2012, Otunga *et al.*, 2014).

6.6 Conclusions

The unprecedented growth in urban population has put too much pressure on the terrestrial ecosystems and has led to the depletion of vegetation. Vegetation is needed

in urban areas to reduce environmental degradation, for carbon and for providing shade. Urbanisation has proved to be the main contributor to vegetation loss and land cover dynamics and causes a global decline in vegetation cover. To examine the spatio-temporal changes in vegetation in the CoT MODIS NDVI 250m was layer stacked and used in the profiling of these variations in NDVI in different landscapes. Seasonal time series analysis was analysed using Mann-Kendall test to show the overall trend in vegetation from 2000 to 2016 and in some land cover classes there was a decrease in vegetation from 2000 to 2016. One of the characteristics of urban areas depicted in most of the temporal profiles was that vegetation in urban areas also follows the seasonal patterns. When a settlement is established, the community and local government will start growing trees in their properties and in their streets. This is the main reason why even the urban environments were following the seasonal patterns of high vegetation in summer and low in winter. The same theory of high vegetation cover in summer and low in winter also applies in both formal and informal settlements. NDVI variations can show the dates when the development in the areas started. After transformation of natural areas into built-up areas, there were reductions in NDVI values and this will be evident on the NDVI profile.

Vegetation in high-density was low as compared to other areas. This was mainly because in the high-density areas people invade the natural vegetation to cut wood for fire. The natural areas were cleared and left with only grass and no trees thereby reducing the NDVI values. Most of the people staying in the high-density suburbs are the low-income earners or the jobless, so they depend on firewood to substantiate their energy. Natural vegetation in the low-density areas or protected areas has high NDVI because there are few people and most of the people in those areas are high income earners, who can afford electricity and can buy firewood if need be without getting into the nearby bushes to destroy the veld. Some of the areas are protected and inaccessible that no one can trespass into those areas that is why they have high NDVI values. Conclusively, MODIS time series analysis offered wealth of information that is important in urban research and provided a base to integrate with other sensors to help in urban studies.

.

CHAPTER SEVEN

7 SPATIO-TEMPORAL VARIATIONS OF LAND SURFACE TEMPERATURES OVER THE COT, SOUTH AFRICA USING LANDSAT TM AND OLI IMAGERY*

7.1 Abstract

Urbanisation in both developed and developing countries has led to the transformation of non-urban environments into urban areas. These changes have implications on the urban ecology and microclimatic conditions. One of the microclimatic conditions is land surface temperature, where the impact of urban surfaces can be seen in the form of urban heat islands. This study reports on the integration of GIS and remote sensing to quantify and assess change in LST in the CoT. Land Surface Temperature (LST) was used as a proxy for urban land cover change and was retrieved using the thermal band and NDVI data from Landsat TM and Landsat OLI. Winter and summer images of 1997 to 2015 were used in the study. Algorithms were used to retrieve LST using emissivity and satellite temperature as the input parameters. The spatial and temporal variations in the LST were retrieved to show the effects of land cover change on LST. Cross-section analysis along transects revealed rises (peaks) and falls (dips) of LST from one land cover class to another and further revealed the temporal variations in LST. This study revealed that non-cropped land have high LST as compared to cropped agricultural land as well as high LST in urban areas than the surroundings. There are some seasonal variations in LST with high values in summer and low values in winter because of the intensity of solar radiation in the different seasons. There was an increase in LST between 1997 and 2015.

Keywords: Landsat TM, Landsat OLI, Urban growth, LST, urban heat island, remote sensing

---

* Submitted in the Urban Climate Journal and is currently under review

7.2 Introduction

Urbanisation is increasing in both developing and developed countries leading to the transformation of non-urban environments into urban environments (Zhang, 2016). Projections by the United Nations shows that more than 70% of the population will be living in urban areas by 2050 and this can be attributed to migration and natural population increase (Zhang, 2016). Transformation of landscapes into urban environments has led to replacement of natural vegetation and agricultural areas by impervious surfaces such as roads, pavements and buildings (UNHABITAT, 2016). This has also led to high concentration of pollutants in the urban areas as a result of release of gases from industries and cars (Abutaleb *et al.*, 2014, Peres *et al.*, 2018). Urban growth has negative impact on the quality of the environments, which include air quality and temperature (Abutaleb *et al.*, 2014, Wray and Cheruiyot, 2015).

Temperature increases were reported in urban areas as a result of impervious surfaces and high concentration of pollutants leading to the establishment of urban heat islands (UHI) (Mallick *et al.*, 2008, Sheng *et al.*, 2017). UHI can be defined as a microclimate where the temperature in the urban areas is higher than that of the surrounding areas (Yue *et al.*, 2007, Abutaleb *et al.*, 2014, Peres *et al.*, 2018). UHI is a result of anthropogenic activities which influence the increase in temperature in the urban areas and these cause an increase in precipitation (Huang *et al.*, 2008, Sheng *et al.*, 2017), affect the quality of air and leads to rise in global warming (Mallick *et al.*, 2008). These effects can be detrimental to the human health which will in turn increase mortality (Yue *et al.*, 2007). UHI thermal profiles are used to graphically illustrate spatial variations of temperature in the urban environment and its surroundings (Sheng *et al.*, 2017). Typical thermal curves of UHI variations will show cliffs, peaks, depressions and plateaus, which reveal the thermal variations (Huang *et al.*, 2008, Abutaleb *et al.*, 2014).

Anthropogenic activities cause changes in the surface (from natural to impervious) which affect albedo, thermal capacity and heat conductivity (Abutaleb *et al.*, 2014). An urban area with green vegetation suffers less from UHI than a non-vegetated urban area (Weng *et al.*, 2004, Mallick *et al.*, 2008, Tomlinson *et al.*, 2012) hence the use of

vegetation indices such as Normalised Difference Vegetation Indices in retrieving LST in satellite imagery (Ngie *et al.*, 2014).

The temperature at the sensor is slightly lower than the temperature measured at meteorological stations (ground level). There is a need to use ground emissivity and atmospheric corrections in order to quantify LST (LST) accurately (Sobrino *et al.*, 2004). Vegetation cover and soil background influence the emissivity and the vegetation vigour hence the use of NDVI in calculating emissivity (Sobrino *et al.*, 2004).

7.3 Study Area

CoT (Figure 50) popularly known as the City of Pretoria is the administrative capital of the Republic of South Africa and located in the North of the Gauteng Province. The city was founded in 1855 by Marthinus Pretorius and renamed to Tshwane in 2000 (Raper, 2008, Van der Vyver, 2015). It merged with Metsweding District following the Gauteng Global City Region Strategy (Matlala, 2015). COT has 7 regions, 105 wards and 210 councillors and is the single largest municipality. CoT lies between latitudes 25°6’34.60” S to 26°4’41.12” S and longitudes 27°53’24.26E to 29°5’54.31” E. The city landmass of 629 618 ha, 2 921 490 people and 911 536 households based on the census data on 2011. The population of the CoT was 1 770 330 in 1996, 2,142,322 in 2001 and 2,921,488 in 2011 (STATSSA, 2012). COT experiences sub-tropical climate with hot and rainy summer and very cold and dry winter.

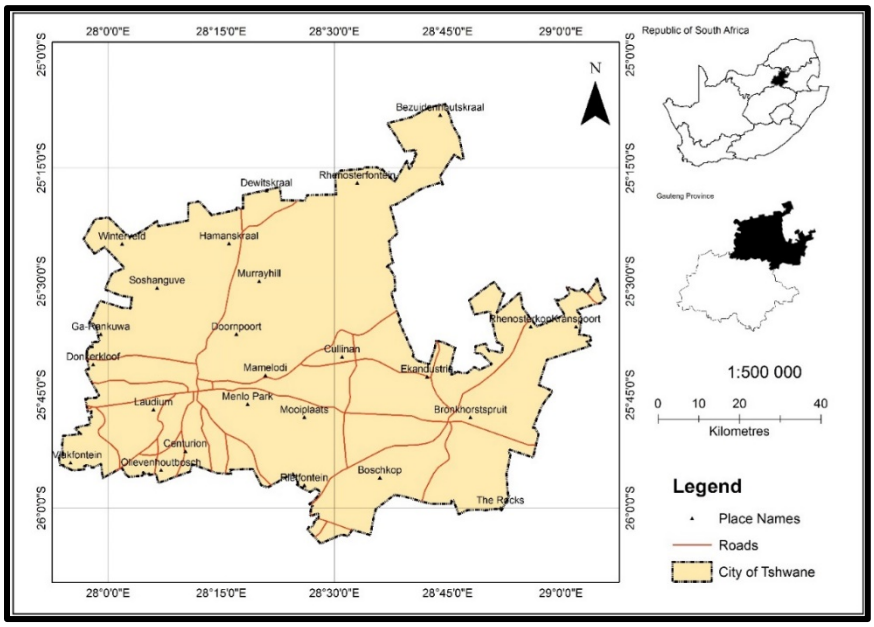

Figure 50: The map of the CoT.

7.4 Data and Methods

Satellite imagery (Landsat OLI and Landsat TM) were downloaded from the USGS' Earth Explorer web portal. Acquired satellite imagery were for both winter and summer seasons as indicated in Table 26. Winter and summer cloud-free images were found in August (1997 and 2016) and December (1997 and 2015) respectively. Figure 51 illustrates the flowchart of the methodology used to retrieve LST in the two years (1997 and 2015).

Table 26: Landsat imagery that was used in the study to retrieve LST

Sensor	Year	Month	Path	Row	Scene Status
Landsat OLI	2015	December	177	77 and 78	Cloud-free
	2015	August			
Landsat TM	1997	December			
	1997	August			

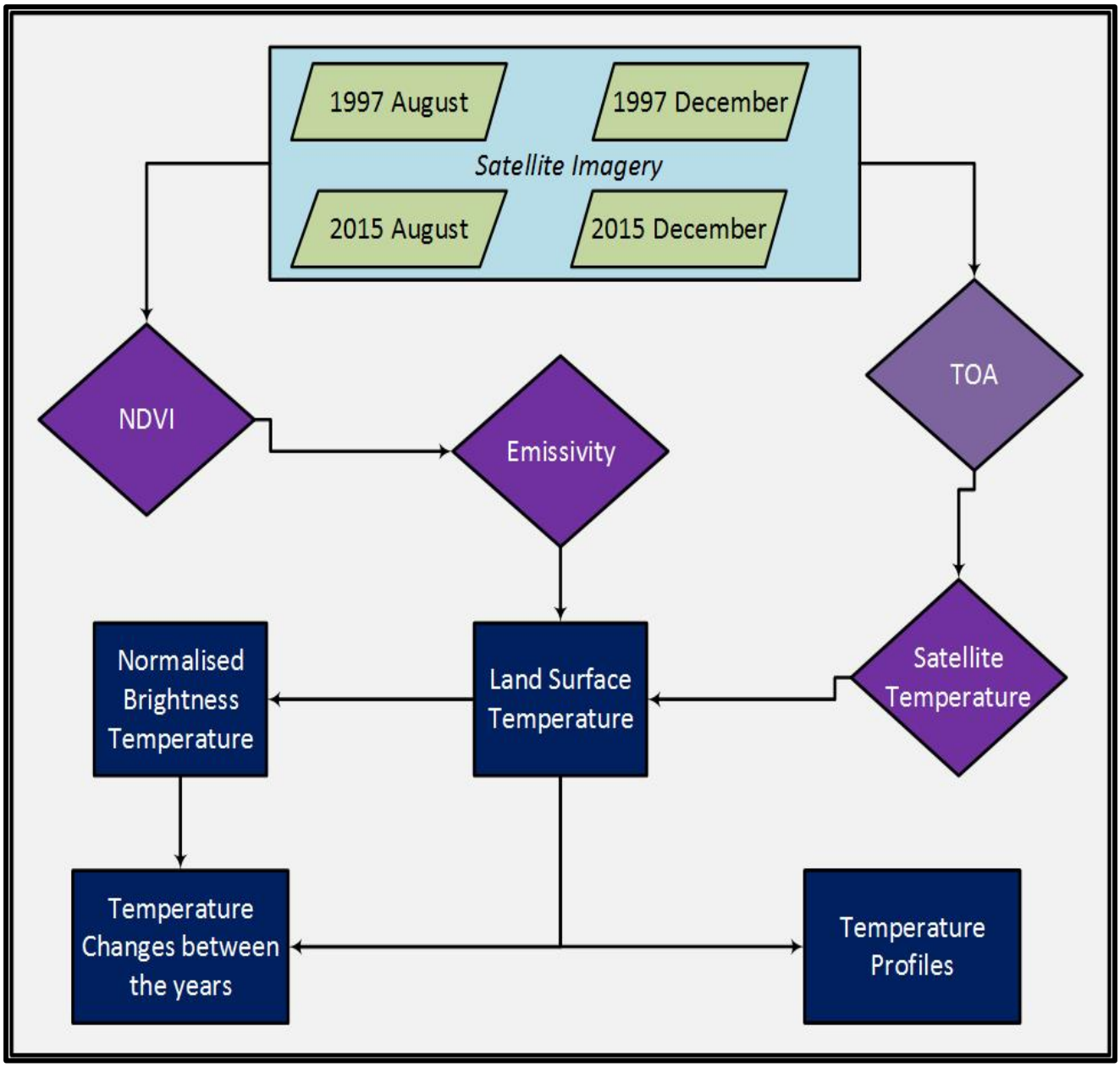

Figure 51: Flowchart showing the methods used to retrieve LST using Landsat OLI and Landsat TM.

7.4.1 Converting to Radiance

In order to convert the downloaded DN values to TOR (Top of Atmosphere Reflectance) for Landsat TM images, the formula on Equation 7-1 was used (Qin *et al.*, 2001).

$$L = (L_{\lambda max} - L_{\lambda min}) * \frac{Q_{\lambda DN} - Q_{\lambda min}}{Q_{\lambda max} - Q_{\lambda min}} + Lmin \qquad 7\text{-}1$$

Where L= is the spectral radiance received by the sensor, $L_{\lambda max}$ is the maximum detected spectral radiance, $L_{\lambda min}$ is the minimum spectral radiance. Q_{DN} is the DN at a given pixel, $Q_{\lambda max}$ = is the maximum DN value (255) and $Q_{\lambda min}$ = is the minimum DN value (0) (Qin *et al.*, 2001)

In order to convert the downloaded DN values to TOR for Landsat OLI images the formula on Equation 7-2 was used (Qin *et al.*, 2001).

$$L_\lambda = M_L Q_{cal} + A_L \qquad 7\text{-}2$$

Where: L_λ = TOA spectral radiance (Watts/(m^2 * srad * μm)), M_L = Band-specific multiplicative rescaling factor from the metadata A_L = Band-specific additive rescaling factor from the metadata and Q_{cal} = Quantized and calibrated standard product pixel values (DN) (Qin *et al.*, 2001).

7.4.2 Calculating Satellite Temperature

Satellite temperature was calculated for Band 6 for TM and band 10 for OLI converted from digital number to spectral radiance using the formula below (Artis and Carnahan, 1982, Kumar *et al.*, 2012).

$$T_{Sat} = \frac{K_2}{ln\left(\left(\frac{K_1}{L_\lambda}\right)+1\right)} \qquad 7\text{-}3$$

Where: T_{Sat} = At-satellite brightness temperature (K), L_λ = TOA spectral radiance (Watts/(m^2 * srad * μm)), K_1 = Band-specific thermal conversion constant (Table 27)

andK_2 = Band-specific thermal conversion constant (Table 27) (Chander and Markham, 2003, Kumar *et al.*, 2012)

Table 27: Thermal Conversion Constants for Landsat

Constant	Landsat 4	Landsat TM	Landsat ETM+	Landsat OLI
K1	671.62	607.76	666.09	In the metadata
K2	1284.30	1260.56	1282.71	In the metadata

7.4.3 Calculating NDVI

NDVI is an indicator calculated from the red bands and the near-infrared bands (Kumar and Shekhar, 2015) of the electromagnetic spectrum using Equation 7-4 illustrated below. NDVI used a standard algorithm of Townshend and Justice (1986) which was adopted by scientists and decision-makers to assess and analyse vegetation greenness (Townshend and Justice, 1986, Kumar and Shekhar, 2015). It estimates the amount of above-ground vegetation cover from red and infrared bands (Kumar and Shekhar, 2015). Green vegetation absorbs the red wavelengths as a result of chlorophyll while scattering near-infrared wavelengths and unhealthy leaves reflect the red band and absorb the near-infrared bands (Kumar and Shekhar, 2015). NDVI ranges between -1 and 1 and values between -1 and 0 where the NDVI above 0.1 is for vegetated areas (Laosuwan *et al.*, 2017).

$$NDVI = \frac{(NIR-RED)}{NIR+RED} \qquad 7\text{-}4$$

Where: NIR is the Near Infra-Red Band (Band 4 in TM and Band 5 in OLI) and RED = Red Band (Band 3 in TM and Band 4 in OLI)

7.4.4 Calculating Emissivity

Emissivity is a function of wavelength, which is influenced by a number of environmental factors such as water content, chemical composition, the density of vegetation, plant species and smoothness of the surface (Sobrino et al., 2004). There

is a correlation between emissivity and NDVI (Sobrino et al., 2004). The conditional formulae used to compute emissivity is shown in Table 28.

Table 28: Estimation of land surface emissivity using NDVI.

NDVI	Land Surface Emissivity (ε)
NDVI<-0.185	0.995
-0.185≤NDVI≤0.157	0.970
0.157≤NDVI≤0.727	1.0094+0.047ln(NDVI)
NDVI>0.727	0.990

7.4.5 Calculating LST

Satellite temperature (T_{Sat}) and emissivity were used to compute LST (LST/$T_{surface}$) using Equation 7-5 below (Artis and Carnahan, 1982, Chander and Markham, 2003, Weng *et al.*, 2004) and this was performed using ArcGIS (ESRI, 2015).

$$T_{Surface} = \frac{T_{Sat}}{\left(1 + \left[\left(\frac{\lambda T_{Sat}}{\rho}\right)\ln(\varepsilon)\right]\right)} \qquad 7\text{-}5$$

where: T_{sat} is Satellite Temperature derived from Equation 7-3, λ = wavelength of emitted radiance and average wavelengths and ε is the surface emissivity derived from Table 28 (Chander and Markham, 2003).and $\rho = h\frac{c}{\sigma}$ (σ is the Stefan-Boltzmann constant ($1.38*10^{-23}$ J/K), h is the Planck's constant ($6.626*10^{-32}$Js) and *c* is the velocity of light ($2.998*10^{8}$ m/s)

7.4.6 Normalising Brightness Temperature

There is need to normalise LST between 0 and 1 to get rid of time difference when images were captured and for easy comparison of LST. Equation 7-6 below was used to compute the normalised LST (Schissau, 2006).

$$N = \frac{T_i - T_{min}}{T_{max} - T_{min}} \qquad 7\text{-}6$$

Where N is the pixel normalised value of the LST, T_i is the LST of the i^{th} pixel, T_{min} is the minimum value of the LST and T_{max} is the maximum LST. The normalised LST can be divided into five zones, which are strong heat islands zone (0.8-1.0), heat islands zone (0.6-0.8), normal zone (0.4-0.6), green islands zone (0.2-0.4) and strong green islands zone (0-0.2) (Xu *et al.*, 2013, El-Magd *et al.*, 2016).

7.4.7 Cross-Sectional Analysis using Transects

Transects were run across different land cover classes using the 3D Analyst in ArcGIS (ESRI, 2015). Transects were run across agricultural areas, across the city centres, across the residential areas and across city outskirts. The LST on each point on the transect was recorded and results were computed graphically.

7.5 Results and Discussions

7.5.1 Land Surface Temperature (LST).

Computed LST maps are depicted in Figure 52 (August 1997), Figure 53 (December 1997) Figure 54 (August 2005) and Figure 55 (December 2015). High temperatures were experienced in summer than in winter as depicted on the visual maps and there was an increase in temperature between 1997 and 2015. From the maps, there was a high LST in December 2015 as compared to December 1997 and there were high temperatures in summer as compared to winter (Figure 56). The average temperature for December 2015 was 35.01°C, August 2015 was 30.44°C, December 1997 was 31.24°C and August 1997 was 20.95°C (Figure 56).

LST in urban areas was high as compared to the surrounding areas for August and December for both years. The results are agreeing with the consensus that there was high LST in urban areas as compared to the surrounding areas. This agrees with the finding from cities such as Cairo in Egypt, where there was little or no vegetation in urban areas. CoT is also known as the Jacaranda City a pseudonym that was derived from the Jacaranda trees in the streets together with other different indigenous and alien tree species. These together with stadiums and parks in the urban areas plays a role on the LST in urban areas. The temperature in the CBD was lower than in urban environments outside the city. The high-density areas have high temperatures as compared to low-density areas and the city centres. This is mainly because there was less vegetation in high-density areas as compared to low-density areas and the city centres.

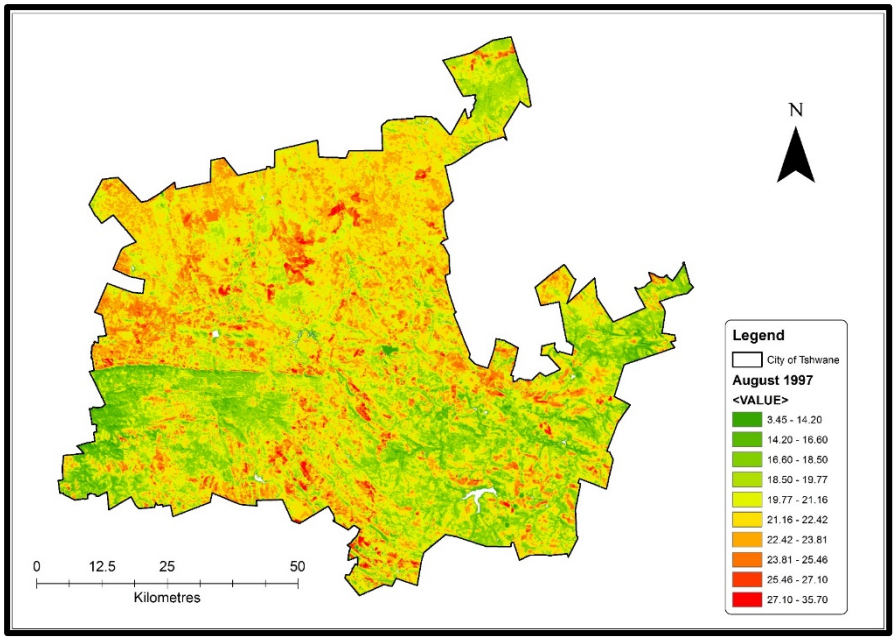

Figure 52: LST map for August 1997 derived from the Landsat TM thermal bands and emissivity.

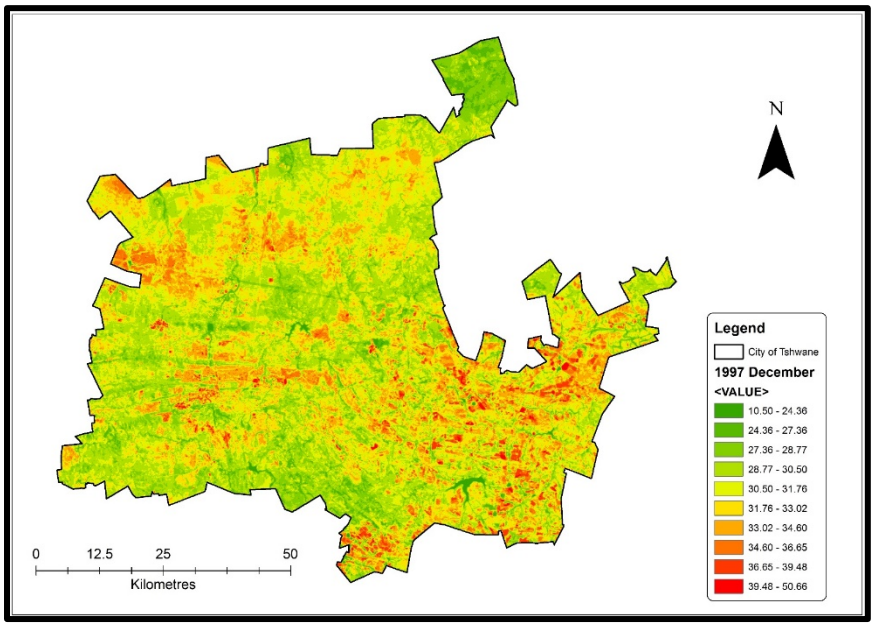

Figure 53: LST map for December 1997 derived from the Landsat TM thermal bands and emissivity.

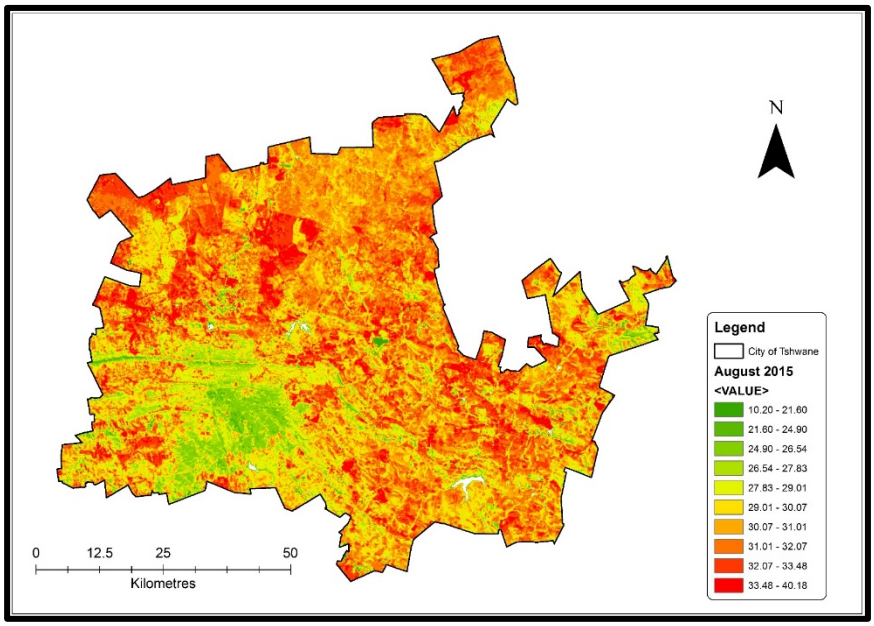

Figure 54: LST map for August 2015 derived from the Landsat OLI thermal bands and emissivity.

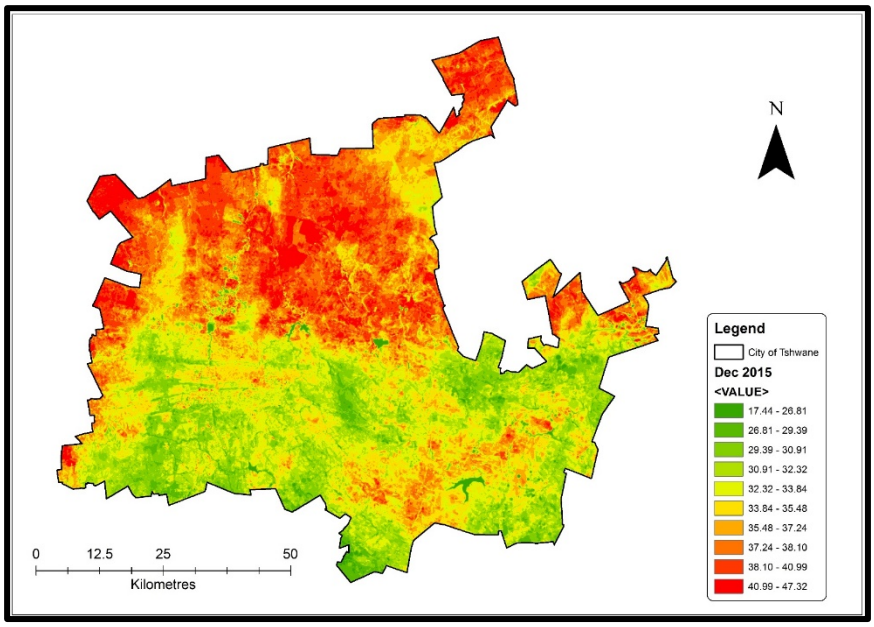

Figure 55: LST map for December 2015 derived from the Landsat OLI thermal bands and emissivity.

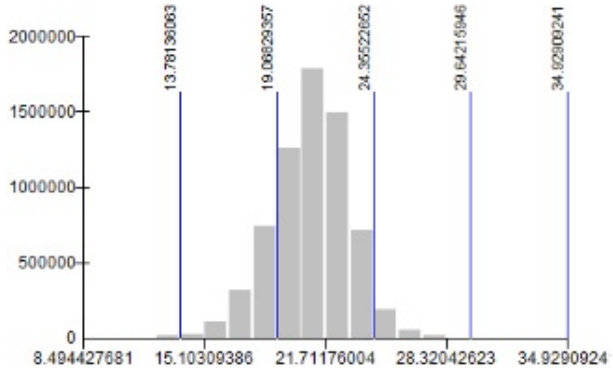

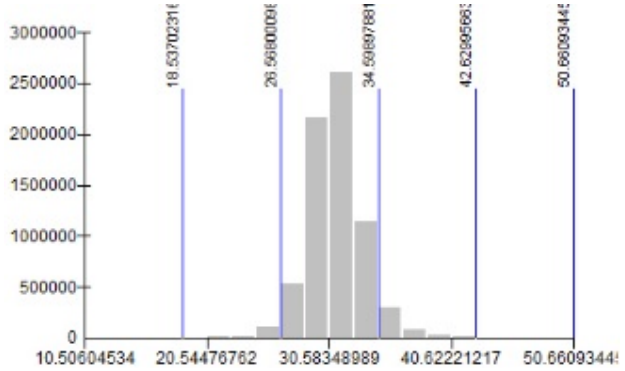

LST 1997 August			
Max:34.93	Min: 8.49	Mean: 20.95	St. Dev: 2.11

LST 1997 December			
Max:50.99	Min: 10.50	Mean: 31.24	St. Dev:2.27

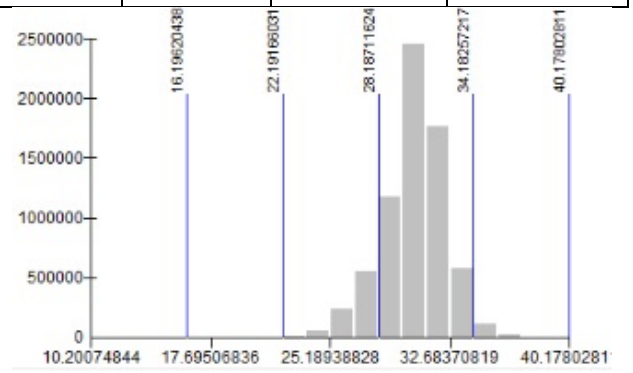

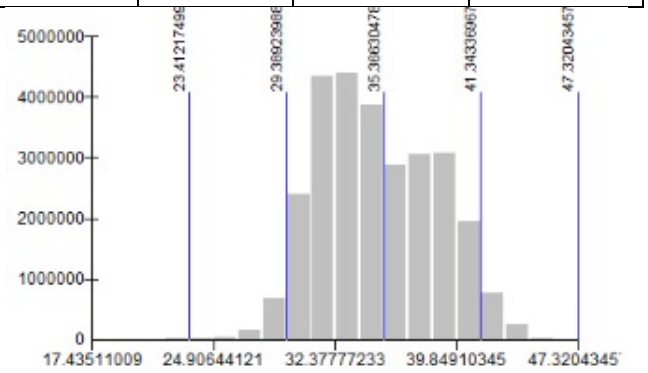

LST 2015 August			
Max:40.17	Min: 10.20	Mean: 30.44	St. Dev:1.97

LST 2015 December			
Max:47.32	Min: 17.44	Mean: 35.01	St. Dev: 3.61

Figure 56: Statistics of LST for 1997 (August and December 1997) and 2015 (August and December).

7.5.2 Normalised LST

In August 1997, the normalised LST (Figure 57) had a mean of 0.47 with the standard deviation of 0.08 (Figure 61). Most of the areas were in the normal zone and green islands zone (0.2-0.4) and few heat islands. In December 1997, the normalised LST (Figure 58) had a mean of 0.51 and standard deviation of 0.06. Most of the areas were in the normal zone and heat zone and fewer patches in strong heat islands (in red) (Figure 58). In August 2015, the normalised LST (Figure 59) had a mean of 0.68 and standard deviation of 0.07. The normalised LST maps show most on the areas in the normal zone and fewer patches in the heat zone. In December 2015, the normalised LST (Figure 60) had a mean of 0.58 and standard deviation of 0.12 (Figure 61). There were significant strong heat islands zone during that season but most the areas were in the normal and heat zones.

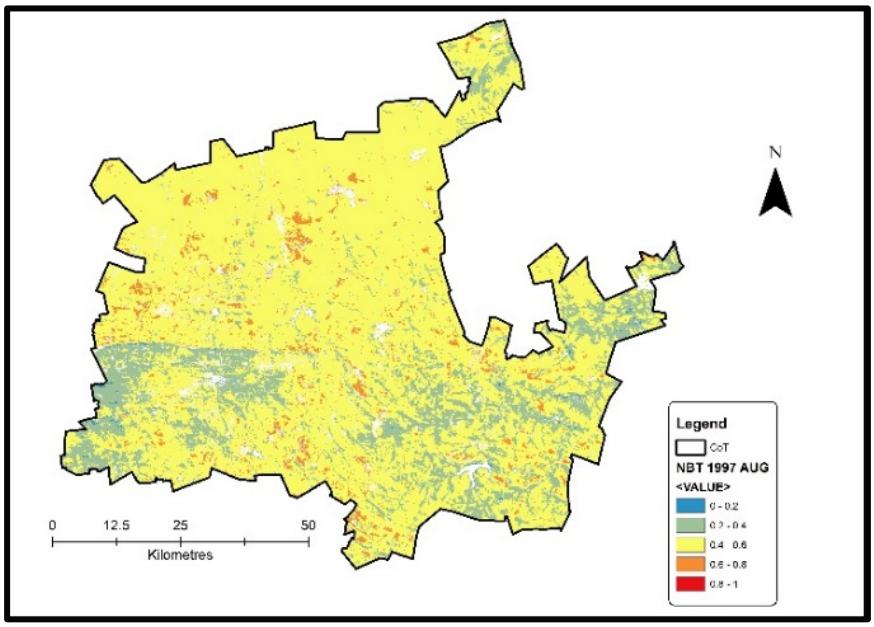

Figure 57: Normalised LST for August 1997.

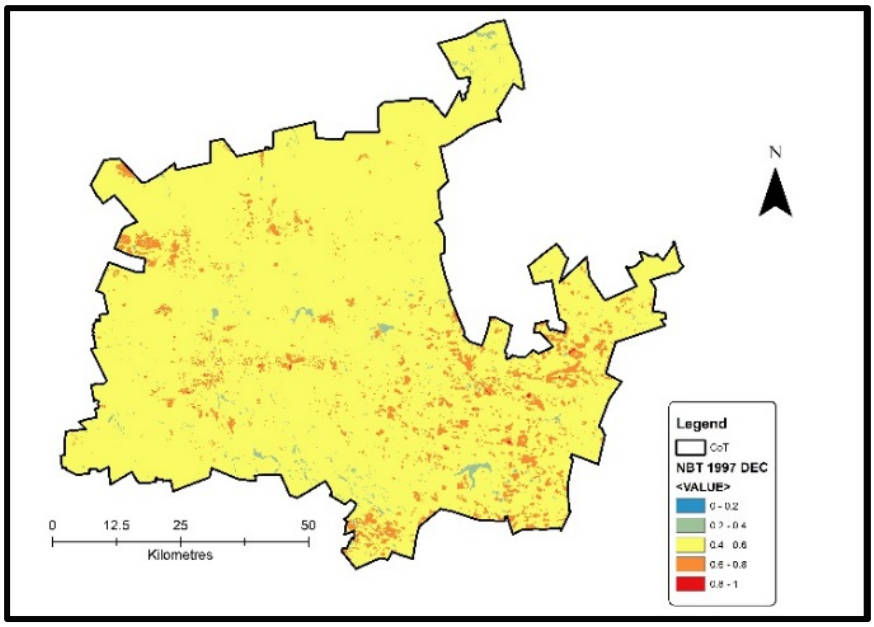

Figure 58: Normalised LST for December 1997

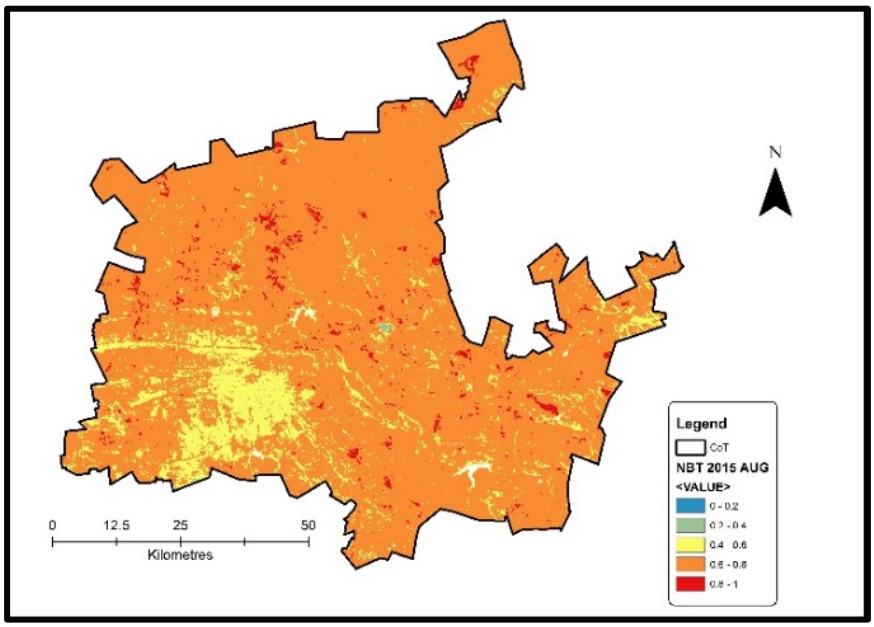

Figure 59: Normalised LST for August 2015.

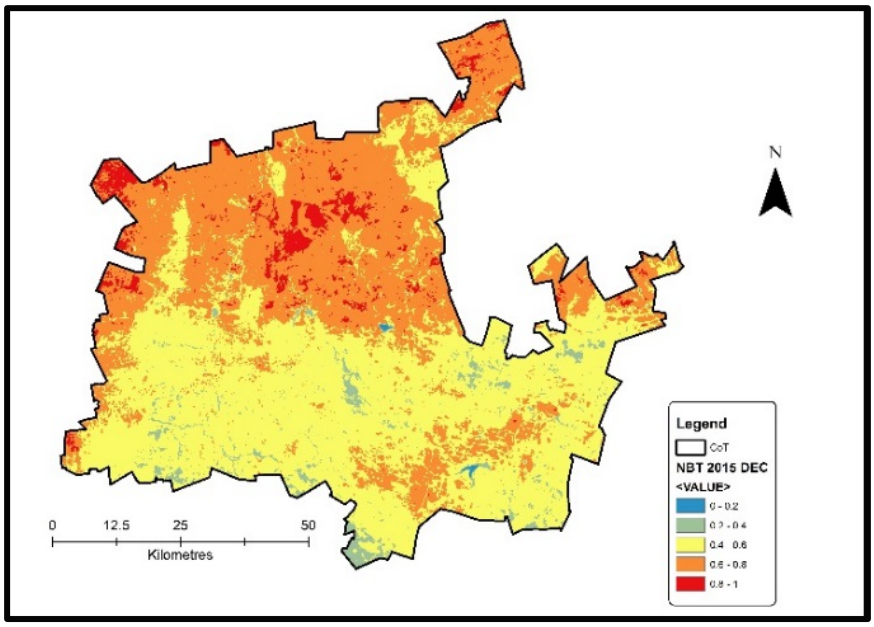

Figure 60: Normalised LST for December 2015.

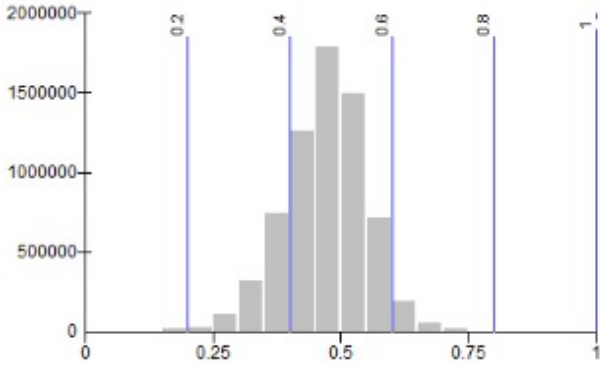

Normalised LST 1997 August			
Max:1	Min: 0	Mean: 0.47	St. Dev: 0.08

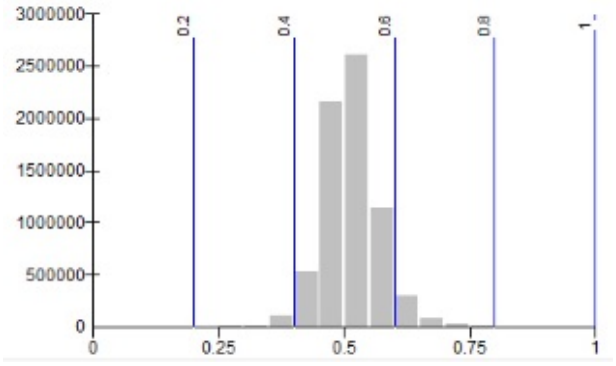

Normalised LST 1997 December			
Max:1	Min: 0	Mean: 0.51	St. Dev:0.06

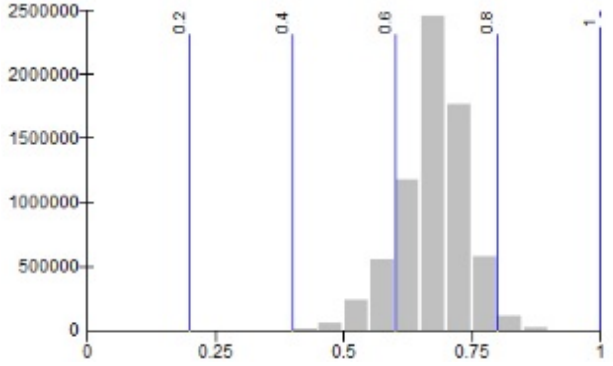

Normalised LST August2015			
Max:1	Min: 0	Mean: 0.68	St. Dev:0.07

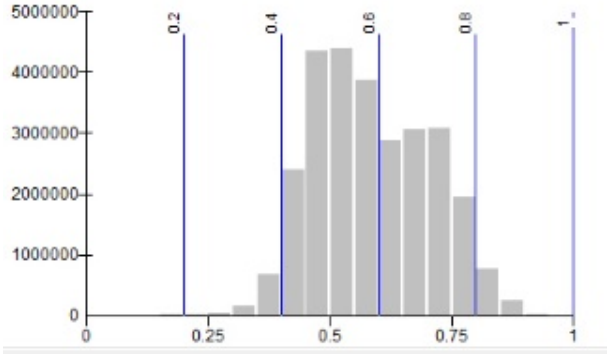

Normalised LST 2015 December			
Max:1	Min: 0	Mean: 0.58	St. Dev: 0.12

Figure 61: Statistics of the normalised LST for 1997 (August and December) and 2015 (August and December).

7.5.3 Spatial profile in Agricultural Areas

Spatial profiles of LST that were run along a transect in the agricultural areas were depicted in Figure 62 (August 1997), Figure 63 (August 2015), Figure 64 (December 1997) and Figure 65 (December 2015). The spatial profiles show the inter-seasonal variations of LST 1997 and 2015 respective. In the winter of 1997, the highest temperature was 26.5°C, the lowest was 18.0°C and in summer of the same year the highest temperature was 33.8°C and the lowest was 28°C. In the winter of 2015, the highest temperature was 33.2°C and lowest, was 23.5°C while in summer highest temperature was 40.9 °C and lowest, was 29.3°C. There were peaks and depression in the spatial profiles in both winter and summer images of 1997 and 2015. Peaks (high LST) were in areas with little or no crops and depressions (low LST) were in cropped areas where the value of greenness was high. Areas with depression in winter were as a result of winter cropping and high peaks because the areas had bare soils (no crops). There was a strong seasonality difference between the winter and summer seasons and it was clear in the spatial profiles of both 1997 and 2015. There was an increase in temperature in agricultural areas between 1997 and 2015 in both seasons.

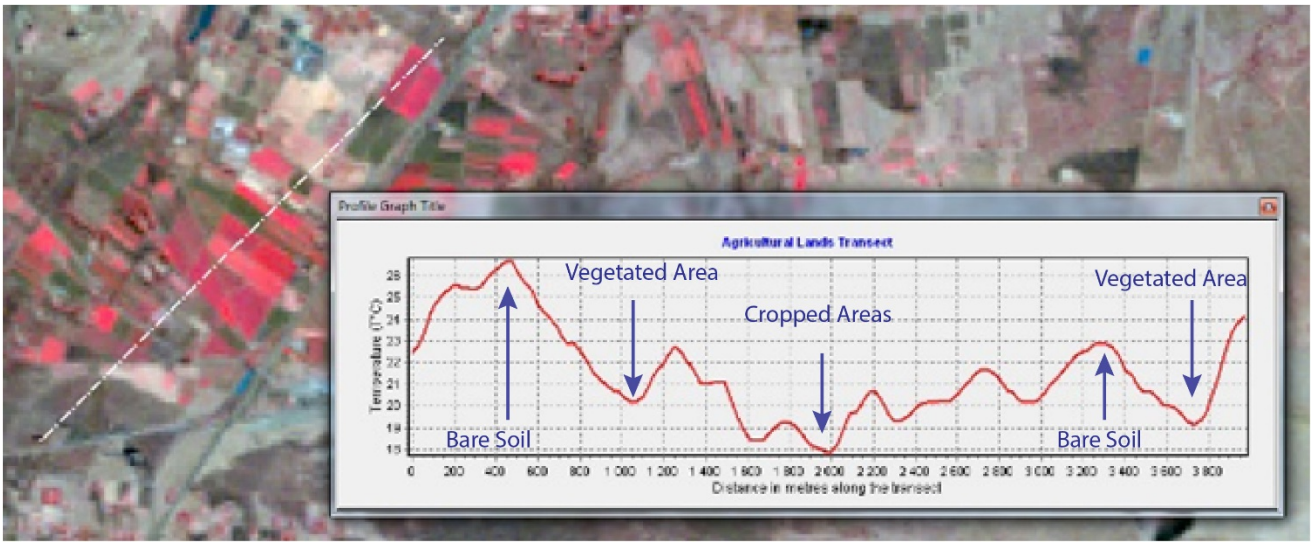

Figure 62: Spatial profile of LST along a transect (white) in the agricultural areas in August 1997.

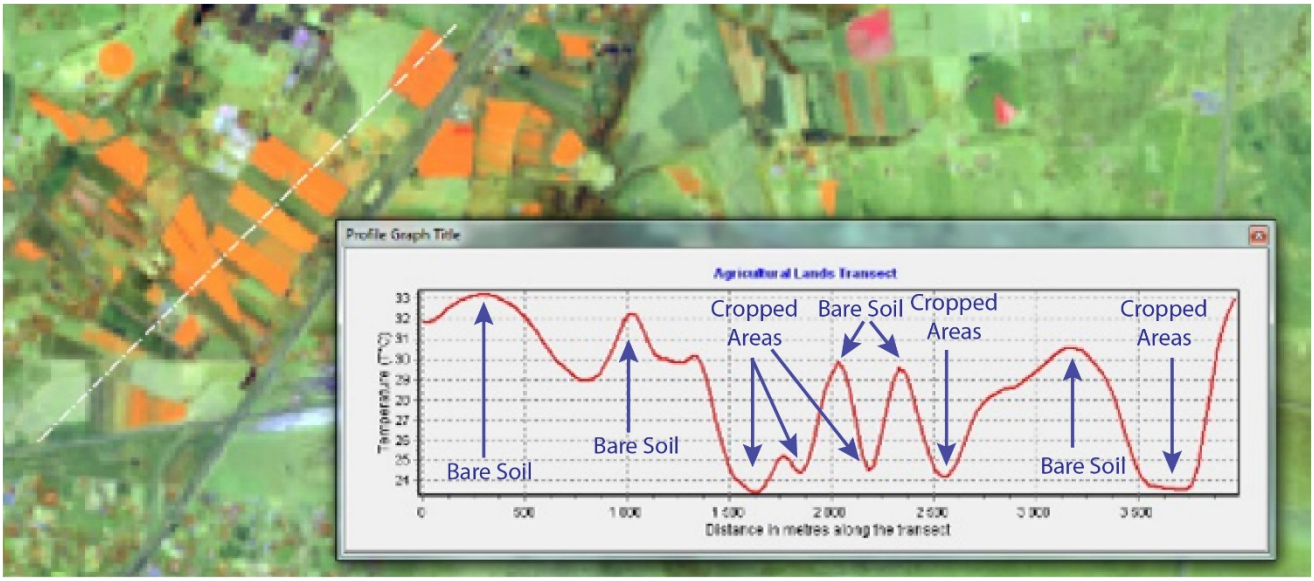

Figure 63: Spatial profile of LST along a transect (white) in the agricultural areas in and August 2015.

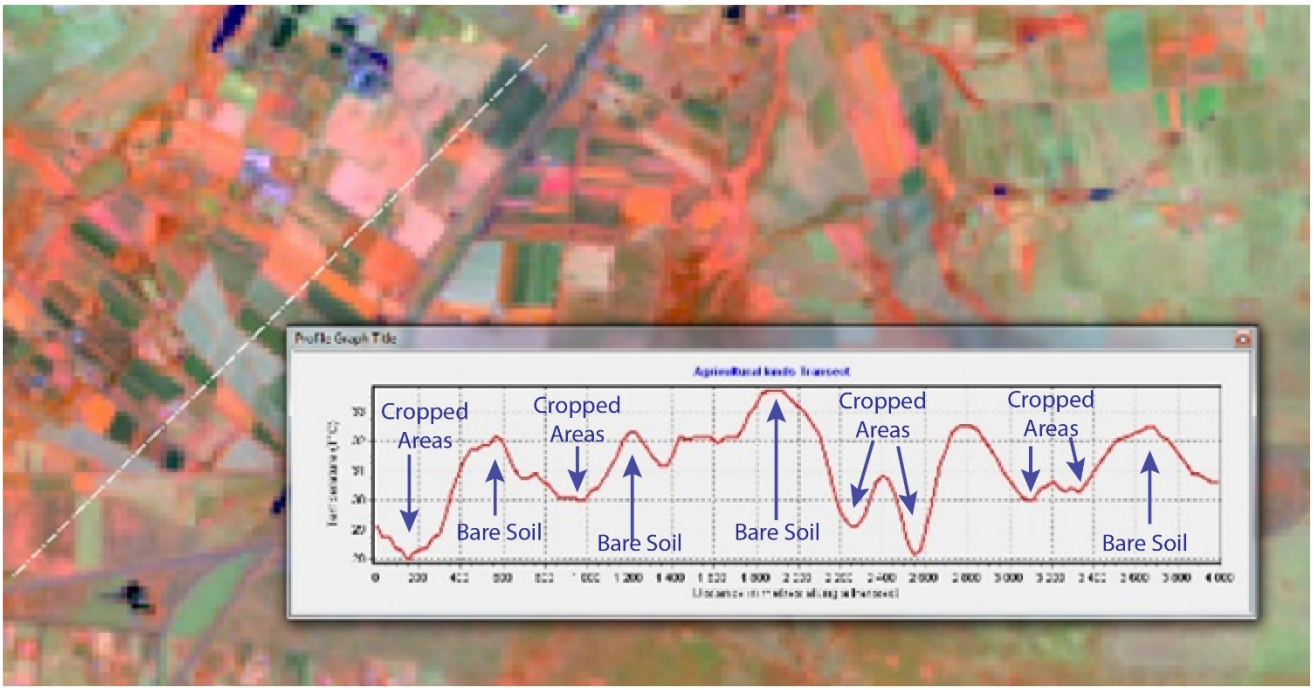

Figure 64: Spatial profile of LST along a transect (white) in the agricultural areas in December 1997

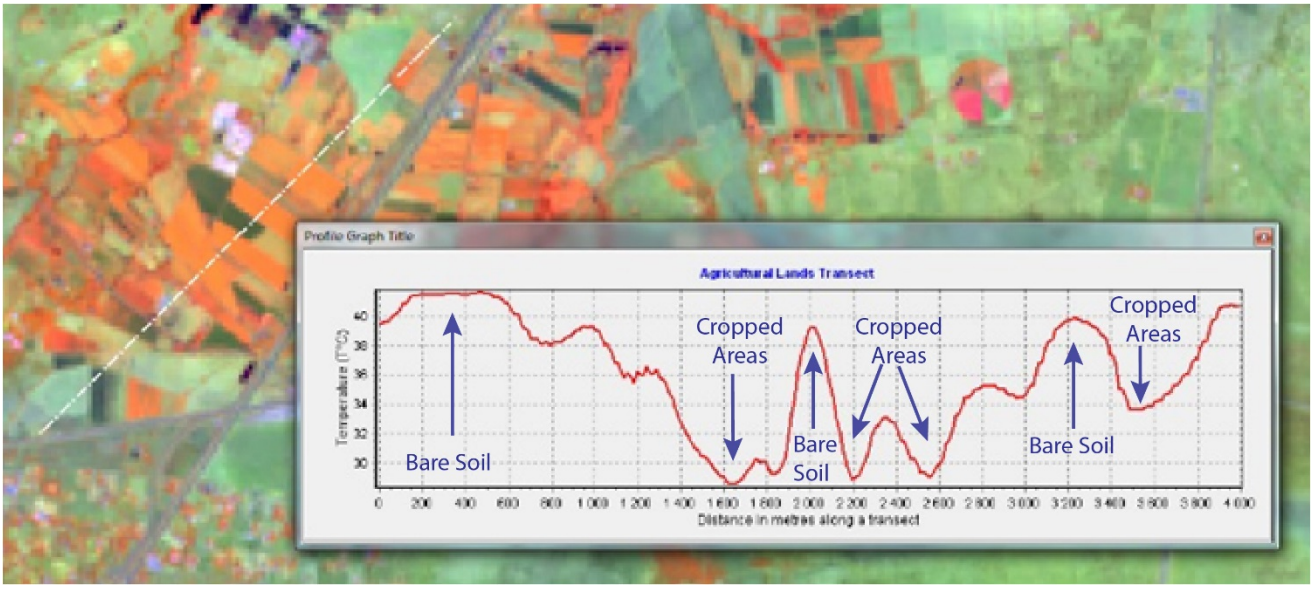

Figure 65: Spatial profile of LST along a transect (white) in the agricultural areas in December 2015.

7.5.4 Spatial Profile in Residential Areas

The residential areas used in the study were in Soshanguve and the inter-seasonal variations for 1997 and 2015 are shown in Figure 66 (August 1997), Figure 67 (August 2015), Figure 68 (December 1997) and Figure 69 (December 2015). In 1997 winter, highest temperature was 26.1°C and lowest, was 15.2°C while in summer highest temperature was 36.5°C and lowest, was 23.1°C. In 2015 winter, highest temperature was 33.6°C and lowest, was 23.2°C while in summer highest temperature was 43.1°C and lowest, was 32.8°C. High peaks were experienced in newly established settlements where there was no vegetation and depression in areas with little or no impervious surface for example the water body which situated at 1500m from the start of the transect.

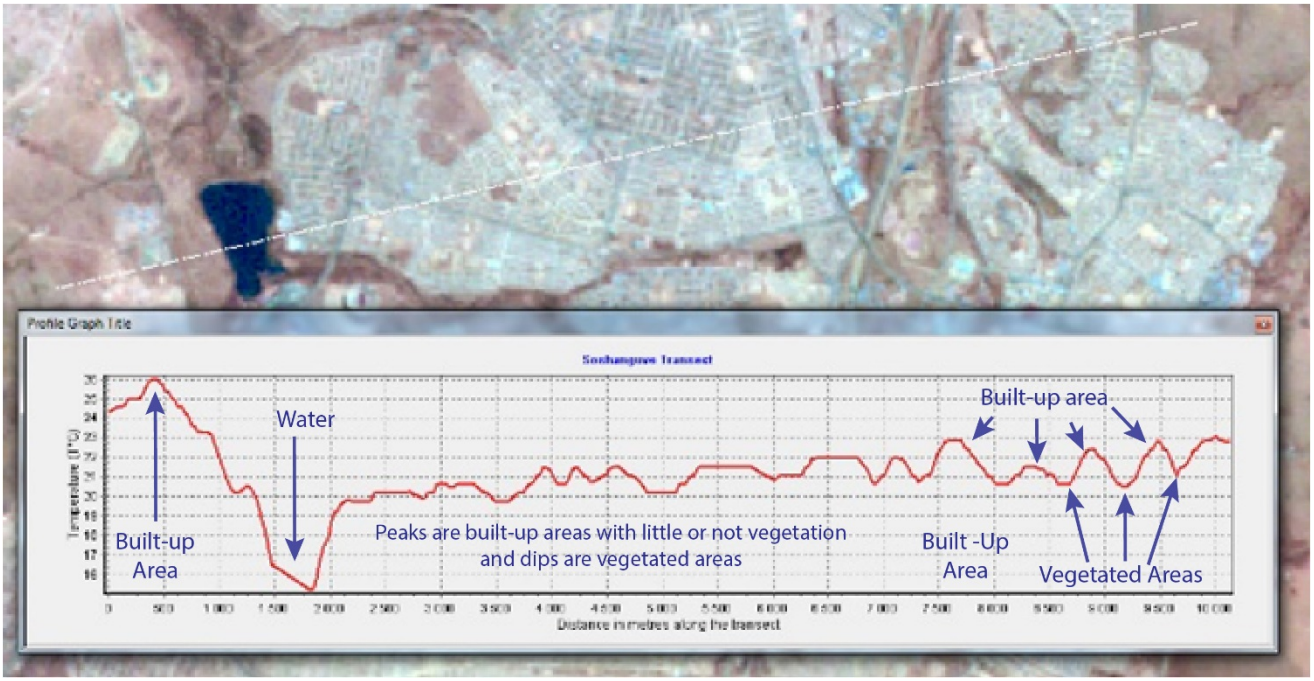

Figure 66: Spatial profile of LST along a transect (white) in the high-density residential areas of Soshanguve in August 1997)

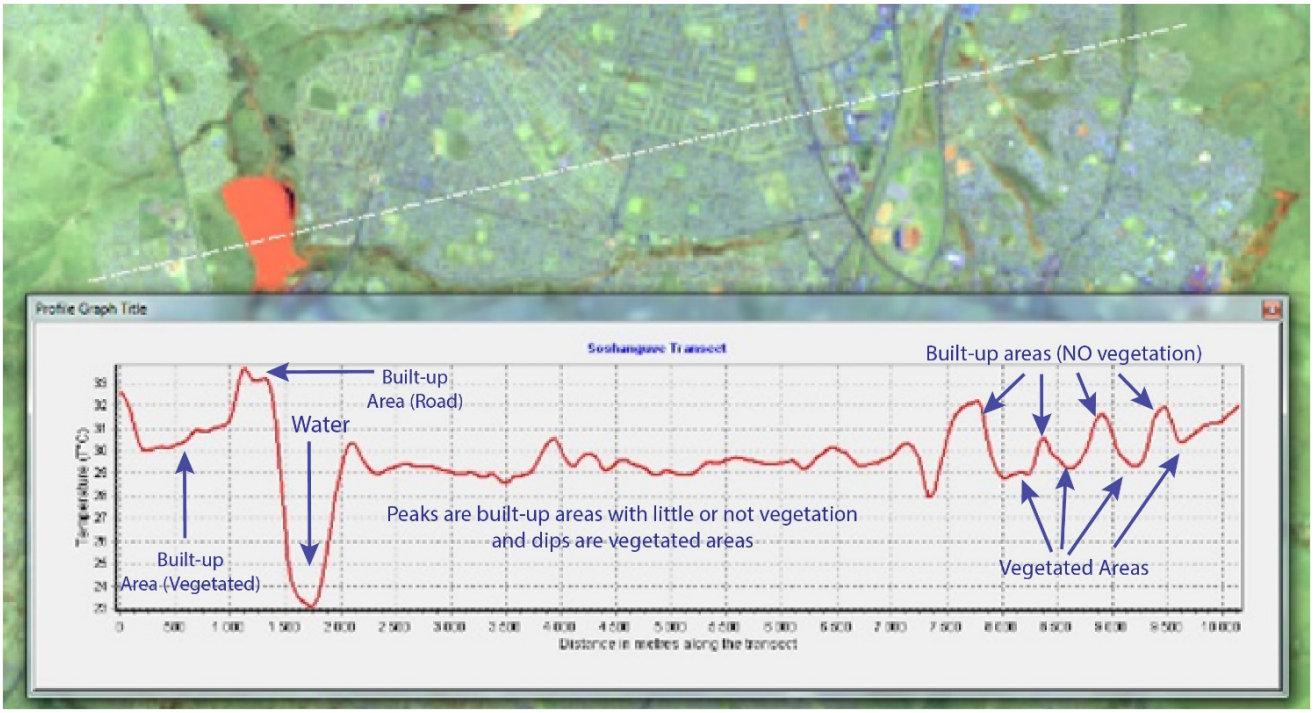

Figure 67 Spatial profile of LST along a transect (white) in the high-density residential areas of Soshanguve in August 2015.

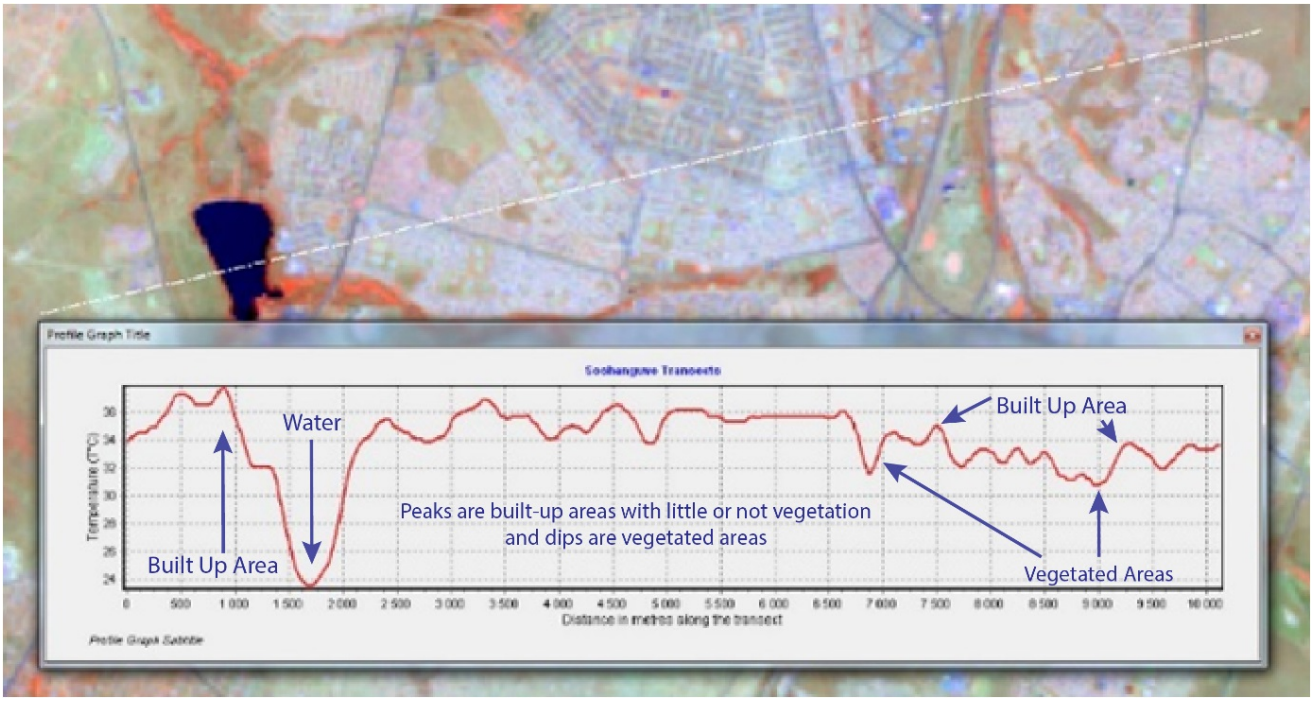

Figure 68: Spatial profile of LST along a transect (white) in the high-density residential areas of Soshanguve in December 1997.

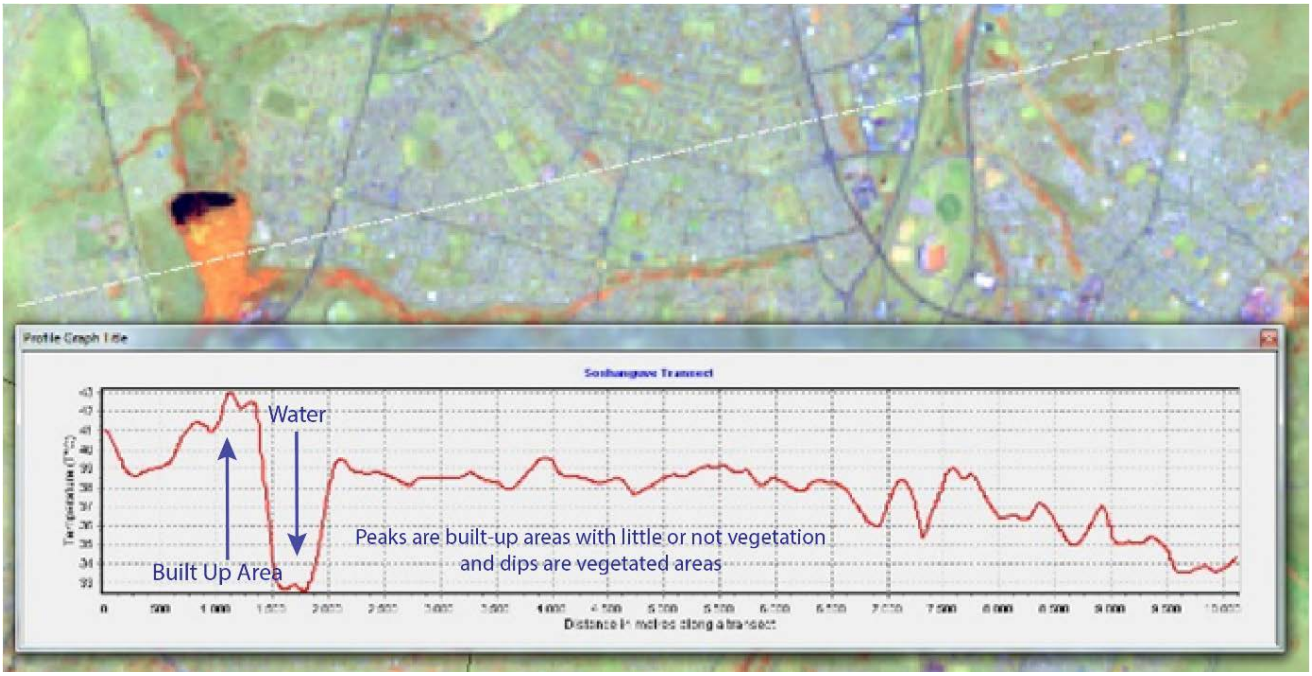

Figure 69: Spatial profile of LST along a transect (white) in the high-density residential areas of Soshanguve in December 2015.

7.5.5 Spatial Profile in the City Centre

There were temperature variations in the City Centre as shown Figure 70 (August 1997), Figure 71 (August 2015), Figure 72 (December 1997) and Figure 73 (December 2015). In the winter of 1997, the highest temperature was 21.0°C and lowest, was 15.1°C while in summer highest temperature was 38.2°C and the lowest, was 27.8°C. In 2015 winter, the highest temperature was 30.0°C and the lowest temperature was 20.8°C while in summer the highest temperature was 36.3°C and the lowest, was 29.8°C. Low LST in urban areas was a result of vegetation growth within the city and peaks were areas where there was no or little vegetation (bare soils and urban areas).

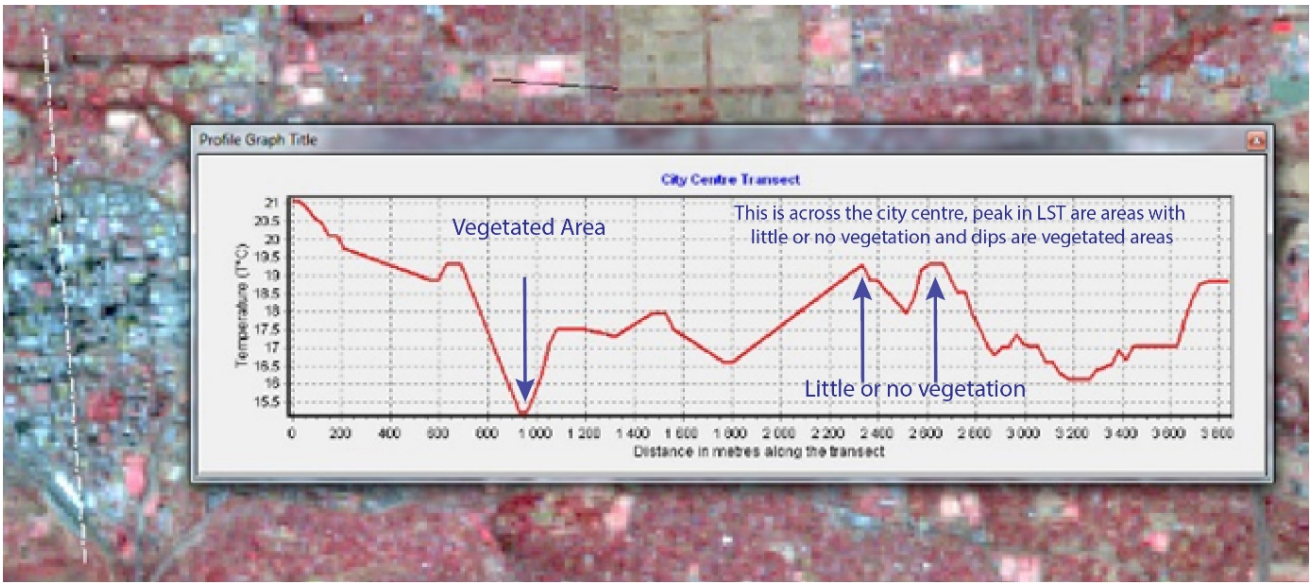

Figure 70: Spatial profile of LST along a transect (white) in the City Centre in August 1997

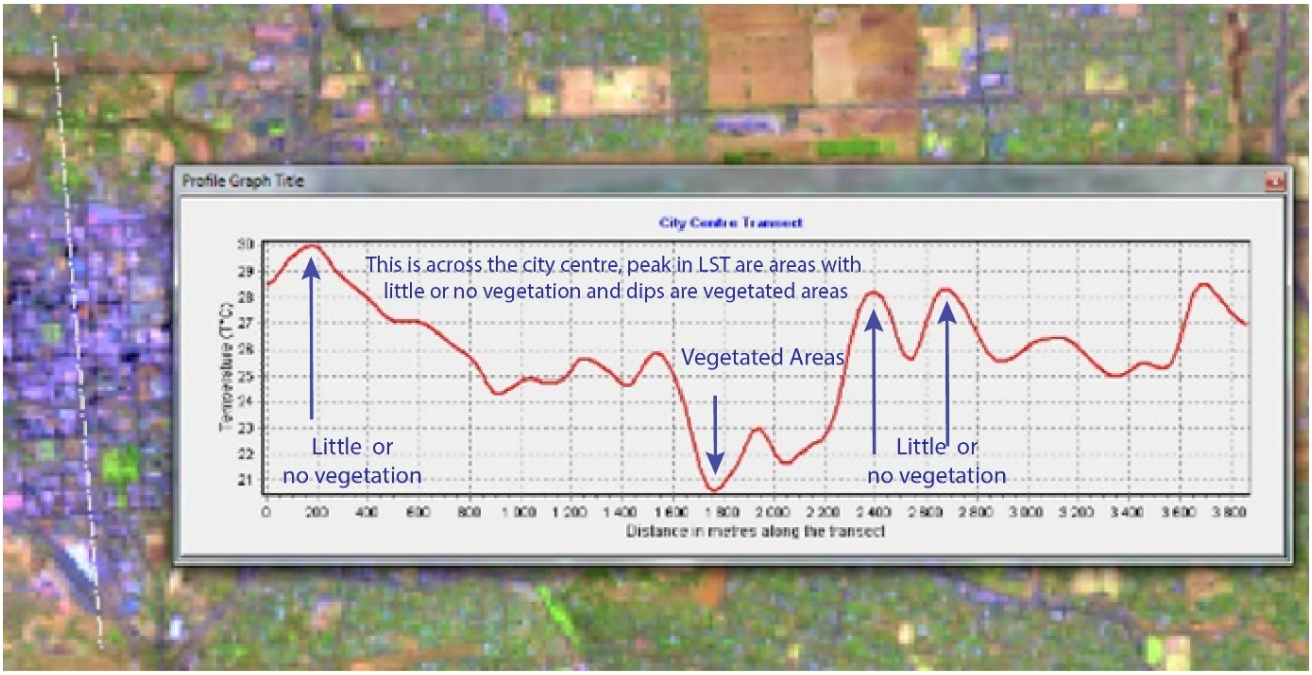

Figure 71: Spatial profile of LST along a transect (white) in the City Centre in August 2015.

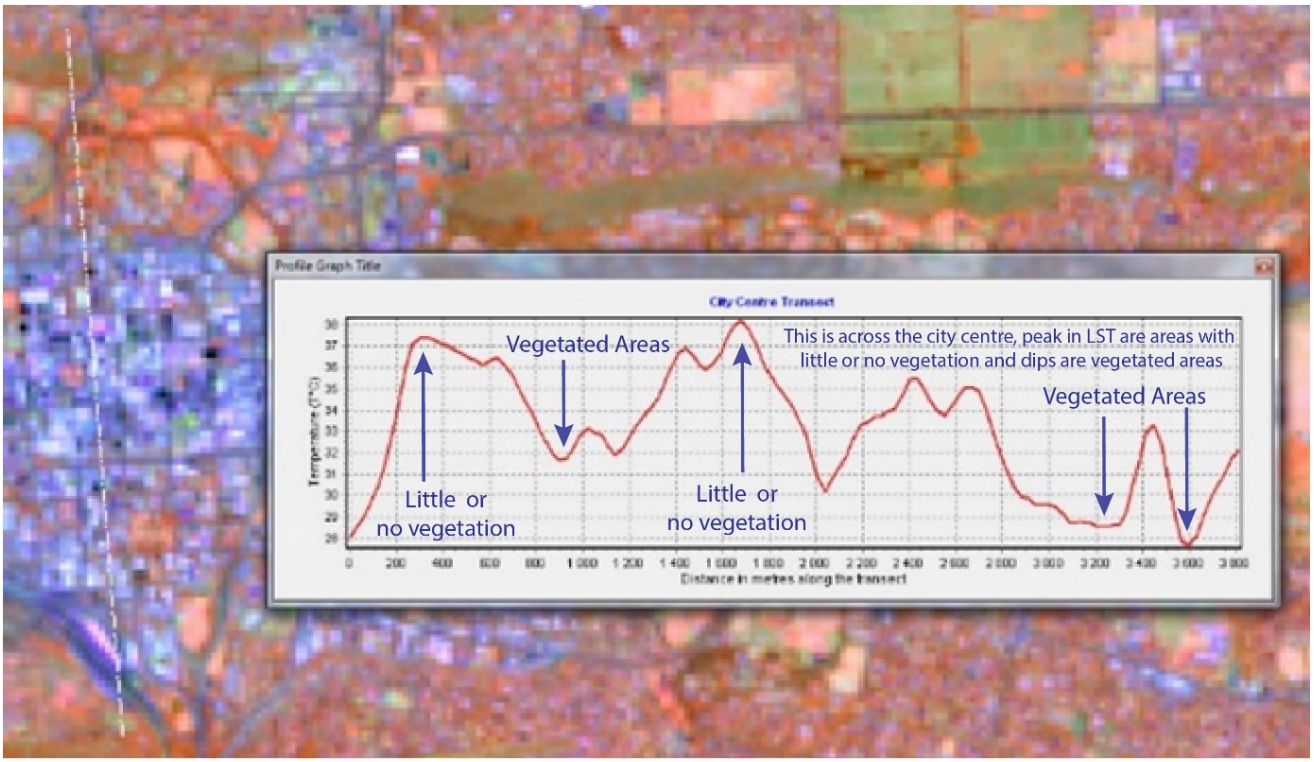

Figure 72: Spatial profile of LST along a transect (white) in the City Centre in December 1997.

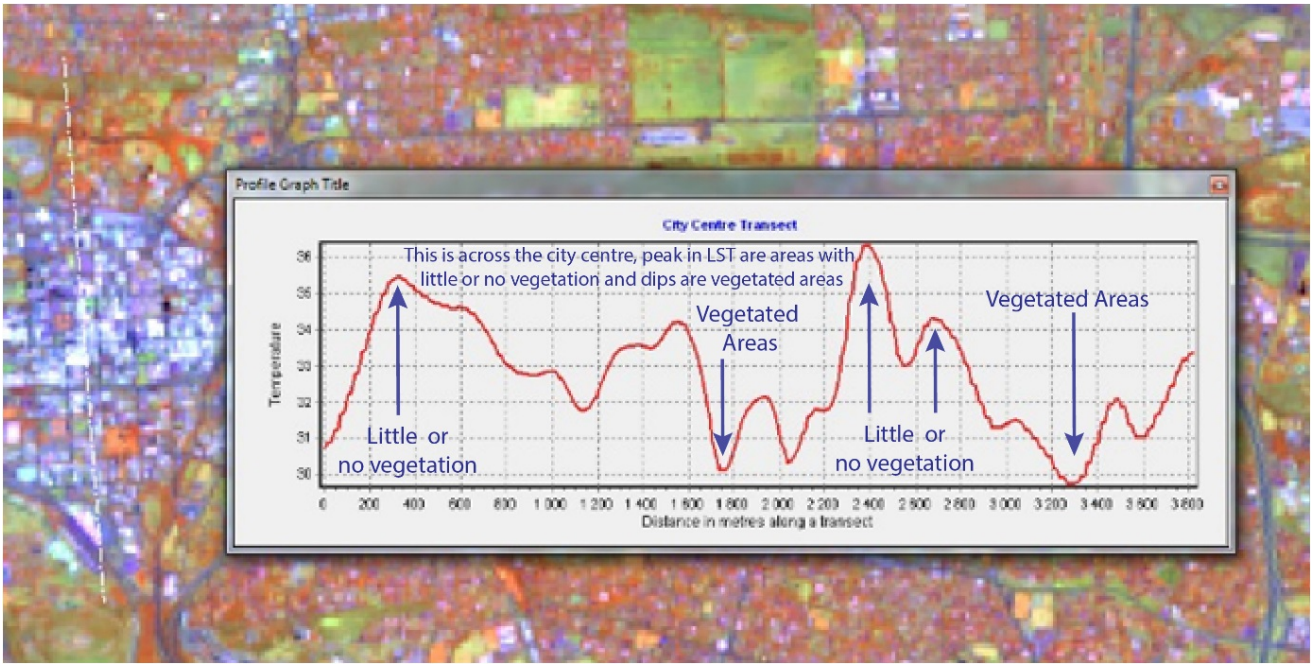

Figure 73: Spatial profile of LST along a transect (white) in the City Centre in December 2015.

7.5.6 Spatial Profile in Mining Areas outside the City

There were temperature variations in the mining area of Cullinan as shown Figure 74 (August 1997), Figure 75 (August 2015), Figure 76 (December 1997) and Figure 77 (December 2015) for the LST spatial profiles of 1997 and 2015 respectively. In winter of 1997, the highest temperature was 25.0°C and the lowest, was 13.0°C while in summer, the highest temperature was 34.8°C and the lowest, was 23.6°C. In winter of 2015, the highest temperature was 34.5°C and the lowest temperature was 17.5°C while in summer, the highest temperature was 38.7°C and the lowest, was 22.0°C. There were some peaks and big depressions (dips) in LST, which was because of the opencast diamond mine, which is full of water. Some of the peaks were because of impervious surfaces and surrounding bare soils in the surrounding agricultural land. The depressions were due to vegetated and cropped areas in and around the Cullinan mine.

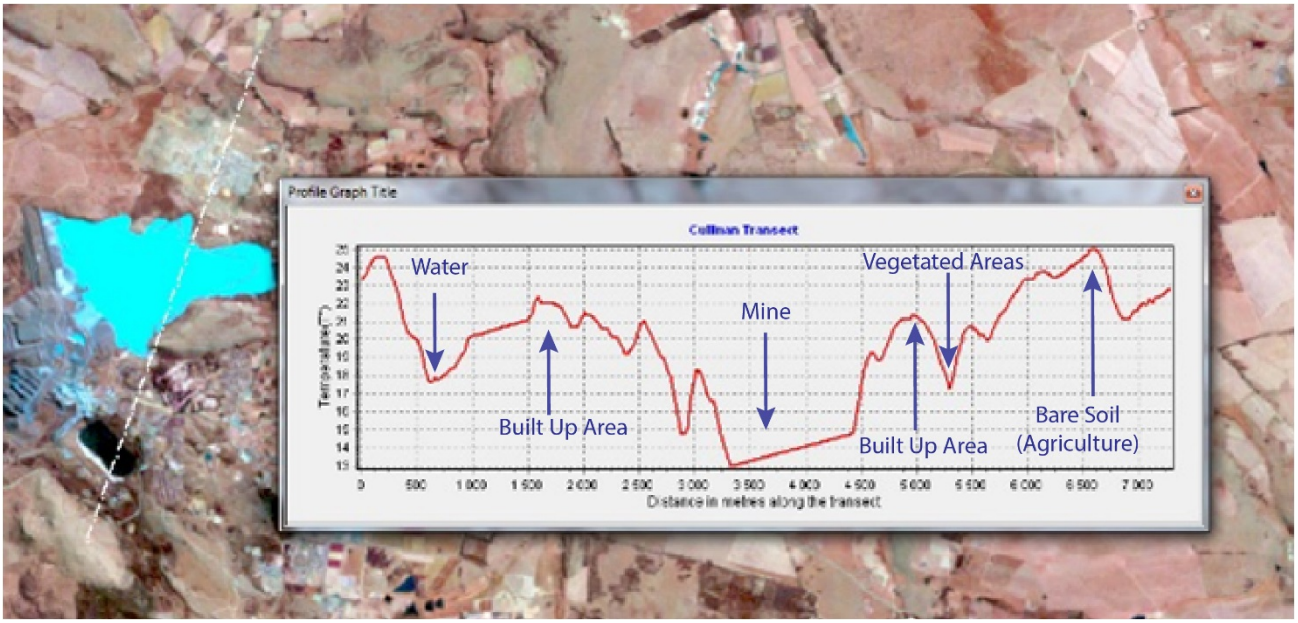

Figure 74: Spatial profile of LST along a transect (white) in mining area of Cullinan in August 1997.

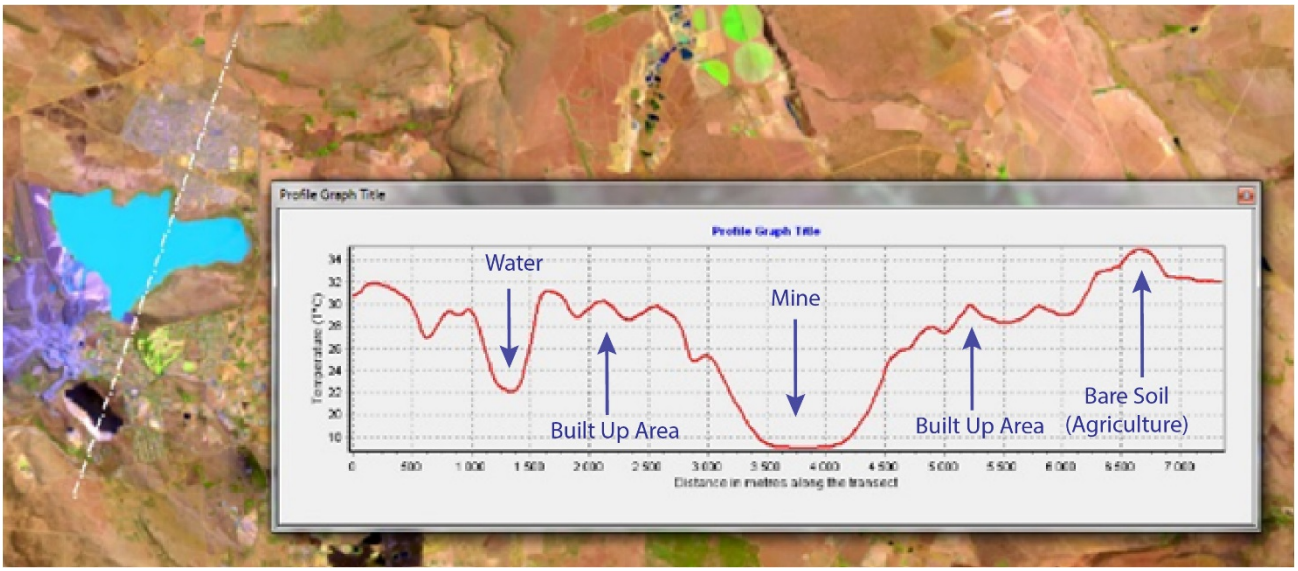

Figure 75: Spatial profile of LST along a transect (white) in mining area of Cullinan in August 2015

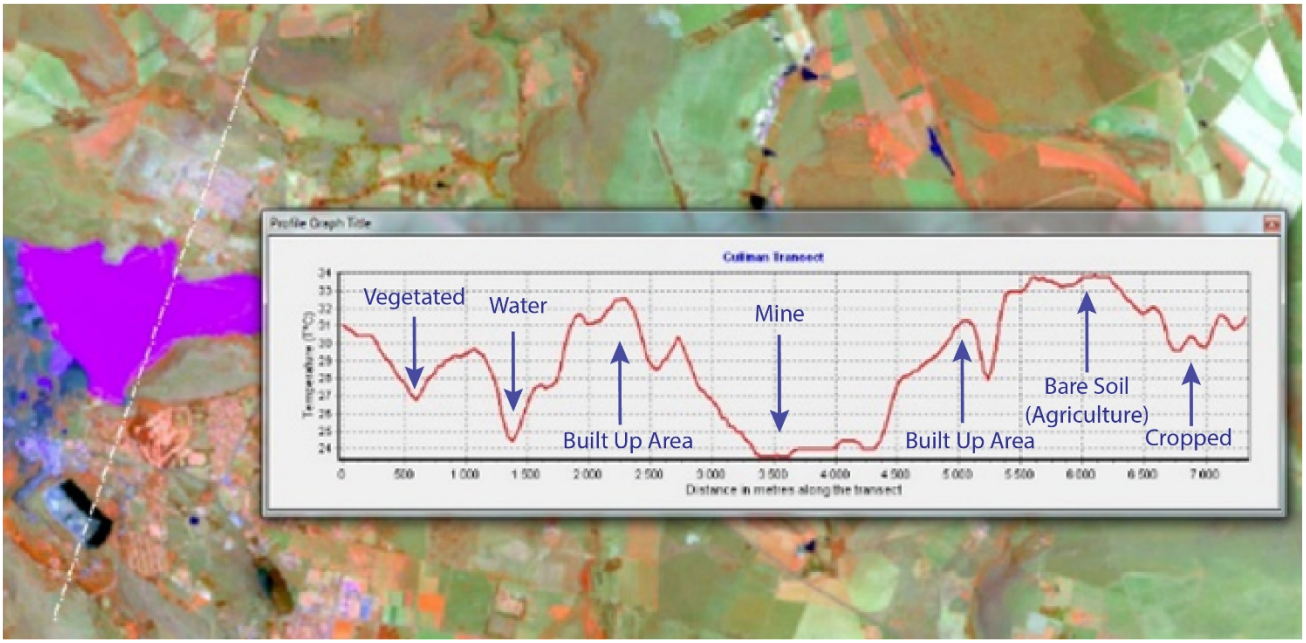

Figure 76 Spatial profile of LST along a transect (white) in mining area of Cullinan in December 1997.

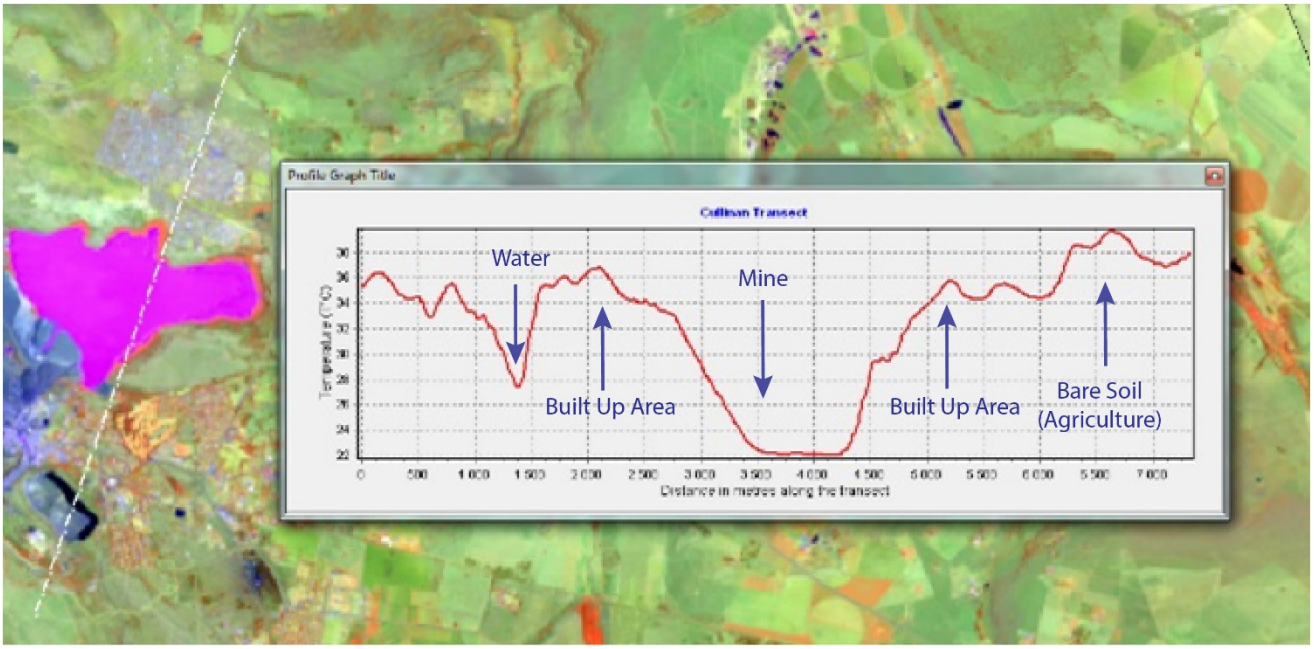

Figure 77: Spatial profile of LST along a transect (white) in mining area of Cullinan in December 2015

Thermal profiles were used to graphically illustrate spatial variations of temperature in the urban environment and its surroundings and it showed curves of UHI variations

with cliffs, peaks, depressions and plateaus, which reveals the thermal variations in different land cover classes (Huang *et al.*, 2008, Abebe, 2013, Ngie *et al.*, 2014, Abutaleb *et al.*, 2014). Anthropogenic activities caused transformation natural to impervious surfaces, which affected the albedo, thermal capacity, heat conductivity (Ngie *et al.*, 2014). Adeyeri *et al.* (2017) argued that bare surfaces and built-up areas have high LST and low LST experienced in vegetated areas. This was in agreement with the results of this research. This argument was also supported by MA *et al.* (2008). In their study of Beijing China, there was a negative correlation between the amount of vegetation and urban heat islands. Bare surfaces experience high temperatures because of incident radiation, which was completely absorbed hence high temperatures (MA *et al.*, 2008, Adeyeri *et al.*, 2017). Yue *et al.* (2007). Research done in Shanghai, China also revealed a negative correlation between NDVI and LST in the study, which indicated that where there was relatively low NDVI and little vegetation in the urban areas, there was high LST (Yue *et al.*, 2007). That was supported in a study done in Kalaburagi, in India by Kumar and Shekhar (2015). A significant increase in temperature and spatial extent of urban heat islands were realised in many cities including Shanghai, China (Li *et al.*, 2009).

Vegetation assists in reducing the temperature of the environment and it also regulates the concentration of carbon in the atmosphere thereby reducing urban heat islands (Li *et al.*, 2013, Ali and Mohammed, 2016). Vegetation provides shade, which reduces incident radiation and evapotranspiration, which helps to regulate overheating (Li *et al.*, 2013, Adeyeri *et al.*, 2017, Mathew *et al.*, 2017). Results of this study agree with research outputs by Adeyeri *et al.* (2017) which show that the lowest LST was in water bodies. Water is a special case in the mapping LST because it has low NDVI and low surface temperature (Kumar and Shekhar, 2015). An urban area with green vegetation suffers less from UHI than a non-vegetated urban area (Tomlinson *et al.*, 2012) and this was the case in the City Centre where low LST is being experienced due to increase in vegetation. There was a variation between winter and summer LST profile and an increase in LST from 1997 to 2015 in both seasons. In winter, there was low temperature as compared to summer hence there was a significant difference in LST between the images of August (winter) and December (summer). In August, LST was

low as compared to December in both 1997 and 2015. There was a significant increase in temperature between 1997 and 2015 in both seasons and this can be attributed to climate change.

7.6 Conclusions

The study revealed that LST can be retrieved from remotely sensed data. Powerful methods used to monitor and quantify urban environment and the information generated helps in understanding urban environments and aid decision-makers in formulating policies that are important in managing urban areas. With this unprecedented urban growth, most of the land surface is no longer natural but impervious. These developments have negative repercussions such as increases in runoff and LST and the creation of an urban microclimate. Land cover affects LST as it was high in areas with impervious surface and low in vegetated areas. Areas of high LST include bare soils and impervious areas as they have low vegetation content. Impervious areas have high LST at inception but as the area becomes vegetated, LST gets lower. This study reveals that non-cropped land have high LST as compared to cropped agricultural land. There was evidence of seasonal variation in LST as it was high in summer and low in winter because of the intensity of solar radiation in the different seasons. This study assessed the seasonal variations in LST and its transition with time. The use of GIS and remote sensing have proved to be a powerful spatial decision support system that can be used in the planning and management of urban environments.

CHAPTER EIGHT

8 AN ASSESSMENT OF THE SPATIO-TEMPORAL URBAN DYNAMICS IN THE COT, SOUTH AFRICA – A SYNTHESIS

8.1 Introduction

Increase in urbanisation in both developing and developed countries has led to uncontrolled urban growth. The main driver of urbanisation is migration, which was brought about by different factors. In South Africa, migration increased from 1994 when the anti-apartheid laws were enacted thereby allowing non-whites to move freely within the country. Migration was also accelerated by the socio-economic and political problems in the Southern African region. This has led to the mass movement of people from different countries into South Africa in search of better living conditions (Chikowore and Willemse, 2017). Urban sprawl, urban morphology and depletion of biodiversity in cities and towns are the major characteristic of most of the urban environments in the world (Kong *et al.*, 2012, Shafizadeh Moghadam and Helbich, 2013). Urban growth and urban sprawl led to traffic congestion, lack of parking, pollution (water, air and land), informal settlements and other socio-economic problems (Shafizadeh Moghadam and Helbich, 2013). The main aim of this study was to assess and quantify spatial and temporal changes in the CoT due to urban growth using different parameters or proxies. These proxies are the extent of urban areas, change in vegetation cover, change in LST and predicting of land cover changes in urban areas.

8.2 Summary of Results

The aim and objectives of the study were successfully achieved. Below is a summary of the findings.

8.2.1 Long-Term Assessment of Urban Sprawl using archival Landsat Imagery

The study was aimed at assessing and quantifying land cover changes in the CoT using Landsat TM. Landsat ETM+ and Landsat OLI imagery from 1984 to 2015.

Remote sensing and GIS techniques were applied in monitoring and quantifying the impacts of urbanisation. Landsat images were downloaded, pre-processed and classified using the maximum likelihood classifier for all the different years into four main classes, which were reclassified into urban and non-urban areas. Post-classification change detection methods and landscape metrics were employed to measure the degree of urban growth from 1984 to 2015. The spatial and attribute data of urban areas in the CoT were attained using landscape metrics. Patchiness, shape index and built-up density landscape metrics and other metrics were calculated. These are necessary for decision-makers to assist them to gain knowledge of the spatio-temporal trends and patterns in urban growth. For the 31 years, urbanisation led to significant land cover changes in the CoT. There was a remarkable increase in urban sprawl as was illustrated in classified maps, landscape metrics and cross-tabulation results. There was an increase in urban areas in relation to other land cover classes such as agriculture and natural vegetation. To ensure sustainable management of urban environments GIS and remote sensing technologies were proven as tools that provide adequate and relevant information that is required in informing researchers and decision-makers. This study demonstrated the use of multi-temporal remote sensing imagery coupled with landscape metrics and change analysis techniques in assessing and quantifying spatio-temporal patterns of urban sprawl in the CoT and these are important in describing urban structures.

8.2.2 Spatial Modelling of Urban Sprawl in the CoT, South Africa.

The aim of this section was to use land cover maps, transitional areas and transitional probabilities to simulate future trends in land cover types using the CA-Markov model. To achieve this objective classified Landsat imagery of 1986, 2005 and 2013 were used to predict future land cover scenarios. Transitional probabilities and transitional areas between 1986 and 2005 coupled with the classified map of 1986 and 2005 were used to predict land cover in 2009. The predicted map of 2009 was validated against the classified map of 2009. Transitional probabilities and transitional areas between 1986 and 2005 coupled with the classified map of 1986 and 2009 were used to predict land cover in 2013. The predicted map of 2013 was validated against the classified map of 2013. Built-up areas were calculated to show the urban patterns, characteristics

and trends in the CoT. Validation of the performance of prediction models was necessary as it indicated that CA-Markov simulation provides good results for planning purposes. Validation results revealed an agreement between the predicted images and classified ones. The validation values derived from the predicted images of 2009 and 2013 show that CA-Markov models can be used to predict urban sprawl. However, there is a need to be cautious about using the CA-Markov in long-term predictions, as they will give unreliable results. Predicting future urban sprawl scenarios revealed that integrated approach of GIS, remote sensing and urban prediction techniques can be used as part of the spatial decision support system that will aid researchers and spatial planners in to gain an understanding of future, patterns and trends in urban growth. This will help policy-makers to formulate land use planning and management policies and strategies that are needed for the sustainable management of the resources.

8.2.3 Short-term Assessment of Urban Sprawl Using Archival SPOT Imagery

The aim of short-term land cover change was to use high-resolution satellite imagery to assess and quantify the land cover changes in specific areas at a larger scale as compared to the long-term land cover change, which utilised Landsat imagery. In this instance, analysis focused on three main areas, Pretoria East (low-density), Pretoria Moot (medium-density) and Eastern Townships (high-density) was carried out. SPOT imagery of 2008, 2012 and 2015 were used to map land cover in these three areas. After pre-processing the SPOT imagery, a maximum likelihood classifier was used to classify built-up and non-built-up areas. Land cover changes were assessed and there was an increase in urban areas between the years in the three study sites. There was a high increase in built-up areas in high-density as compared to low-density and medium-density areas. The study revealedthat, the main contributor of urban change in Pretoria whether low-density, medium-density or high-density were RDP Houses, property development by private developers, the establishment of backyard houses and informal settlements and the improvement of transport networks. This study also analysed the impact of urbanisation in areas earmarked for conservation (CBAs and their ESAs). These CBAs and ESAs were affected by urban growth and it was evident in high-density areas followed by medium-density areas but in the low-density areas these changes but were minimal. The maps revealed an impact of urban growth on

sensitive areas and there is a need for local government to enact policies that ensure protection of these CBAs and ESAs as they are needed in maintaining conservation targets.

8.2.4 Monitoring Vegetation Phenology Using MODIS NDVI 250m

Urban growth has exerted too much pressure on the terrestrial ecosystems, which has led to the depletion of vegetation. Urbanisation has proved to be the main contributor to vegetation loss and has caused a global decline in vegetation cover. To examine spatio-temporal variations in vegetation spatio-temporal variation in vegetation cover, the study utilised MODIS NDVI with a 250m spatial resolution and 16 days temporal resolution. The study used time series plots, Mann-Kendall statistics and Sen's slope estimator to analyse seasonal trends in vegetation cover from 2000 to 2016. One of the characteristics of the urban areas as depicted in most of the time series plots was that vegetation in urban areas follows the seasonal patterns. When an area is set aside and cleared for urban development, the local government, residents and land managers (local government) of that area will start to grow vegetation. Alien species and local species will start to grow in those disturbed or +transformed areas. This is the main reason why even the urban environments were following the seasonal patterns of high vegetation in summer and low in winter. There is an overall decreasing trend of vegetation cover in all the different land cover types. Time series plots showed the dates when the developments in some of the areas started. Vegetation cover in high-density areas was low as compared to other areas. Most of the people staying in the high-density suburbs are the low-income earners who are dependent on firewood to substantiate their energy. Natural vegetation in the low-density areas or protected areas have high NDVI because there are few or no people dwelling in those areas. Most of the people in the low-density areas are high-income earners who can afford electricity and can buy firewood if need be without getting into the nearby bushes to destroy vegetation. Some of the areas are protected and inaccessible that no one can trespass into those areas, hence the high NDVI values.

8.2.5 Spatio-Temporal Variations of LST

With the increase in urban growth, one of the proxies that can be affected by these anthropogenic influences is LST. The thermal band in Landsat images was used to extract the satellite brightness temperature for August (1997 and 2015) and December (1997 and 2015). NDVI was used to extract emissivity, which was used to retrieve LST. There was a negative correlation between NDVI and LST. Using algorithms embedded in ArcGIS (ESRI, 2015) and ERDAS Imagine (Intergraph, 2014) satellite brightness temperature, NDVI, emissivity and LST were retrieved. Spatio-Temporal changes in LST were analysed in different land cover classes and revealed an increase in LST between 1997 and 2015. There were difference in LST between different land cover types with high LST in bare and impervious surfaces and low in vegetated and cropped areas. Impervious areas for example settlement have high LST at inception but as the area becomes vegetated, LST was reduced. This study revealed that non-cropped land (bare) have high LST as compared to cropped agricultural land. There was evidence of seasonal variations in LST as it was high in summer and low in winter. There was a high intensity of solar radiation in summer as compared to winter hence the high LST in summer than in winter. GIS and remote sensing have proved to be powerful spatial decision support tools in the planning and management of urban environments.

8.3 Conclusions

There was an increase in urban growth in the CoT between 1984 and 2015 as shown in the land cover maps and landscape metric results. The highest degree of urban growth occurred in high-density areas as compared to low-density and medium-density. There was generally an increase in urban growth, which resultantly led to the LST increases and reduction in vegetation cover. Vegetation in urban areas followed the sinusoidal pattern with low greenness in winter and high in summer. This was evident on the temporal profiles but vegetation cover had a decreasing trend in all the different land cover types. There were seasonal variations in vegetation cover in different land uses in the COT. There was a decreasing trend of vegetation and this can only be attributed to urbanisation. There was an increase in LST with time and that was a result of climate change, which was induced by urbanisation. The unprecedented urban growth in some of the areas such as informal settlements, has

led to the encroachment of urban-like environments into areas that were earmarked for conservation (CBAs and ESAs). There was unprecedented growth of informal settlements (constructed without adherence to the guidelines and by-laws of the municipalities) hence the development of urban areas in areas earmarked for conservation. There was anticipated growth in urban areas due to continued urbanisation, which were revealed using the urban prediction models.

8.4 Limitations of the Study

Below are limitations of this study

8.4.1 Lack of Data

One of the challenges experienced in the research was the lack of data to use in the research. The research used only MODIS, Landsat and SPOT imagery whereas there are better and very high-resolution imagery such as IKONOS, QUICKBIRD, WorldView and many others that are on the market but they were beyond the budget of this study. There are also data restrictions for students in some organisations that are responsible for the distribution of remotely sensed data, which makes it difficult to acquire data required for a project.

8.5 Recommendations

Below are some of the recommendations from this research.

8.5.1 High-resolution Imagery

There is a need for very high-resolution satellite data for researcher and policy-makers to accurately quantify and assess urban environments. SPOT imagery cannot be compared to sensors such as QUICKBIRD, IKONOS, GeoEye and WorldView with very high-resolution. The above-mentioned sensors will improve urban mapping and will produce large scape urban land cover maps. It will be easy to map informal settlements using very high-resolution sensors. In future and if the budget permits, researchers are encouraged to use very high-resolution satellite sensor coupled with aerial photogrammetry such as drones surveys. There is need to make use of drones,

aerial photogrammetry and LIDAR systems to assist in the mapping, monitoring and quantification of urban growth.

Future urban research requires the use of high-resolution and very high-resolution satellite imagery (for example IKONOS, WorldView) and the use of drones and aerial photogrammetry. There is a need to automate the urban mapping and change detection initiative so that there can be enough and constant supply of information to support land use decision-making process.

8.5.2 Automating the Urban Mapping Process

There is a need to automate the process of urban mapping using remotely sensed data. That same process will be able to assess, quantify and predict of land cover processes. This can be a very important tool needed to sustainably manage urban environments. The importance of automating the process of mapping urban areas and assessing change in the urban growth will be to allow researchers and planners to access timely data needed in ther decision-making process.

8.5.3 Improved Access to Data

There is a need for improved access to geo-spatial data in South Africa. Remotely sensed data must be made easily available and student support needs to be enhanced so that they will not struggle to acquire data regardless of cost and logistical challenges. There should be no limit to remote sensing data for researchers and remotely sensed data from commercial satellite sensors must be easily available.

REFERENCES

ABEBE, G. A. 2013. Quantifying Urban growth pattern in developing Countries Using Remote Sensing and Spatial Metrics: A case study of Kampala, Uganda. *Msc Thesis*.

ABUTALEB, K., ADELINE, N., AHMED, F., AHMED, M., ELKAFRAWY, S., ARAFAT, S. & DARWISH, A. 2014. Investigation of Urban Heat Island Using Landsat Data. *Proceedings of the 10th International Conference of AARSE***,** 223.

ABUTALEB, K., TAIWO, O.-J., AHMED, F. & NGIE, A. 2013. Modeling urban change using cellular automata: the case study of Johannesburg, South Africa. *Proceedings of the IGU Urban Geography Commission***,** 64.

ADDINSOFT 2017. XLSTAT 2017: Data Analysis and Statistical Solution for Microsoft Excel. *Paris, France*

ADEYERI, O. E., AKINSANOLA, A. A. & ISHOLA, K. A. 2017. Investigating surface urban heat island characteristics over Abuja, Nigeria: Relationship between land surface temperature and multiple vegetation indices. *Remote Sensing Applications: Society and Environment,* 7**,** 57-68.

ADUAH, M. & BAFFOE, P. 2013. Remote Sensing for Mapping Land-Use/Cover Changes and Urban Sprawl in Sekondi-Takoradi, Western Region of Ghana. *The International Journal of Engineering and Science (IJES),* 2**,** 66-72.

AGUILERA, F., VALENZUELA, L. M. & BOTEQUILHA-LEITÃO, A. 2011. Landscape metrics in the analysis of urban land use patterns: A case study in a Spanish metropolitan area. *Landscape and Urban Planning,* 99**,** 226-238.

AHMED, B. & AHMED, R. 2012. Modeling urban land cover growth dynamics using multi-temporal satellite images: a case study of Dhaka, Bangladesh. *ISPRS International Journal of Geo-Information,* 1**,** 3-31.

AITHAL, B. & RAMACHANDRA, T. 2013. Measuring urban sprawl in Tier II cities of Karnataka, India. *Global Humanitarian Technology Conference: South Asia Satellite (GHTC-SAS), 2013 IEEE*, 321-329.

AL-SHALABI, M., PRADHAN, B., BILLA, L., MANSOR, S. & ALTHUWAYNEE, O. F. 2013. Manifestation of Remote Sensing Data in Modeling Urban Sprawl Using the SLEUTH Model and Brute Force Calibration: A Case Study of Sana'a City, Yemen. *Journal of the Indian Society of Remote Sensing,* 41**,** 405-416.

AL-SHARIF, A. A. A. & PRADHAN, B. 2014. Monitoring and predicting land use change in Tripoli Metropolitan City using an integrated Markov chain and cellular automata models in GIS. *Arabian Journal of Geosciences,* 7**,** 4291-4301.

ALI, A. & MOHAMMED, E. 2016. Impact of Industrial Activities on Land Surface Temperature Using Remote Sensing and GIS Techniques-A Case Study in Jubail, Saudi Arabia. *J Geogr Nat Disast S,* 6**,** 2167-0587.

ALSHARIF, A. A. A. & PRADHAN, B. 2014. Urban Sprawl Analysis of Tripoli Metropolitan City (Libya) Using Remote Sensing Data and Multivariate Logistic Regression Model. *Journal of the Indian Society of Remote Sensing,* 42**,** 149-163.

ARAYA, Y. H. & CABRAL, P. 2010. Analysis and modeling of urban land cover change in Setúbal and Sesimbra, Portugal. *Remote Sensing,* 2**,** 1549-1563.

ARTIS, D. A. & CARNAHAN, W. H. 1982. Survey of emissivity variability in thermography of urban areas. *Remote Sensing of Environment,* 12**,** 313-329.

ASTRIUM 2017. SPOT 6 | SPOT 7, Technical Sheet. *http://www.intelligence-airbusds.com/files/pmedia/edited/r18072_9_spot_6_technical_sheet.pdf (Accessed on: 5/9/2015)*.

BHATTA, B. 2009. Analysis of urban growth pattern using remote sensing and GIS: a case study of Kolkata, India. *International Journal of Remote Sensing,* 30**,** 4733-4746.

BHATTA, B., SARASWATI, S. & BANDYOPADHYAY, D. 2010. Urban sprawl measurement from remote sensing data. *Applied Geography,* 30**,** 731-740.

CAMERON, R. 1996. The reconstruction and development programme. *Journal of Theoretical Politics,* 8**,** 283-294.

CARROLL, C. R. 1992. Ecological management of sensitive natural areas. *Conservation Biology***,** 347-372.

CHANDER, G. & MARKHAM, B. 2003. Revised Landsat-5 TM radiometric calibration procedures and postcalibration dynamic ranges. *IEEE Transactions on geoscience and remote sensing,* 41**,** 2674-2677.

CHIKOWORE, T. & WILLEMSE, L. 2017. Identifying the changes in the quality of life of Southern African Development Community (SADC) migrants in South Africa from 2001 to 2011. *South African Geographical Journal= Suid-Afrikaanse Geografiese Tydskrif,* 99**,** 86-112.

CHISHALESHALE, M., SHACKLETON, C. M., GAMBIZA, J. & GUMBO, D. 2015. The prevalence of planning and management frameworks for trees and green spaces in urban areas of South Africa. *Urban Forestry & Urban Greening,* 14**,** 817-825.

CILLIERS, D. P. 2010. *The development and use of a land-use suitability model in spatial planning in South Africa/DP Cilliers.* North-West University.

COBBINAH, P. B. & AMOAKO, C. 2012. Urban sprawl and the loss of peri-urban land in Kumasi, Ghana. *International Journal of Social and Human Sciences,* 6**,** 397.

COHEN, B. 2006. Urbanization in developing countries: Current trends, future projections, and key challenges for sustainability. *Technology in society,* 28**,** 63-80.

CONGALTON, R. G. 1991. A review of assessing the accuracy of classifications of remotely sensed data. *Remote sensing of Environment,* 37**,** 35-46.

DE JONG, R., DE BRUIN, S., DE WIT, A., SCHAEPMAN, M. E. & DENT, D. L. 2011. Analysis of monotonic greening and browning trends from global NDVI time-series. *Remote Sensing of Environment,* 115**,** 692-702.

DEEP, S. & SAKLANI, A. 2014. Urban sprawl modeling using cellular automata. *The Egyptian Journal of Remote Sensing and Space Science,* 17**,** 179-187.

DEEPA, R. & RAMACHANDRA, T. 1999. Impact of Urbanization in the Interconnectivity of Wetlands. *National Symposium on Remote Sensing Applications for Natural Resources: Retrospective and Perspective (XIX-XXI 1999), Indian Society of Remote Sensing, Banglore*.

DEKA, J., TRIPATHI, O. P. & KHAN, M. L. 2011. Urban growth trend analysis using Shannon Entropy approach-A case study in North-East India. *International Journal of Geomatics and Geosciences,* 2**,** 1062-1068.

DICKIE, I. A., BENNETT, B. M., BURROWS, L. E., NUÑEZ, M. A., PELTZER, D. A., PORTÉ, A., RICHARDSON, D. M., REJMÁNEK, M., RUNDEL, P. W. & VAN WILGEN, B. W. 2014. Conflicting values: ecosystem services and invasive tree management. *Biological Invasions,* 16**,** 705-719.

DODMAN, D., LECK, H., RUSCA, M. & COLENBRANDER, S. 2017. African Urbanisation and Urbanism: Implications for risk accumulation and reduction. *International Journal of Disaster Risk Reduction,* 26**,** 7-15.

DU PLESSIS, J. 2010. Injecting a rapid rail link into a metropolis. *Civil Engineering***,** 63.

EASTMAN, J. 2015. TerrSet: Geospatial Monitoring and Modeling Software. *Clark Labs, Clark University*.

ECKERT, S., HÜSLER, F., LINIGER, H. & HODEL, E. 2015. Trend analysis of MODIS NDVI time series for detecting land degradation and regeneration in Mongolia. *Journal of Arid Environments,* 113**,** 16-28.

EL-MAGD, I. A., ISMAIL, A. & ZANATY, N. 2016. Spatial Variability of Urban Heat Islands in Cairo City, Egypt using Time Series of Landsat Satellite Images. *International Journal of Advanced Remote Sensing and GIS***,** pp. 1618-1638.

EL GAROUANI, A., MULLA, D. J., EL GAROUANI, S. & KNIGHT, J. 2017. Analysis of urban growth and sprawl from remote sensing data: Case of Fez, Morocco. *International Journal of Sustainable Built Environment*.

ESCH, T., TAUBENB, H., X00F, CK, FELBIER, A., HELDENS, W., WIESNER, M. & DECH, S. Monitoring of global urbanization-time series analyses for mega cities based on optical and SAR data. Earth Observation and Remote Sensing Applications (EORSA), 2012 Second International Workshop on, 8-11 June 2012 2012. 21-25.

ESPINDOLA, G. M. D., CARNEIRO, E. L. N. D. C. & FAÇANHA, A. C. 2017. Four decades of urban sprawl and population growth in Teresina, Brazil. *Applied Geography,* 79**,** 73-83.

ESRI 2015. ArcGIS Desktop: Release 10. *Environmental Systems Research Institute*.

FAROOQ, S. & AHMAD, S. 2008. Urban sprawl development around Aligarh city: a study aided by satellite remote sensing and GIS. *Journal of the Indian Society of Remote Sensing,* 36**,** 77-88.

FU, Q., MAO, F., ZHOU, W. & SONG, J. 2010. Simulation of urban land use change using Cellular Automata and Agent integrated model. *Environmental Science and Information Application Technology (ESIAT), 2010 International Conference on,* 1**,** 866-869.

GARENNE, M. Migration, urbanisation and child health in Africa: a global perspective. Conference on African Migration in Comparative Perspective. Johannesburg, 2003. 4-7.

GOLDBLATI, P. 1978. An analysis of the flora of southern Africa: its characteristics, relationships, and orgins. *Annals of the Missouri Botanical Garden***,** 369-436.

GRARD 2014. Technical Report for the Gauteng Conservation Plan (Gauteng C-Plan v3.3). *Gauteng Department of Agriculture and Rural Development: Nature Conservation Directorate***,** 60.

GRIGGS, D., STAFFORD-SMITH, M., GAFFNEY, O., ROCKSTRÖM, J., ÖHMAN, M. C., SHYAMSUNDAR, P., STEFFEN, W., GLASER, G., KANIE, N. & NOBLE, I. 2013. Policy: Sustainable development goals for people and planet. *Nature,* 495**,** 305.

GRIZANS, J. 2009. Urban issues and solutions in the context of sustainable development: A review of the literature. Working Paper, Department of Environmental and Business Economics, University of Southern Denmark.

GROBLER, C. H., BREDENKAMP, G. J. & BROWN, L. R. 2006. Primary grassland communities of urban open spaces in Gauteng, South Africa. *South African Journal of Botany,* 72**,** 367-377.

GUSTAFSON, E. J. 1998. Quantifying landscape spatial pattern: what is the state of the art? *Ecosystems,* 1**,** 143-156.

HARDY, C. & NEL, A. 2015. Data and techniques for studying the urban heat island effect in Johannesburg. *The International Archives of Photogrammetry, Remote Sensing and Spatial Information Sciences,* 40**,** 203.

HEGAZY, I. R. & KALOOP, M. R. 2015. Monitoring urban growth and land use change detection with GIS and remote sensing techniques in Daqahlia governorate Egypt. *International Journal of Sustainable Built Environment,* 4**,** 117-124.

HEROLD, M., COUCLELIS, H. & CLARKE, K. C. 2005. The role of spatial metrics in the analysis and modeling of urban land use change. *Computers, Environment and Urban Systems,* 29**,** 369-399.

HEROLD, M., GOLDSTEIN, N. C. & CLARKE, K. C. 2003. The spatiotemporal form of urban growth: measurement, analysis and modeling. *Remote sensing of Environment,* 86**,** 286-302.

HEROLD, M., MENZ, G. & CLARKE, K. C. 2001. Remote sensing and urban growth models-demands and perspectives. *Symposium on remote sensing of urban areas,* 35.

HUANG, L., LI, J., ZHAO, D. & ZHU, J. 2008. A fieldwork study on the diurnal changes of urban microclimate in four types of ground cover and urban heat island of Nanjing, China. *Building and environment,* 43**,** 7-17.

HUANG, S.-L., WANG, S.-H. & BUDD, W. W. 2009. Sprawl in Taipei's peri-urban zone: Responses to spatial planning and implications for adapting global environmental change. *Landscape and Urban Planning,* 90**,** 20-32.

INTERGRAPH 2014. Erdas Imagine 2014. *Atlanta, Georgia, USA*.

ITT 2007. ENVI 4.4. *Boulder, Colorado*.

JANTZ, C. A., GOETZ, S. J. & SHELLEY, M. K. 2004. Using the SLEUTH urban growth model to simulate the impacts of future policy scenarios on urban land use in the Baltimore-Washington metropolitan area. *Environment and Planning B,* 31**,** 251-272.

JAT, M. K., GARG, P. K. & KHARE, D. 2008. Monitoring and modelling of urban sprawl using remote sensing and GIS techniques. *International journal of Applied earth Observation and Geoinformation,* 10**,** 26-43.

JENSEN, J. R. & COWEN, D. C. 1999. Remote sensing of urban/suburban infrastructure and socio-economic attributes. *Photogrammetric engineering and remote sensing,* 65**,** 611-622.

JENSEN, J. R. & IM, J. 2007. Remote sensing change detection in urban environments. *Geo-spatial technologies in urban environments.* Springer.

JENSEN, J. R. & LULLA, K. 1987. Introductory digital image processing: a remote sensing perspective.

JI, W., MA, J., TWIBELL, R. W. & UNDERHILL, K. 2006. Characterizing urban sprawl using multi-stage remote sensing images and landscape metrics. *Computers, Environment and Urban Systems,* 30**,** 861-879.

JIANG, G., MA, W., QU, Y., ZHANG, R. & ZHOU, D. 2016. How does sprawl differ across urban built-up land types in China? A spatial-temporal analysis of the Beijing metropolitan area using granted land parcel data. *Cities,* 58**,** 1-9.

JIN, K., WANG, F. & LI, P. 2018. Responses of Vegetation Cover to Environmental Change in Large Cities of China. *Sustainability,* 10**,** 270.

JOUBERT, H. 2009. Needed: a paradigm shift in the provision of road infrastructure in Gauteng. *SATC 2009*.

KAMUSOKO, C. & ANIYA, M. 2007. Land use/cover change and landscape fragmentation analysis in the Bindura District, Zimbabwe. *Land degradation & development,* 18**,** 221-233.

KAMUSOKO, C. & ANIYA, M. 2009. Hybrid classification of Landsat data and GIS for land use/cover change analysis of the Bindura district, Zimbabwe. *International journal of remote sensing,* 30**,** 97-115.

KAMUSOKO, C., ANIYA, M., ADI, B. & MANJORO, M. 2009. Rural sustainability under threat in Zimbabwe–simulation of future land use/cover changes in the Bindura district based on the Markov-cellular automata model. *Applied Geography,* 29**,** 435-447.

KENDALL, M. G. 1938. A new measure of rank correlation. *Biometrika,* 30**,** 81-93.

KERR, Y. H., LAGOUARDE, J. P. & IMBERNON, J. 1992. Accurate land surface temperature retrieval from AVHRR data with use of an improved split window algorithm. *Remote Sensing of Environment,* 41**,** 197-209.

KITYUTTACHAI, K., TRIPATHI, N. K., TIPDECHO, T. & SHRESTHA, R. 2013. CA-Markov analysis of constrained coastal urban growth modeling: Hua Hin seaside city, Thailand. *Sustainability,* 5**,** 1480-1500.

KLEYN, L., MANGARA, P. & REMAS, H. Implementation of Automatic Spectral Rule-Based Preliminary Mapping for Enhanced Object-Based Classification of South African Land Cover Classes. Proceedings of AfricaGEO Conference.

KONG, F., YIN, H., NAKAGOSHI, N. & JAMES, P. 2012. Simulating urban growth processes incorporating a potential model with spatial metrics. *Ecological Indicators,* 20**,** 82-91.

KOWE, P., PEDZISAI, E., GUMINDOGA, W. & RWASOKA, D. 2015. An analysis of changes in the urban landscape composition and configuration in the Sancaktepe District of Istanbul Metropolitan City, Turkey using landscape metrics and satellite data. *Geocarto International,* 30**,** 506-519.

KUMAR, D. & SHEKHAR, S. 2015. Statistical analysis of land surface temperature–vegetation indexes relationship through thermal remote sensing. *Ecotoxicology and Environmental Safety,* 121**,** 39-44.

KUMAR, K. S., BHASKAR, P. U. & PADMAKUMARI, K. 2012. Estimation of land surface temperature to study urban heat island effect using LANDSAT ETM+ image. *International journal of Engineering Science and technology,* 4**,** 771-778.

LANDAU, L. B., SEGATTI, A. & MISAGO, J. P. 2011. Governing Migration and Urbanisation in South African Municipalities: Developing Approaches to Counter Poverty and Social Fragmentation. *South African Local Government Association: Pretoria*.

LAOSUWAN, T., GOMASATHIT, T. & ROTJANAKUSOL, T. 2017. Application of Remote Sensing for Temperature Monitoring: The Technique for Land Surface Temperature Analyis. *Journal of Ecological Engineering,* 18**,** 53-60.

LE ROUX, A. 2012. *Quantifying the spatial implications of future land use policies in South Africa: reshaping a city through land use modelling.* University of Utrecht, The Netherlands.

LE ROUX, A. & AUGUSTIJN, P. 2017. Quantifying the spatial implications of future land use policies in South Africa. *South African Geographical Journal= Suid-Afrikaanse Geografiese Tydskrif,* 99**,** 29-51.

LEE, Y. & CHANG, H. 2011. The simulation of land use change by using CA-Markov Model: A case study of Tainan City, Taiwan. *Geoinformatics, 2011 19th International Conference on***,** 1-4.

LEMANSKI, C. 2009. Augmented informality: South Africa's backyard dwellings as a by-product of formal housing policies. *Habitat International,* 33**,** 472-484.

LI, H., HARVEY, J. T., HOLLAND, T. & KAYHANIAN, M. 2013. The use of reflective and permeable pavements as a potential practice for heat island mitigation and stormwater management. *Environmental Research Letters,* 8**,** 015023.

LI, J.-J., WANG, X.-R., WANG, X.-J., MA, W.-C. & ZHANG, H. 2009. Remote sensing evaluation of urban heat island and its spatial pattern of the Shanghai metropolitan area, China. *Ecological Complexity,* 6**,** 413-420.

LILLESAND, T. M., KIEFER, R. W. & CHIPMAN, J. W. 2007. *Remote sensing and image interpretation*, John Wiley & Sons Ltd.

LITTLE, F. 2014. Jacaranda City Pretoria, South Africa. *ChinAfrica,* 11**,** 004.

LIU, Y., HOU, S., KONG, X. & XU, Y. 2011. The analysis on land use change in urban fringe area based on the GIS technology. *Remote Sensing, Environment and Transportation Engineering (RSETE), 2011 International Conference on***,** 6444-6447.

LUCAS, R. E. B. 2015. Chapter 26 - African Migration. *In:* BARRY, R. C. & PAUL, W. M. (eds.) *Handbook of the Economics of International Migration.* North-Holland.

LUCK, M. & WU, J. 2002. A gradient analysis of urban landscape pattern: a case study from the Phoenix metropolitan region, Arizona, USA. *Landscape ecology,* 17**,** 327-339.

MA, W., CHEN, Y.-H. & ZHOU, J. 2008. Quantitative analysis of land surface temperature-vegetation indexes relationship based on remote sensing. *Proc. 21st ISPRS Congress, Youth Forum***,** 261-264.

MAKTAV, D., ERBEK, F. & JÜRGENS, C. 2005. Remote sensing of urban areas. *International journal of remote sensing,* 26**,** 655-659.

MALLICK, J., KANT, Y. & BHARATH, B. 2008. Estimation of land surface temperature over Delhi using Landsat-7 ETM+. *J. Ind. Geophys. Union,* 12**,** 131-140.

MANDAL, U. K. 2014. Geo-information Based Spatio-temporal Modeling of Urban Land Use and Land Cover Change in Butwal Municipality, Nepal. *The International Archives of Photogrammetry, Remote Sensing and Spatial Information Sciences,* 40**,** 809.

MANN, H. B. 1945. Nonparametric tests against trend. *Econometrica: Journal of the Econometric Society***,** 245-259.

MAREE, K. & VROMANS, D. 2010. The biodiversity sector plan for the Saldanha Bay, Bergrivier, Cederberg and Matzikama municipalities: Supporting land-use planning and decision-making in Critical Biodiversity Areas and Ecological Support Areas. *Produced by CapeNature as part of the CAPE Fine-scale Biodiversity Planning Project. Kirstenbosch*.

MARSCHALL, S. 2017. Transnational migrant home visits as identity practice: The case of African migrants in South Africa. *Annals of Tourism Research,* 63**,** 140-150.

MARTINUZZI, S., GOULD, W. A. & RAMOS GONZÁLEZ, O. M. 2007. Land development, land use, and urban sprawl in Puerto Rico integrating remote

sensing and population census data. *Landscape and Urban Planning,* 79**,** 288-297.

MATHEW, A., KHANDELWAL, S. & KAUL, N. 2017. Investigating spatial and seasonal variations of urban heat island effect over Jaipur city and its relationship with vegetation, urbanization and elevation parameters. *Sustainable Cities and Society,* 35**,** 157-177.

MATLALA, R. L. 2015. *Institutional arrangements for the implementation of local economic development in Gauteng Province, with special reference to the City of Tshwane Metropolitan Municipality.*

MCGARIGAL, K., CUSHMAN, S., NEEL, M. & ENE, E. 2002. FRAGSTATS: spatial pattern analysis program for categorical maps. *Department of Agriculture, Forest Service, Pacifica Northwest Research Station*.

MCGARIGAL, K. & MARKS, B. J. 1995. Spatial pattern analysis program for quantifying landscape structure. *Gen. Tech. Rep. PNW-GTR-351. US Department of Agriculture, Forest Service, Pacific Northwest Research Station*.

MCGARIGAL, K., TAGIL, S. & CUSHMAN, S. A. 2009. Surface metrics: an alternative to patch metrics for the quantification of landscape structure. *Landscape ecology,* 24**,** 433.

MCGRANAHAN, G., MITLIN, D., SATTERTHWAITE, D., TACOLI, C. & TUROK, I. 2009. Africa's urban transition and the role of regional collaboration. *International Institute for Environmental Development*.

MCLENNAN, D., NOBLE, M. & WRIGHT, G. 2016. Developing a spatial measure of exposure to socio-economic inequality in South Africa. *South African Geographical Journal,* 98**,** 254-274.

MISAGO, J. P., MONSON, T., POLZER, T. & LANDAU, L. 2010. May 2008 violence against foreign nationals in South Africa: Understanding causes and evaluating

responses. *Johannesburg: Forced Migration Studies Programme (FMSP), University of the Witwatersrand*.

MUBEA, K., NGIGI, T. & MUNDIA, C. 2011. Assessing Application of Markov Chain Analysis in Nakuru. *AGSE 2011***,** 182.

MUBIWA, B. & ANNEGARN, H. 2015. Historical spatial change in the Gauteng City-Region.

MUDAU, N., MHANGARA, P. & GEBRESLASIE, M. 2014. Monitoring urban growth around Rustenburg, South Africa, using SPOT 5. *South African Journal of Geomatics,* 3**,** 185-196.

MUNDIA, C. & ANIYA, M. 2006. Dynamics of landuse/cover changes and degradation of Nairobi City, Kenya. *Land Degradation & Development,* 17**,** 97-108.

MUNDIA, C. N. & ANIYA, M. 2005. Analysis of land use/cover changes and urban expansion of Nairobi city using remote sensing and GIS. *International Journal of Remote Sensing,* 26**,** 2831-2849.

MUNYATI, C. & MOTHOLO, G. L. 2014. Inferring urban household socio-economic conditions in Mafikeng, South Africa, using high spatial resolution satellite imagery. *Urban, Planning and Transport Research,* 2**,** 57-71.

MUSAKWA, W. & VAN NIEKERK, A. 2014. Monitoring Urban Sprawl and Sustainable Urban Development Using the Moran Index: A Case Study of Stellenbosch, South Africa. *International Journal of Applied Geospatial Research (IJAGR),* 5**,** 1-20.

MUTAMBIRWA, C. & POTTS, D. 1990. Changing patterns of African rural-urban migration and urbanisation in Zimbabwe. *Eastern and Southern Africa Geographical Journal,* 1**,** 26-39.

NADOUSHAN, M., SOFFIANIAN, A. & ALEBRAHIM, A. 2015. Modeling Land Use/Cover Changes by the Combination of Markov Chain and Cellular

Automata Markov (CA-Markov) Models. *Journal of Earth, Environment and Health Sciences,* 1**,** 16-21.

NATIONAL PLANNING COMMISSION, N. 2012. National Development Plan 2030: Our future–make it work. *Pretoria: National Planning Commission*.

NGIE, A., ABUTALEB, K., AHMED, F., DARWISH, A. & AHMED, M. 2014. Assessment of urban heat island using satellite remotely sensed imagery: a review. *South African Geographical Journal,* 96**,** 198-214.

NGIE, A., ABUTALEB, K., AHMED, F. & TAIWO, O.-J. 2013. Spatial modelling of urban change using satellite remote sensing. *Life in a Changing Urban Landscape,* 1**,** 3.

NGIE, A., ABUTALEB, K., AHMED, F., TAIWO, O., DARWISH, A. & AHMED, M. 2016. An estimation of land surface temperatures from landsat ETM+ images for Durban, South Africa. *Rwanda Journal,* 1.

NOOR, N. M. & ROSNI, N. A. 2013. Determination of Spatial Factors in Measuring Urban Sprawl in Kuantan Using Remote Sensing and GIS. *Procedia - Social and Behavioral Sciences,* 85**,** 502-512.

NOURI, J., GHARAGOZLOU, A., ARJMANDI, R., FARYADI, S. & ADL, M. 2014. Predicting Urban Land Use Changes Using a CA-Markov Model. *Arabian Journal for Science & Engineering (Springer Science & Business Media BV),* 39.

NPC, S. E. A. 2011. State of energy in South African Cities. *City Energy Support Unit of Sustainable Energy Africa*.

ODINDI, J. & MHANGARA, P. 2012. Green spaces trends in the city of Port Elizabeth from 1990 to 2000 using remote sensing. *International Journal of Environmental Research,* 6**,** 653-662.

ODINDI, J., MHANGARA, P. & KAKEMBO, V. 2012. Remote sensing land-cover change in Port Elizabeth during South Africa's democratic transition. *South African Journal of Science,* 108**,** 60-66.

ODINDI, J. O. & MHANGARA, P. 2011. THE TRANSFORMATION OF URBAN BUILT-UP AREAS DURING SOUTH AFRICA'S DEMOCARTIC TRANSITION: A CASE OF PORT ELIZABETH CITY USING REMOTE SENSING. *Journal of Sustainable Development in Africa,* Volume 13, .

OGRA, A. & ONATU, G. 2013. Metropolitan housing development in urban fringe areas-a case study of three metropolitan cities of South Africa: Johannesburg, Ekurhuleni and Tshwane.

OGUZ, H., KLEIN, A. & SRINIVASAN, R. 2007. Using the SLEUTH urban growth model to simulate the impacts of future policy scenarios on urban land use in the Houston-Galveston-Brazoria CMSA. *Research Journal of Social Sciences,* 2**,** 72-82.

OMAR, N. Q., AHAMAD, M. S. S., WAN HUSSIN, W. M. A., SAMAT, N. & BINTI AHMAD, S. Z. 2013. Markov CA, Multi Regression, and Multiple Decision Making for Modeling Historical Changes in Kirkuk City, Iraq. *Journal of the Indian Society of Remote Sensing,* 42**,** 165-178.

OSMAN, T., DIVIGALPITIYA, P. & ARIMA, T. 2016. Driving factors of urban sprawl in Giza Governorate of Greater Cairo Metropolitan Region using AHP method. *Land Use Policy,* 58**,** 21-31.

OTUNGA, C., ODINDI, J. & MUTANGA, O. 2014. Land Use Land Cover Change in the fringe of eThekwini Municipality: Implications for urban green spaces using remote sensing. *South African Journal of Geomatics,* 3**,** 145-162.

PAUCHARD, A., AGUAYO, M., PEÑA, E. & URRUTIA, R. 2006. Multiple effects of urbanization on the biodiversity of developing countries: the case of a fast-

growing metropolitan area (Concepción, Chile). *Biological conservation,* 127**,** 272-281.

PAUDEL, S. & YUAN, F. 2012. Assessing landscape changes and dynamics using patch analysis and GIS modeling. *International Journal of Applied Earth Observation and Geoinformation,* 16**,** 66-76.

PENCE, G. Q. 2008. CAPE Fine-scale systematic conservation planning assessment: Technical report. *Produced for CapeNature as part of the GEF-funded CAPE Fine-Scale Biodiversity Planning Project. Cape Town, South Africa*.

PENCE, G. Q. 2014. Western Cape Biodiversity Framework 2014 Status Update: Critical Biodiversity Areas of the Western Cape. *Unpublished CapeNature project report. Cape Town, South Africa*.

PERES, L. D. F., LUCENA, A. J. D., ROTUNNO FILHO, O. C. & FRANÇA, J. R. D. A. 2018. The urban heat island in Rio de Janeiro, Brazil, in the last 30 years using remote sensing data. *International Journal of Applied Earth Observation and Geoinformation,* 64**,** 104-116.

PIETER, K. & MARK, C. 2006. Migration and urbanization in South Africa.

. *Report 03-04-02, Pretoria:,* Statistics South Africa. **,** 29.

PILI, S., GRIGORIADIS, E., CARLUCCI, M., CLEMENTE, M. & SALVATI, L. 2017. Towards sustainable growth? A multi-criteria assessment of (changing) urban forms. *Ecological Indicators,* 76**,** 71-80.

POHLERT, T. 2016. Non-parametric trend tests and change-point detection. *CC BY-ND,* 4.

PONTIUS, G. R. & MALANSON, J. 2005. Comparison of the structure and accuracy of two land change models. *International Journal of Geographical Information Science,* 19**,** 243-265.

POTTS, D. 2005. Counter-urbanisation on the Zambian copperbelt? Interpretations and implications. *Urban Studies,* 42**,** 583-609.

QIN, Z., KARNIELI, A. & BERLINER, P. 2001. A mono-window algorithm for retrieving land surface temperature from Landsat TM data and its application to the Israel-Egypt border region. *International Journal of Remote Sensing,* 22**,** 3719-3746.

RALSTON, S., DE VILLIERS, C., MANUEL, J., TE ROLLER, K. & PENCE, G. 2009. Where are we going? Fine scale systematic conservation plans and their contribution to environmental assessment. *IAIAsa 2009 National Conference Proceedings* [Online].

RAMACHANDRA, T. & AITHAL, B. H. 2013. Urbanisation and Sprawl in the Tier II City: Metrics, Dynamics and Modelling Using Spatio-Temporal Data. *International Journal of Remote Sensing Applications,* 3.

RAMACHANDRA, T., AITHAL, B. H. & BEAS, B. 2014. Urbanisation Pattern of Incipient Mega Region in India. *Tema. Journal of Land Use, Mobility and Environment,* 7**,** 83-100.

RAPER, P. E. 2008. Tshwane, a San Name for Pretoria, South Africa. *Names,* 56**,** 221-230.

RENDENIEKS, Z., TĒRAUDS, A., NIKODEMUS, O. & BRŪMELIS, G. 2017. Comparison of input data with different spatial resolution in landscape pattern analysis – A case study from northern Latvia. *Applied Geography,* 83**,** 100-106.

REVESHTY, M. A. 2011. The assessment and predicting of land use changes to urban area using multi-temporal satellite imagery and GIS: A case study on Zanjan, IRAN (1984-2011). *Journal of Geographic Information System,* 3**,** 298.

RHINANE, H., HILALI, A., BAHI, H. & BERRADA, A. 2012. Contribution of Landsat TM data for the detection of urban heat islands areas case of Casablanca. *Journal of Geographic Information System,* 4**,** 20.

RICHARD, Y. & POCCARD, I. 1998. A statistical study of NDVI sensitivity to seasonal and interannual rainfall variations in Southern Africa. *International Journal of Remote Sensing,* 19**,** 2907-2920.

ROSSETTI, L. A., DOS ANJOS F PINTO, S. & DE ALMEIDA, C. M. 2013. Cellular automata-based spatial dynamic modeling for analyzing urban land use change. *Urban Remote Sensing Event (JURSE), 2013 Joint***,** 1-4.

RUI, Y. & BAN, Y. Multi-agent simulation for modeling urban sprawl in the greater toronto area. 13th AGILE International Conference on Geographic Information Science 2010, Guimarães, Portugal, 10-14 May 2010, 2010.

SAFF, G. 1994. The changing face of the South African city: from urban apartheid to the deracialization of space. *International Journal of Urban and Regional Research,* 18**,** 377-391.

SCHISSAU, R. 2006. Strafverfahren wegen MfS-Unrechts : die Strafprozesse bundesdeutscher Gerichte gegen ehemalige *Mitarbeiter des Ministeriums für Staatssicherheit der DDR*.

SCHOEMAN, F., NEWBY, T., THOMPSON, M. & VAN DEN BERG, E. C. 2014. South African national land-cover change map. *South African Journal of Geomatics,* 2**,** 94-105.

SEEKINGS, J. 2000. Introduction: Urban studies in South Africa after apartheid. *International Journal of Urban and Regional Research,* 24**,** 832-840.

SEN, P. K. 1968. Estimates of the regression coefficient based on Kendall's tau. *Journal of the American Statistical Association,* 63**,** 1379-1389.

SETO, K. C. & FRAGKIAS, M. 2005. Quantifying Spatiotemporal Patterns of Urban Land-use Change in Four Cities of China with Time Series Landscape Metrics. *Landscape Ecology,* 20**,** 871-888.

SHAFIZADEH MOGHADAM, H. & HELBICH, M. 2013. Spatiotemporal urbanization processes in the megacity of Mumbai, India: A Markov chains-cellular automata urban growth model. *Applied Geography,* 40**,** 140-149.

SHENG, L., TANG, X., YOU, H., GU, Q. & HU, H. 2017. Comparison of the urban heat island intensity quantified by using air temperature and Landsat land surface temperature in Hangzhou, China. *Ecological Indicators,* 72**,** 738-746.

SHOKO, M. & SMIT, J. 2013. Use of Agent Based Modelling in the Dynamics of Slum Growth. *South African Journal of Geomatics,* 2**,** 54-67.

SHOKO, M. & SMIT, J. 2014. Use of Agent Based Modelling to Investigate the Dynamics of Slum Growth. *South African Journal of Geomatics,* 2**,** 54-67.

SINGH, A. 1989. Review Article Digital change detection techniques using remotely-sensed data. *International journal of remote sensing,* 10**,** 989-1003.

SISODIA, P. S., TIWARI, V. & KUMAR, A. Analysis of supervised maximum likelihood classification for remote sensing image. Recent Advances and Innovations in Engineering (ICRAIE), 2014, 2014. IEEE, 1-4.

SMIT, S., MUSANGO, J. K., KOVACIC, Z. & BRENT, A. C. 2017. Conceptualising slum in an urban African context. *Cities,* 62**,** 107-119.

SOBRINO, J. A., JIMÉNEZ-MUÑOZ, J. C. & PAOLINI, L. 2004. Land surface temperature retrieval from LANDSAT TM 5. *Remote Sensing of environment,* 90**,** 434-440.

STATISTICS SOUTH AFRICA, S. 2015. Millennium Development Goals: Country report 2015. *Stats SA Library Cataloguing-in-Publication (CIP) Data*.

STATSSA, S. S. A. 2012. Census 2011 Municipal Report - Gauteng. *Stats SA Library Cataloguing-in-Publication (CIP) Data*.

SUBEDI, P., SUBEDI, K. & THAPA, B. 2013. Application of a Hybrid Cellular Automaton–Markov (CA-Markov) Model in Land-Use Change Prediction: A Case Study of Saddle Creek Drainage Basin, Florida. *Applied Ecology and Environmental Sciences,* 1**,** 126-132.

SUDHIRA, H. & RAMACHANDRA, T. 2007. Characterising urban sprawl from remote sensing data and using landscape metrics.

SUDHIRA, H., RAMACHANDRA, T. & JAGADISH, K. 2003a. Urban sprawl pattern recognition and modeling using GIS. *map India***,** 28-31.

SUDHIRA, H., RAMACHANDRA, T. & JAGADISH, K. 2003b. Urban sprawl: metrics, dynamics and modelling using GIS. *International Journal of Applied Earth Observation and Geoinformation,* 5**,** 29-39.

SUDHIRA, H., RAMACHANDRA, T. & JAGADISH, K. 2004. Urban sprawl: metrics, dynamics and modelling using GIS. *International Journal of Applied Earth Observation and Geoinformation,* 5**,** 29-39.

SUDHIRA, H., RAMACHANDRA, T., RAJ, K. S. & JAGADISH, K. 2003c. Urban growth analysis using spatial and temporal data. *Journal of the Indian Society of Remote Sensing,* 31**,** 299-311.

SUDHIRA, H., RAMACHANDRA, T., WYTZISK, A. & JEGANATHAN, C. 2005. Framework for integration of agent-based and cellular automata models for dynamic geospatial simulations. *Centre for Ecological Sciences, Indian Institute of Science) Bangalore*.

TAIWO, O. J., ABU-TALEB, K. A.-B. A., NGIE, A. & AHMED, F. EFFECTS OF POLITICAL DISPENSATIONS ON THE PATTERN OF URBAN EXPANSION IN THE OSOGBO METROPOLIS, OSUN STATE, NIGERIA. Proceedings of the 10th International Conference of AARSE, 2014. 242.

TAJBAKHSH, M., MEMARIAN, H. & SHAHROKHI, Y. 2016. Analyzing and modeling urban sprawl and land use changes in a developing city using a CA-Markovian

approach. *Global Journal of Environmental Science and Management,* 2**,** 397-410.

TAO, J., KONG, X., WANG, Y. & CHEN, R. 2016. A study of vegetation phenology in the analysis of urbanization process based on time-series MODIS data. *Geoscience and Remote Sensing Symposium (IGARSS), 2016 IEEE International***,** 2826-2829.

TAUBENBÖCK, H. & ESCH, T. 2011. Remote Sensing–An effective data source for urban monitoring. *Earth Observation, Urban Monitoring. www. earthzine. org/2011/07/20 (accessed 29th February 2012)*.

TAUBENBÖCK, H., ESCH, T., FELBIER, A., WIESNER, M., ROTH, A. & DECH, S. 2012. Monitoring urbanization in mega cities from space. *Remote sensing of Environment,* 117**,** 162-176.

TAUBENBÖCK, H., ESCH, T. & ROTH, A. 2006. An urban classification approach based on an object-oriented analysis of high resolution satellite imagery for a spatial structuring within urban areas. *Proceedings of the 1st EARSel Workshop of the SIG Urban Remote Sensing*.

TAUBENBÖCK, H., WEGMANN, M., ROTH, A., MEHL, H. & DECH, S. 2009. Analysis of urban sprawl at mega city Cairo, Egypt using multisensoral remote sensing data, landscape metrics and gradient analysis. *Proceedings of the ISRSE conference, Stresa, Italy. S,* 4.

TEWOLDE, M. G. & CABRAL, P. 2011. Urban sprawl analysis and modeling in Asmara, Eritrea. *Remote Sensing,* 3**,** 2148-2165.

THDA, T. H. D. A. 2012. South Africa: Informal settlements status. *Research Report.*

THOMPSON, M. 1996. A standard land-cover classification scheme for remote-sensing applications in South Africa. *South African Journal of Science,* 92**,** 34-42.

TIWARI, P., RAO, J. & DAY, J. 2016. Housing in South Africa. *Development Paradigms for Urban Housing in BRICS Countries***,** 183-219.

TOMLINSON, C., CHAPMAN, L., THORNES, J. & BAKER, C. 2012. Derivation of Birmingham's summer surface urban heat island from MODIS satellite images. *International Journal of Climatology,* 32**,** 214-224.

TORRENS, P. M. & ALBERTI, M. 2000. Measuring sprawl. *Centre for Advanced Spatial Analysis*.

TOWNSHEND, J. R. & JUSTICE, C. 1986. Analysis of the dynamics of African vegetation using the normalized difference vegetation index. *International Journal of Remote Sensing,* 7**,** 1435-1445.

TUCKER, C. J. 1979. Red and photographic infrared linear combinations for monitoring vegetation. *Remote sensing of Environment,* 8**,** 127-150.

TUROK, I. & BOREL-SALADIN, J. 2016. Backyard shacks, informality and the urban housing crisis in South Africa: stopgap or prototype solution? *Housing Studies,* 31**,** 384-409.

UN-HABITAT 2010. *State of the World's Cities 2010/11: Bridging the Urban Divide*, Earthscan.

UNHABITAT 2016. Urbanisation and Development: Emerging Futures. *World Cities Report 2016: United Nations Human Settlements Programme*

UNITED NATIONS, U. 2014. World Urbanization Prospects: The 2014 Revision, Highlights *Department of Economic and Social Affairs, Population Division, ST/ESA/SER.A/352*.

UNITED NATIONS, U. 2015. The Millennium Development Goals Report 2015. *Department of Economic and Social Affairs, Population Division,* United Nations, New York.

UNITED NATIONS, U. 2016. The World's Cities in 2016. *Economic and Social Affairs*.

VAN DER VYVER, Y. 2015. Situating Geography and the powers of Law, State and Church in the dynamic of Change that lead to the establishment of Pretoria. *South African Journal of Art History,* 30**,** 151-171.

VAN DER WESTHUIZEN, J. 2007. Glitz, glamour and the Gautrain: Mega-projects as political symbols. *Politikon,* 34**,** 333-351.

VAZ, E. 2014. Managing urban coastal areas through landscape metrics: An assessment of Mumbai's mangrove system. *Ocean & Coastal Management,* 98**,** 27-37.

VAZ, E., TAUBENBÖCK, H., KOTHA, M. & ARSANJANI, J. J. 2017. Urban change in Goa, India. *Habitat International,* 68**,** 24-29.

VERMEIREN, K., VAN ROMPAEY, A., LOOPMANS, M., SERWAJJA, E. & MUKWAYA, P. 2012. Urban growth of Kampala, Uganda: Pattern analysis and scenario development. *Landscape and Urban Planning,* 106**,** 199-206.

WALTERS, J. 2013. Overview of public transport policy developments in South Africa. *Research in Transportation Economics,* 39**,** 34-45.

WANG, L., FANG, L., HU, Y., HU, X., WU, L. & TIAN, Y. 2010. Dynamic land use change in rapidly urbanizing region. *Geoinformatics, 2010 18th International Conference on***,** 1-5.

WEBER, C. & PUISSANT, A. 2003. Urbanization pressure and modeling of urban growth: example of the Tunis Metropolitan Area. *Remote sensing of environment,* 86**,** 341-352.

WEN, Z., WU, S., CHEN, J. & LÜ, M. 2017. NDVI indicated long-term interannual changes in vegetation activities and their responses to climatic and anthropogenic factors in the Three Gorges Reservoir Region, China. *Science of The Total Environment,* 574**,** 947-959.

WENG, Q. 2012. Remote sensing of impervious surfaces in the urban areas: Requirements, methods, and trends. *Remote Sensing of Environment,* 117**,** 34-49.

WENG, Q., LU, D. & SCHUBRING, J. 2004. Estimation of land surface temperature–vegetation abundance relationship for urban heat island studies. *Remote Sensing of Environment,* 89**,** 467-483.

WENG, Y.-C. 2007. Spatiotemporal changes of landscape pattern in response to urbanization. *Landscape and Urban Planning,* 81**,** 341-353.

WOOD, A. 2014. Moving policy: global and local characters circulating bus rapid transit through South African cities. *Urban Geography,* 35**,** 1238-1254.

WRAY, C. 2010. Working towards a successful Gauteng City-Region. *PositionIT–Jan/Feb*.

WRAY, C. & CHERUIYOT, K. 2015. Key Challenges and Potential Urban Modelling Opportunities in South Africa, with Specific Reference to the Gauteng City-Region. *South African Journal of Geomatics,* 4**,** 14-35.

XIAN, G. & CRANE, M. 2005. Assessments of urban growth in the Tampa Bay watershed using remote sensing data. *Remote Sensing of Environment,* 97**,** 203-215.

XIAN, G., HOMER, C., BUNDE, B., DANIELSON, P., DEWITZ, J., FRY, J. & PU, R. 2012. Quantifying urban land cover change between 2001 and 2006 in the Gulf of Mexico region. *Geocarto International,* 27**,** 479-497.

XIE, Y., MA, W., ZHANG, H., CHEN, W., CHEN, M. & ZHOU, L. 2007. Using CA-Markov Models to Simulate the Land-use Changes in Pudong New Area, Shanghai City.

XU, L. Y., XIE, X. D. & LI, S. 2013. Correlation analysis of the urban heat island effect and the spatial and temporal distribution of atmospheric particulates using TM images in Beijing. *Environmental Pollution,* 178**,** 102-114.

XU, X. & MIN, X. 2013. Quantifying spatiotemporal patterns of urban expansion in China using remote sensing data. *Cities,* 35**,** 104-113.

YA, W., ZHI-FENG, W., XIAONAN, L. & JIONG, C. 2010. Use of RS and GIS to Identify of Farmland Loss in the Coastal Area of Pearl River Estuary. *Education Technology and Computer Science (ETCS), 2010 Second International Workshop on,* 1**,** 312-316.

YANG, L., QIAN, F., SONG, D.-X. & ZHENG, K.-J. 2016. Research on Urban Heat-Island Effect. *Procedia Engineering,* 169**,** 11-18.

YANG, Y., LIU, Y., LI, Y. & DU, G. 2018. Quantifying spatio-temporal patterns of urban expansion in Beijing during 1985–2013 with rural-urban development transformation. *Land Use Policy,* 74**,** 220-230.

YU, X. J. & NG, C. N. 2007. Spatial and temporal dynamics of urban sprawl along two urban–rural transects: A case study of Guangzhou, China. *Landscape and Urban Planning,* 79**,** 96-109.

YUE, W., XU, J., TAN, W. & XU, L. 2007. The relationship between land surface temperature and NDVI with remote sensing: application to Shanghai Landsat 7 ETM+ data. *International Journal of Remote Sensing,* 28**,** 3205-3226.

ZEILHOFER, P. & TOPANOTTI, V. P. 2008. GIS and ordination techniques for evaluation of environmental impacts in informal settlements: A case study from Cuiaba, central Brazil. *Applied Geography,* 28**,** 1-15.

ZENG, C., LIU, Y., STEIN, A. & JIAO, L. 2015. Characterization and spatial modeling of urban sprawl in the Wuhan Metropolitan Area, China. *International Journal of Applied Earth Observation and Geoinformation,* 34**,** 10-24.

ZHANG, X. Q. 2016. The trends, promises and challenges of urbanisation in the world. *Habitat International,* 54**,** 241-252.

ZHAO, P. 2010. Sustainable urban expansion and transportation in a growing megacity: Consequences of urban sprawl for mobility on the urban fringe of Beijing. *Habitat International,* 34**,** 236-243.